University of Alberta

Identification and characterization of novel ribosome biogenesis factors

by

Yaroslav Sydorskyy 

A thesis submitted to the Faculty of Graduate Studies and Research in partial fulfillment of the requirements for the degree of Doctor of Philosophy

Department of Cell Biology

Edmonton, Alberta

Fall 2005

Abstract

Ribosome biogenesis is one of the major cellular activities in a eukaryotic cell. Sequential biogenesis events occurring in the nucleolus, the nucleoplasm and the cytoplasm, indicate that the ribosomal assembly is inextricably linked to nucleocytoplasmic transport. Existence of such a link in *Saccharomyces cerevisiae* was made clear by the investigation of the stationary and mobile phases of the nucleocytoplasmic transport machinery. Proteomic analysis of an enriched nuclear pore complex (NPC) fraction revealed that ribosomal biogenesis factors constituted a large fraction of the proteins, likely reflecting their abundance and transit through the pore. Among these was Nop53p, which we have characterized as a novel ribosomal biogenesis factor. A genetic study based on the nucleocytoplasmic transport mobile phase receptor, β-karyopherin Kap123p, also identified a ribosome biogenesis factor termed Rai1p, which functions with the exonuclease Rat1p. In addition, this screen identified three karyopherins, Kap121p/Pse1p, Sxm1p/Kap108p and Nmd5p/Kap119p, which we propose are able to supplant Kap123p's role in nuclear import of numerous ribosomal proteins and biogenesis components.

This thesis focuses on the characterization of Rai1p and Nop53p. Mutations in both *RAI1* and *NOP53* are deleterious to cell growth and cause defects in rRNA processing. This in turn leads to an imbalance of the 60S:40S ratio and, due to the paucity of functional 60S subunits, the appearance of "halfmers", which results from an accumulation of 40S subunits stalled on mRNA. Rai1p and Nop53p are involved in two

separate stages of 60S subunit biogenesis. Nop53p is likely involved in an early processing step, as it localizes to the nucleolus, physically interacts with early rRNA processing factors Cbf5p and Nop2p, and cofractionates specifically with pre-60S particles on sucrose gradients. Rai1p likely acts in one of the later maturation steps. It localizes predominantly to the nucleus, where it interacts with Rat1p and pre-60S particles. Emphasizing the relationship between nucleocytoplasmic transport and ribosome biogenesis, we also demonstrated that Kap123p imports the essential 60S ribosomal subunit export factor Nmd3p. The observed genetic interaction between *KAP123* and *RAI1* is interpreted to result from a combination of compromised Kap123p-mediated nuclear import of Nmd3p and a *rai1Δ*-induced decrease in the overall efficiency of ribosomal biogenesis.

Acknowledgements

First of all, I want to thank my supervisor, John Aitchison for his advice, support and encouragement. I also want to thank John for broadening my scientific horizons and giving me the freedom to work independently and to follow my own ideas. His dedication to work, perseverance and readiness to follow exciting scientific projects into unrelated research fields is an inspiration to us all. Thank you, John.

I want to express my gratitude to the members of the Aitchison lab in Edmonton and Seattle, talented young scientists from whom I've learned and received a lot of help. Over time all of them became my good friends, ready to share happiness and sorrow. In particular I would like to thank David Dilworth, Marcello Marelli, Brendan Halloran, Rosanna Baker and Taras Makhnevych for their contributions to my projects.

In addition, I want to acknowledge the organizations which provided funding for this study: the Canadian Institutes for Health Research and Alberta Heritage Foundation for Medical Research, the Institute for Systems Biology, and Merck & Co., Inc. I am also a recipient of a University of Alberta CHIA Fellowship for Foreign Students.

Finally, I want to express my gratitude to the members of my supervisory committee, Richard Rachubinski, Paul Melançon and Richard Wozniak for setting a high standard level and guiding me to reach it.

Technical Acknowledgements

I would like to thank Deena Leslie, Kelly Hjertaas, Dwayne Weber, Richard Rogers, Jennifer Smith, Tatiana Iouk and Vladmir Titorenko for technical assistance, and to acknowledge Eugene Yi and David Goodlett for the mass spectrometry analysis of my samples.

I also want to express my gratitude to those who directly contributed to various parts of this study. John Aitchison, Rosanna Baker and Adriana Antunz-de-Mayolo performed introductory stages of the *KAP123* synthetic fitness screen and constructed several plasmids for the analysis of resulting mutants; David Dilworth, Brendan Halloran and Scott Wyzykowski for construction of *NOP53* plasmids and strains, and for co-immunoprecipitation of the interacting proteins; Taras Makhnevych, Marcello Marelli, Ramsey Saleem, Halyna Shcherbata and Mike Rout for critical reading, and helpful discussions of my manuscripts; Mike Rout, Arlen Johnson, Gunter Blobel, John Woolford and Olivier Gadal for sharing strains and plasmids.

These people were a pleasure to work with and are very much appreciated.

Table of Contents

Chapter 3 Intersection of the Kap123p-mediated nuclear import and ribosome export pathways **76**

Chapter 4 Nop53p is a novel nucleolar 60S ribosomal subunit biogenesis protein **106**

Chapter 5 Perspectives **124**

Chapter 6 References **136**

List of Tables

List of Figures

List of Symbols and Abbreviations

ETS	external transcribed spacer
Amp	Ampere
AAA-ATPases	ATPases associated with various cellular activities
ATP	adenosine tiphosphate
ATPase	adenosine tiphosphate hydrolase
bp	base pair
BSA	bovine serum albumin
c	centi ($x10^{-2}$)
°C	degrees Celsius
Ci	Curie
cpm	counts per minute
d	day
D.	*Drosophila*
Da	Dalton
DFC	dense fibrillar component
DNA	deoxyribonucleic acid
dNTP	deoxynucleotide triphosphates
E.	*Escherichia*
ECL	enhanced chemiluminescence
EM	electron micrograph
F	Farad
g	gram
g	force of gravity
GC	granular component
GFP	green fluorescent protein
GTPase	guanosine triphosphat hydrloase
h	hour
HRP	horseradish peroxidase
IgG	immunoglobulin G
ITS	internal transcribed spacers
J	Joule
k	kilo ($x10^{3}$)
Kap	Karyopherin
L	litre
LSU	large subunit
m	meter or milli ($x10^{-3}$)
M	moles per litre
min	minute
mRNA	messenger RNA
n	nano (10^{-9})
NCBI	National Center for Biotechnology Information
NE	nuclear envelope
NES	nuclear export sequence
NLM	National Library of Medicine
NLS	nuclear localization sequence

NPC	nuclear pore complex
NTS	nontranscribed spacers
Nup	Nucleoporin
OD	optical dencity
ORF	open reading frame
pA	*Staphylococcus aureus* protein A
PAGE	polyacrylamide gel electrophoresis
PCR	polymerase chain reaction
pH	$-\log[H^+]$
PKA	protein kinase A
Pol I	RNA polymerase I
Pol II	RNA polymerase II
RanGAP	GTPase activating protein
RanGEF	guanosine nucleotide exchange factor
RB	retinoblastoma proteins
rRNA	ribosomal DNA
RFP	red fluorescent protein
RNA	ribonucleic acid
RNase	ribonuclease
RNase MRP	mitochondrial RNA processing RNase
r-proteins	ribosomal proteins
rpS#/rpL#	small/large subunit r-protein
rRNA	ribosomal RNA
S	Svedberg unit (sedimentation coefficient of a particle)
S.	*Saccharomyces*
sc	*Saccharomyces cerevisiae*
SDS	sodium dodecyl sulphate
sec	second
SGD	Saccharomyces Genome Database
snoRNA	small nucleolar RNA
snoRNP	small nucleolar ribonucleoprotein particle
snRNA	small nuclear RNA
sp	*Schizosaccharomyces pombe*
SSU	small subunit processome
TCA	trichloracetic acid
TOR	target of rapamycin
tRNA	transfer RNA
U	units of enzymatic activity
UBF	upstream binding factor
v	volume
V	Volt
w	weight
λ	wavelength
μ	micro ($x10^{-6}$)
Ω	Ohm
Ψ	pseudouridine

Chapter 1

Introduction

1.1 The ribosome and translation

Proteins constitute more than half the total dry mass of a cell, and their synthesis is central to cell maintenance, growth, and development. Protein synthesis occurs on ribosomes, which are complexes of RNA and protein molecules. Here, mRNA and aminoacyl-tRNA meet during the translation of the genetic message. The ribosome provides the structural framework for the decoding process, and contains the catalytic centre responsible for formation of the peptide bond, so-called peptidyl transferase centre.

Ribosomes were first discovered in the early 1950s (Porter et al., 1945; Schachman et al., 1952; Palade, 1955) but their role in protein synthesis didn't become apparent until more than a decade later. The name "ribosome" was given to the particles in 1958 (Tissieres and Watson, 1958).

Eukaryotic and prokaryotic ribosomes are very similar in design and function, but differ in size. Both are composed of one large and one small subunit that fit together to make up the complete ribosome, a complex with a mass of several million daltons (Da) (Fig. 1.1A). The ribosomal subunits are commonly designated in Svedberg units (S), a measure of particle sedimentation rate during centrifugation. When measured in these units, the large subunits are 50S or 60S, the small subunits are 30S or 40S, and the complete ribosomes are 70S or 80S (prokaryotic or eukaryotic ribosomes, respectively). A ribosome contains four binding sites for RNA molecules: one for mRNA and three for tRNAs (Fig. 1.1A, C). One tRNA binding site is called the peptidyl-tRNA binding site, or P-site, and it holds the tRNA molecule that is linked to the growing end of the polypeptide chain. The other tRNA binding site, called the aminoacyl-tRNA binding

Figure 1.1. The structure of a ribosome. (A) Both eukaryotic and prokaryotic ribosomes are composed of one large (60S) and one small (40S) subunit that fit together to make up the complete ribosome. The large subunit has three tRNA binding sites necessary for translation: peptidyl-tRNA binding site (P-site), aminoacyl-tRNA binding site (A-site) and tRNA exit site (E-site) (adapted from http://nobelprize.org/medicine/educational/). (B) Schematic representation of a loaded ribosome. The small subunit is bound to the template mRNA, while the large subunit guides aminoacyl-tRNA and peptidyl-tRNA to the template, forcing base pairing with appropriate codons (adapted from Alberts, 1994). (C) Space-filling representations of the bacterial large (50S) subunit with the three tRNA molecules loaded into the binding sites. The proteins are in pink and the rRNA in blue. A backbone ribbon representation of the A-, P-, and E-sites are shown in yellow, red, and white, respectively. The whole subunit in a rotated crown view is on the left, and a closer view showing the numbered r-proteins is on the right (reproduced from Nissen et al., 2000).

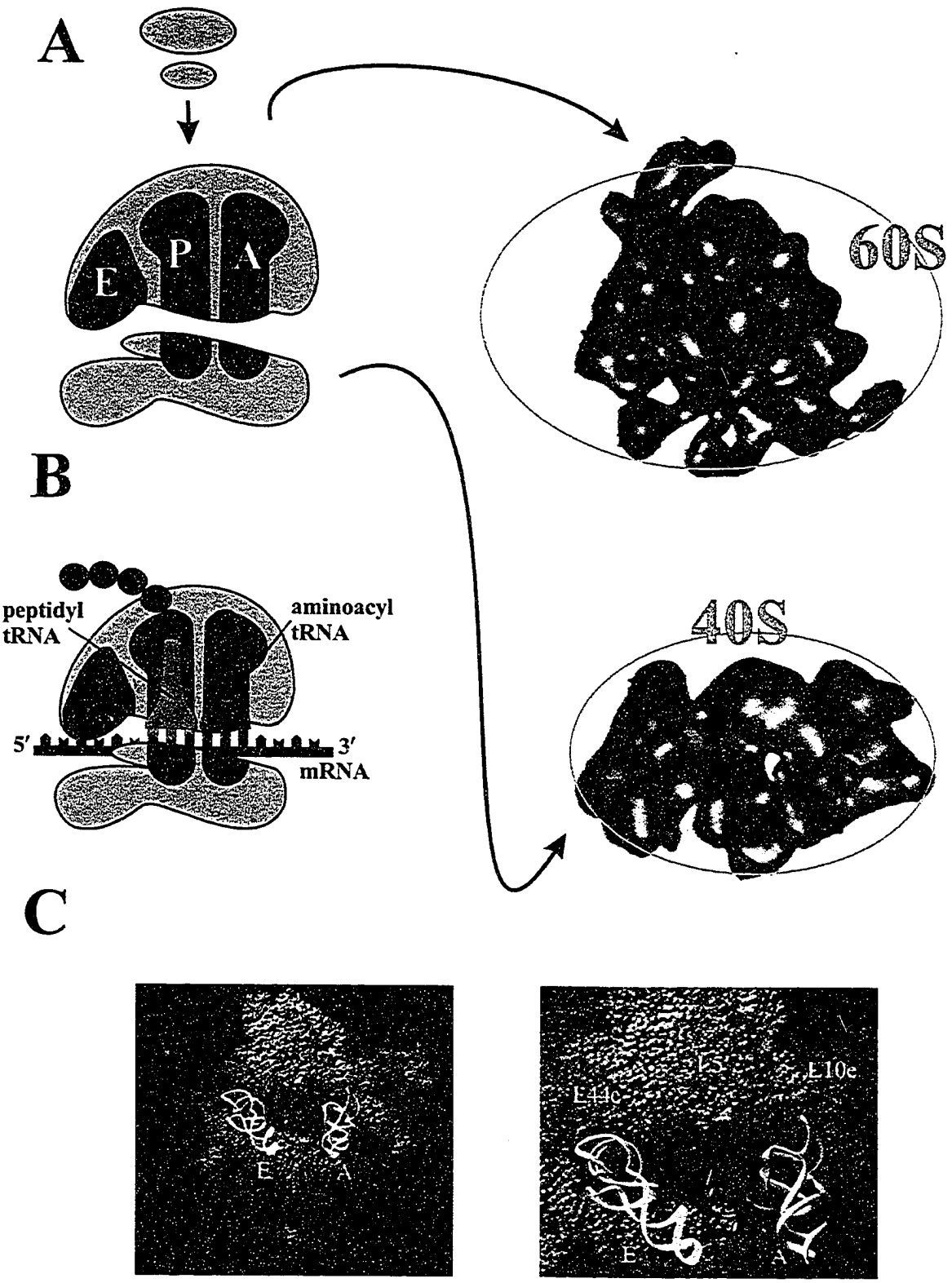

site, or A-site, holds the incoming tRNA molecule charged with an amino acid. During translation the small subunit binds the mRNA and tRNAs, while the large subunit catalyzes peptide bond formation (Fig. 1.1B).

Mature ribosomes are located at the sites of translation; either free floating in the cytoplasm of a cell, or bound to the cytoplasmic face of rough endoplasmic reticulum (Fig. 1.2A, B). One mRNA molecule is usually translated by multiple ribosomes simultaneously. These structures are called polyribosomes or polysomes (Fig. 1.2C). A new ribosome initiates translation as soon as the previous 40S subunit, bound to the mRNA molecule recruits a 60S subunit and then moves along the template. This frees-up approximately 80 nucleotides, including the start codon and a binding site for the next 40S subunit (Alberts, 1994). Ribosomes can also be found in mitochondria and chloroplasts where they translate the organelle's mRNA. These ribosomes, however, resemble bacterial ribosomes rather than eukaryotic ones.

The *S. cerevisiae* ribosome contains 79 highly basic ribosomal proteins (r-proteins) (Fig. 1.3A, B). These proteins are generally small and are encoded by 138 genes; usually one r-protein is encoded by two nearly identical genes. The mRNAs for the r-proteins are transcribed by RNA polymerase II. Although r-protein genes represent only 2% of the yeast genome, they contain almost half of the genome's introns and the resultant mRNAs require extensive splicing (Spingola et al., 1999).

Many r-proteins are not essential for translation. Because of this, it has been suggested that a ribosome is actually a ribozyme, and that the ribosomal proteins mainly enhance the catalytic function of ribosomal RNA (rRNA), by performing structural,

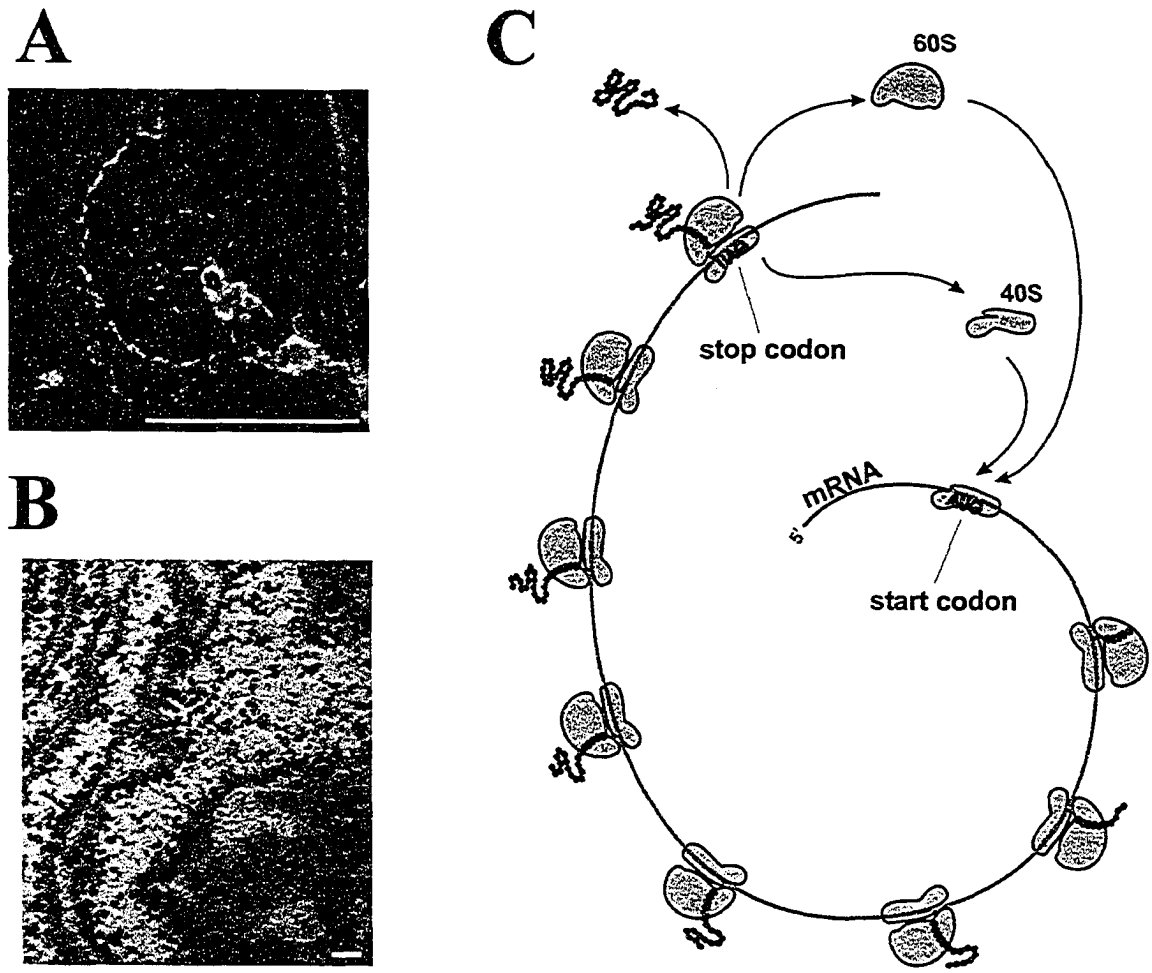

Figure 1.2. Polysomes contain multiple ribosomes translating the same mRNA molecule. Shown are polysomes in electron micrographs of eukaryotic cells. (A) A freeze-etch EM shows a cytosolic polysome in its characteristic spiral shape. (B) A transmission EM shows membrane-bound polysomes which lack the spiral shape (reproduced from Alberts, 1994). Bar, 100 nm. (C) A scheme showing a series of ribosomes simultaneously translating the same mRNA (reproduced from Alberts, 1994).

signaling and regulatory functions (Nissen et al., 2000; Noller et al., 1992). Accordingly, more than half of the mass of a ribosome is RNA, and there is increasing evidence that the rRNA molecules play central roles in the ribosome's catalytic activities. While the size and the nucleotide sequence of both the small subunit and large subunit rRNAs vary

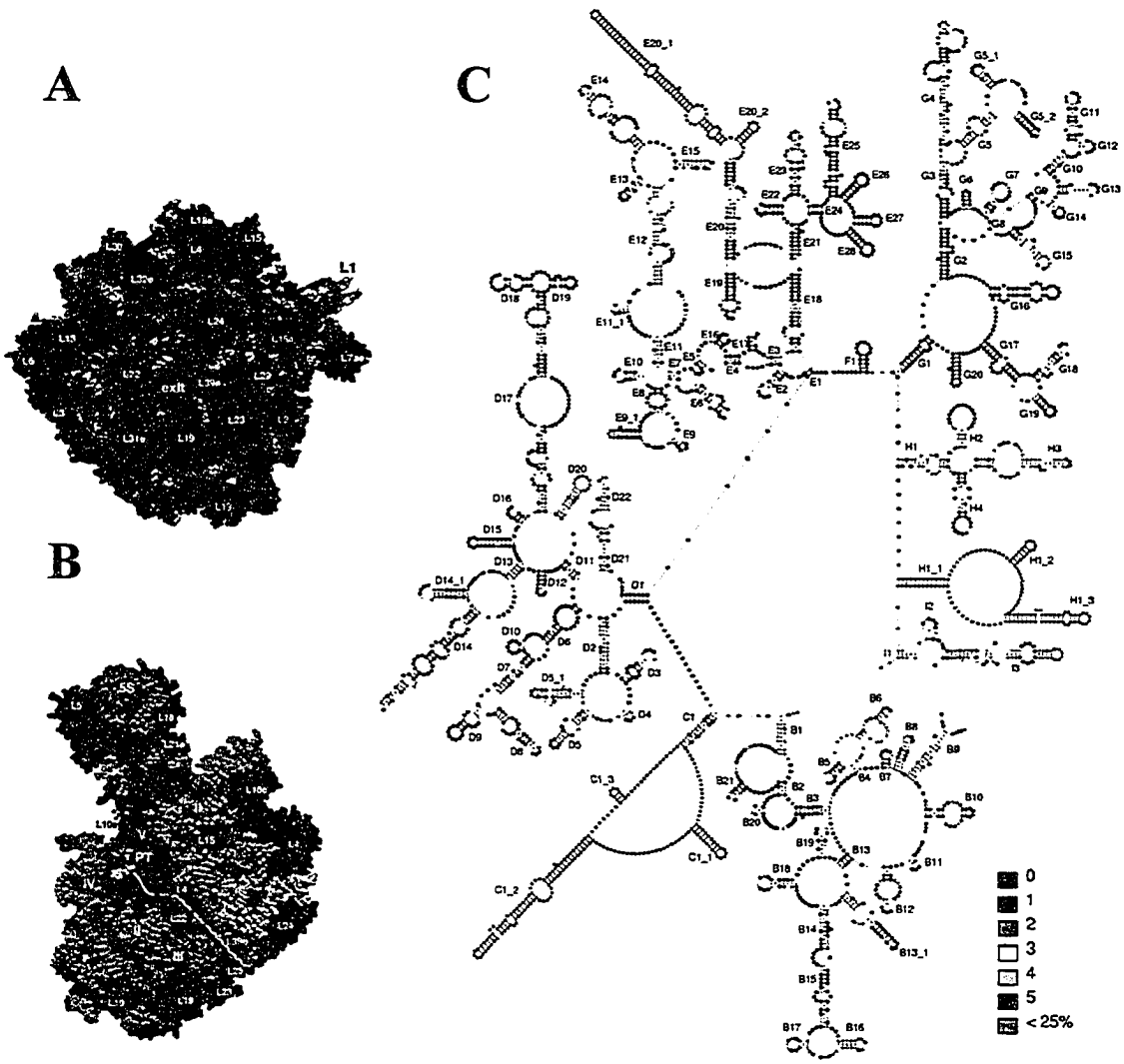

Figure 1.3. A detailed model of a large ribosomal subunit and rRNA. (A) A space-filling representation of the prokaryotic large subunit surface at the polypeptide tunnel exit showing the arrangement of r-proteins (blue), rRNA (white and orange). (B) A model of the large subunit section along the polypeptide tunnel. R-proteins are shown in blue, all other colors represent the large subunit rRNA (23S) domains I through V and 5S rRNA (reproduced from Nissen et al., 2000). (C) Map of nucleotide variability among 77 eukaryote species, superimposed on a secondary structure model of *S. cerevisiae* large subunit rRNA (25S). The variability of each nucleotide is indicated with a colored dot. Red dots represent sites that are least conserved, while blue indicates the most conserved ones. Sites that are completely conserved in all tested species are represented by purple dots. Sites which represent nucleotides that are present in *S. cerevisiae*, but are absent in 75% or more of the other sequences are represented by grey dots (reproduced from Ben Ali et al., 1999).

in different organisms, there are large regions of sequence homology and their folded structures remain highly conserved (Fig. 1.3C) (Ben Ali et al., 1999).

1.2 Ribosomes and human health

1.2.1 Genetic diseases (r-protein deficiencies)

Although the ribosome is essential for cell growth and development, the effects of mutations in r-proteins and their roles in human disease have been largely ignored. One might predict that genetic defects in r-proteins would cause serious problems with the translational apparatus and hence result in early embryonic death. However, there is strong evidence in *Drosophila melanogaster* that a quantitative deficiency of any one of the ribosomal proteins can still yield viable but abnormal phenotypes (reviewed in Uechi et al., 2001). A group of mutations (over 50) collectively known as *minute*, are scattered in the *D. melanogaster* genome and are all associated with similar dominant phenotypes, displaying a slower rate of mitosis, reduced body size, diminished fertility, and short, thin bristles. Interestingly, the *minute* mutations do not affect cell size (Neufeld et al., 1998). Several genes responsible for these mutations have been characterized at the molecular level, and all, so far, have been found to encode r-proteins (Kongsuwan et al., 1985; Lambertsson, 1998). Thus, the *minute* phenotype appears to result from a reduced capacity for protein synthesis in flies caused by expression of functional copy of a given r-protein gene only from one allele rather than two.

Because ribosomal proteins are highly conserved among eukaryotes, it is likely that quantitative deficiencies in human ribosomal proteins, as in *D. melanogaster*, would

result in reduced translation capacity and thereby yield abnormal phenotypes. Surprisingly, there are very few reports of haploinsufficiency of r-protein genes in the human population. Diamond-Blackfan anaemia is a classical case of a human syndrome, in which a variety of mutations in the gene for r-protein S19 have been identified in 25% of the patients (Da Costa et al., 2001; Draptchinskaia et al., 1999). These mutations lead to anaemia, increased susceptibility to cancer, hypotrophy at birth and severe growth retardation (Da Costa et al., 2001).

In light of recent findings on Diamond-Blackfan anaemia, a suggestion made more than a decade ago becomes very attractive. It was proposed that haploinsufficiency of ribosomal protein S4 (RPS4), encoded by both the X and the Y chromosomes, is an important factor in Turner syndrome (Fisher et al., 1990; Watanabe et al., 1993). This syndrome is a complex human disorder classically associated with the lack of a Y chromosome. One example of a well characterized mammalian r-protein gene mutation is *Bst* in mice, which is semidominant and homozygous lethal (Oliver et al., 2004). It was characterized as a deletion within the gene encoding r-protein L24. The resulting heterozygous phenotype includes disrupted pigmentation and skeletal abnormalities, as well as decreased rates of protein synthesis and proliferation. Interestingly, however, a *S. cerevisiae* ortholog of mouse L24 protein is one of the few r-proteins that is not essential for growth (Baronas-Lowell and Warner, 1990). In conclusion, the lack of r-protein gene haploinsufficiency cases found in mammals is likely caused by the severity of defects which render the embryos inviable at early stages of development (Rudra and Warner, 2004).

1.2.2 Cancer (deregulation of translation machinery)

Although it has long been known that in cancer cells components of the translation machinery are deregulated or misexpressed, their precise roles in tumorigenesis have largely been overlooked. For example, as early as 1970, changes in the nucleolus were recognized as a reliable marker of cellular transformation. However, these findings were dismissed as non-consequential to the overall transformation process (Ruggero and Pandolfi, 2003). Recent research shows that several proto-oncogenes and tumour suppressors directly regulate ribosome production, the initiation of protein translation, or both (reviewed in Ruggero and Pandolfi, 2003).

An example of this is the family of retinoblastoma proteins (RB), tumor suppressors involved in a wide range of tumors, which have been shown to regulate rRNA synthesis by controlling Pol I-dependent transcription. Several findings indicate that the RB gene product restricts the production of rRNA through direct association with an upstream binding factor (UBF) in the rRNA gene, preventing it from recruiting other cofactors required for Pol I activity (Cavanaugh et al., 1995; Ciarmatori et al., 2001; Voit et al., 1997). Proto-oncogene product MYC, a transcription factor involved in several B-cell-specific malignancies, directly regulates ribosome biogenesis normally through the transcriptional activation of r-proteins and ribosome assembly factors (Boon et al., 2001; Menssen and Hermeking, 2002).

Cancer and human disease have also been associated recently with mutations in genes encoding proteins that are directly involved in ribosome biogenesis. The *DKC1* gene is mutated in patients with *dyskeratosis congenita*, a disease that is characterized by premature ageing and an increased susceptibility to cancer (Heiss et al., 1998; Ruggero et

al., 2003). *DKC1* encodes a pseudouridine synthase that mediates posttranscriptional modification of rRNA.

Although mutations in genes that are directly responsible for ribosome biogenesis, such as those encoding the r-protein S19 and *DKC1*, have been found in cancer susceptibility syndromes, the molecular mechanisms by which these proteins contribute to cancer remain largely unknown. Further investigation will be required to clarify to what extent defects in the translation process contribute to tumorigenesis. This is important because components of the translation machinery that are overexpressed or deregulated in cancer cells could represent targets for cancer therapy. For example, the macrolide rapamycin, which affects the translation machinery, has already been used in clinical trials as a tumor inhibitory agent. However, a deeper knowledge of basic ribosomal processes, including ribosome biogenesis will be required to identify the triggers that will enable the fine-tuning of damaged translation machinery.

1.3 Ribosome biogenesis

1.3.1 rRNA operon

In a rapidly growing yeast cell the approximate distribution of RNA species is: 80% rRNA, 15% tRNA and 5% mRNA. One cell can contain approximately 200 000 ribosomes. With a doubling time of about 100 minutes, a growing cell must produce 2000 ribosomes per minute to maintain a constant level of ribosomes (Warner, 1999). In order to support this rapid ribosome production, the yeast genome contains 100 to 200 head-to-tail copies of the rRNA operon. The *S. cerevisiae* rRNA operon encodes the four

rRNA species found in the mature ribosome: 5S, 18S, 5.8S, and 25S (28S in mammals). The basic organization of the nuclear rRNA operon which includes the last three rRNA species is similar in all eukaryotes including yeast (Fig. 1.4). These three rRNAs (18S, 5.8S, and 25S/28S) are transcribed by RNA polymerase I (Pol I) as a single large precursor, the 35S pre-rRNA (45S in mammals), which contains the mature rRNA sequences separated by two internal transcribed spacers, ITS1 and ITS2, and flanked by two external transcribed spacers, the 5'-ETS and 3'-ETS. The remaining part of the *S. cerevisiae* 9.1-kb long rRNA operon is formed by two nontranscribed spacers, NTS1 and NTS2, which flank the 5S rRNA gene, which is transcribed by RNA polymerase III. The presence of the 5S rRNA gene within the rRNA operon is a unique feature of *S. cerevisiae* since in other eukaryotic species it is usually located on a different chromosome (Paule and White, 2000).

1.3.2 Ribosome assembly factors and the maturation pathway

Due to the ease of genetic and biochemical manipulations, the ribosome biogenesis pathway is best characterized in the budding yeast *S. cerevisiae*. In this organism, mature 60S ribosomal subunits contain the 5S, 5.8S and 25S rRNAs, whereas the small 40S subunit contains the 18S rRNA. Maturation of the ribosomal rRNA and its assembly into ribosomal subunits involves at least 170 accessory proteins comprising endo- and exoribonucleases, putative ATP-dependent RNA helicases, 'chaperones' or 'assembly factors' (Kressler et al., 1999b; Venema and Tollervey, 1999), and as many as 66 or more small nucleolar RNAs (snoRNAs), which serve to guide enzymatic modifications along

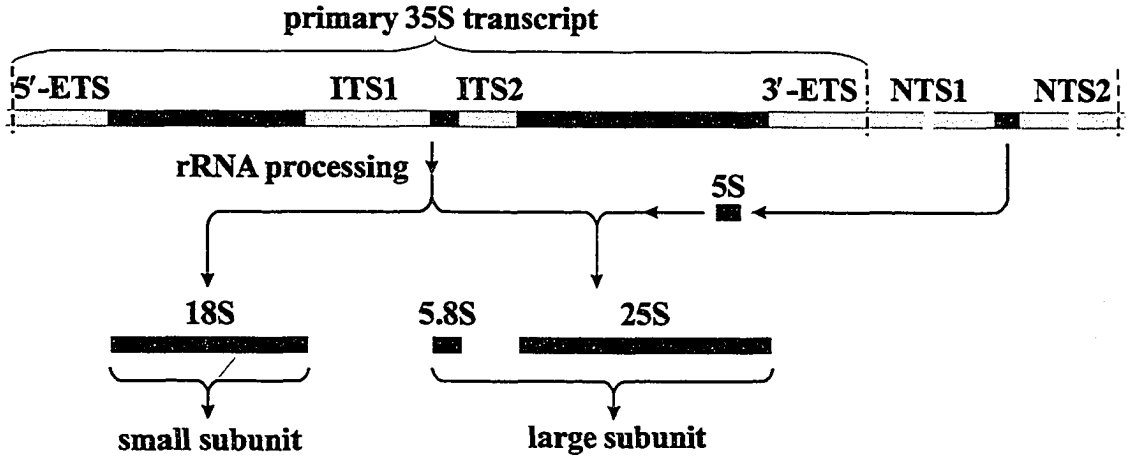

Figure 1.4. The structure of the *S. cerevisiae* rRNA operon. The primary 35S rRNA transcript is processed to form three mature rRNAs: 18S, 5.8S and 25S (blue). Nearly half of the nucleotide sequence of a primary rRNA transcript is excised and/or degraded. The four degraded sequences (grey) include: two internal transcribed spacers (ITS1/ITS2) and two external transcribed spacers (5'-ETS/3'-ETS). The 5S gene (purple) is flanked by two nontranscribed spacers (NTS1/NTS2) (grey) (adapted from Alberts, 1994).

the rRNA during ribosome biogenesis (Fromont-Racine et al., 2003). In most cases, snoRNAs must also assemble with protein counterparts and undergo maturation before they are transported to the nucleolus, which adds to the complexity of ribosome biogenesis (Fromont-Racine et al., 2003).

35S pre-rRNA was first found in 90S ribosome precursor particles in the early 1970s by sedimentation analysis. These particles were detected along with 66S and 43S precursor ribosomal subunits (Udem and Warner, 1972; Warner et al., 1972). Further studies revealed the basic features behind the ribosomal maturation pathway: the 90S precursors split to form 66S and 43S pre-ribosome subunits, which then undergo a series of maturation steps until they get exported from the nucleus and become the mature 60S and 40S subunits. Over the ensuing three decades, studies of the rRNA processing

pathway have revealed a number of additional specific intermediates. Combining this knowledge with recent developments in proteomic-based technology has allowed one to start assigning roles to the long list of accessory proteins and to define the points at which they enter and exit the ribosome maturation pathway (Fig. 1.5) (Bassler et al., 2001; Grandi et al., 2002; Harnpicharnchai et al., 2001; Nissan et al., 2002; Saveanu et al., 2003; Schafer et al., 2003). However, the lack of simple correspondence between the individual protein factors and specific steps in rRNA maturation suggests that the ribosome biogenesis pathway is not as linear and simple as is depicted in the classical schemes. The apparent heterogeneity of rRNA species and the varying yield of different protein factors observed in various high-throughput co-purification studies led to an alternative hypothesis in which multiple assembly and processing reactions are proceeding in parallel. If this is true, the key steps of the processing pathway must be regulated by quality control systems to ensure that irreversible reactions do not occur prematurely (Dez and Tollervey, 2004). Ribosomal biogenesis factors Rlp7p and Ssf1p, which are required for processing of the pre-60S particles beyond a certain point, and which localize exclusively to the nucleolus, may well be the members of such a quality control system - the guardians of the processing pathway checkpoints (Fatica and Tollervey, 2002; Gadal et al., 2002). In short, the specific details of how ribosomal subunits are processed and assembled remain unclear.

1.3.3 rRNA processing pathway

As with eukaryotic mRNA processing, the 35S pre-rRNA processing begins while transcription is still taking place. The terminal knobs visualized by electron microscopy

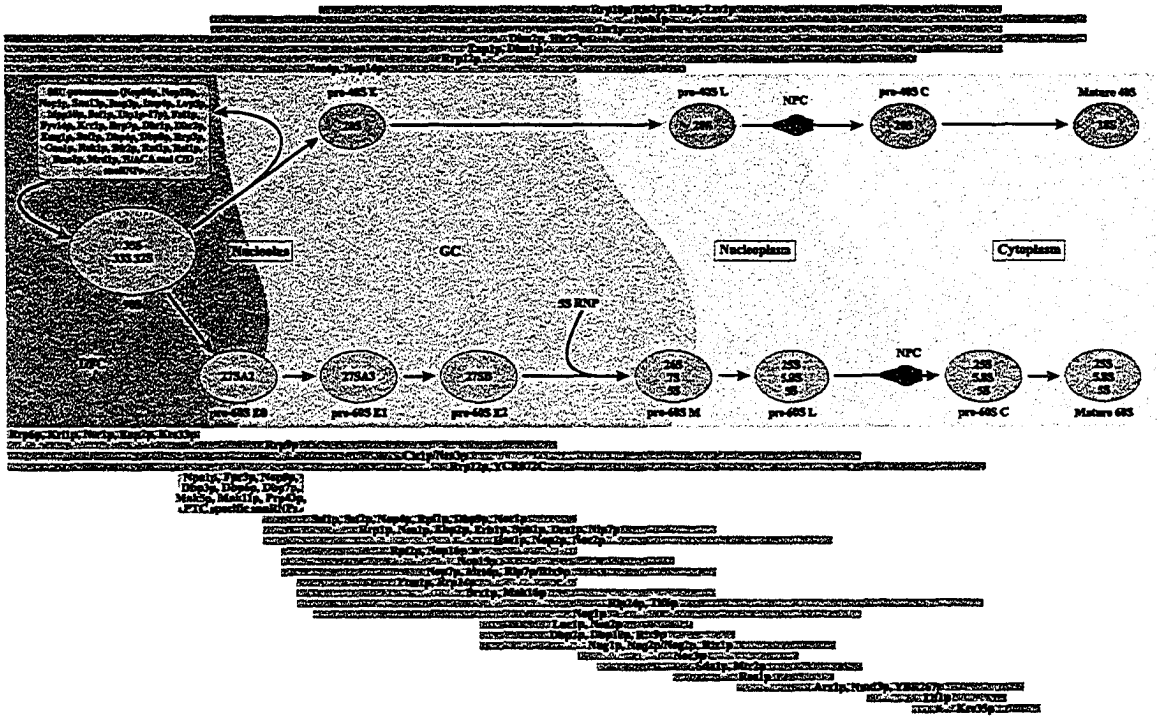

Figure 1.5. Chart of the assembly/disassembly of protein trans-acting factors with pre-ribosomal particles along the ribosome biogenesis pathway. The ribosome biogenesis pathway consists of multiple pre-ribosomal particles which differ in their protein composition and the level of rRNA processing. The upper panel indicates 40S subunit synthesis factors. The lower panel indicates 60S synthesis factors. The central panel depicts the pre-ribosomal particles and their predicted subcellular locations. The pre-rRNA intermediates and the mature rRNA species are indicated within the respective particles. The pre-rRNA is transcribed in the dense fibrillar component (DFC) of the nucleolus and the maturing pre-ribosomes move from the DFC to the more peripheral granular component (GC) of the nucleolus. The particles are then released into the nucleoplasm prior to transport through the nuclear pore complex (NPC) into the cytoplasm. The 90S particles largely contain factors required for 40S subunits synthesis. Most factors required for 60S synthesis associate with the pre-60S particles during their maturation following separation from the pre-40S pathway. As indicated by their names, the pre-ribosomes are classified as early (E), middle (M), late (L) and cytoplasmic (C). The beginning and the end of lines in the upper and lower panels indicate the points at which respective ribosome biogenesis factors are bound and released from the pre-ribosomal particles, as identified by proteomic analyses (reproduced from Dez and Tollervey, 2004).

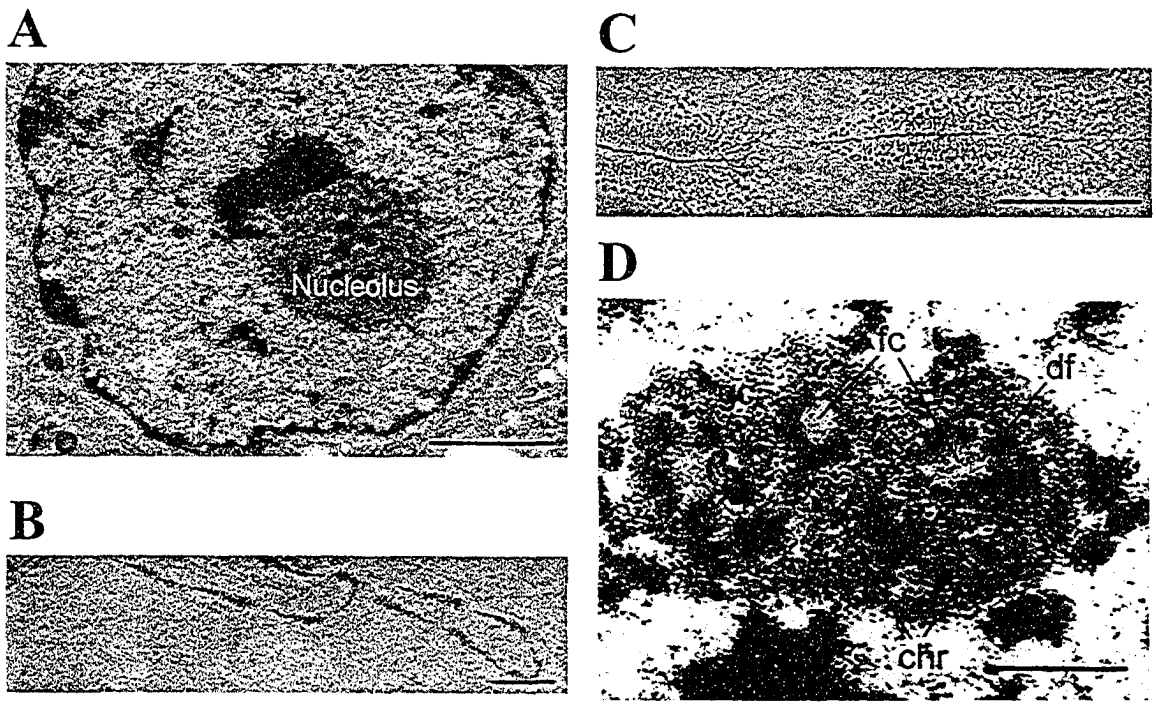

Figure 1.6. Ribosome biogenesis begins in a specialized nuclear compartment called the nucleolus. (A) An electron micrograph of a human fibroblast nucleolus (reproduced from http://www.biols.susx.ac.uk/home/Julian_Thorpe/TEM29.htm). Bar, 5 μm. (B) Electron micrograph of chromatin spread preparation from the *Triturus viridescens* oocyte (Miller spreads); transcription from tandemly arranged rRNA genes (reproduced from Alberts, 1994). Bar, 2 μm. (C) Rapid transcription of each rRNA gene by about 100 densely packed RNA polymerases makes transcription units appear shaped as Christmas trees. Terminal knobs, the large particles at the 5' end of each rRNA transcript, are believed to be the small subunit processome (see text for details) (reproduced from Alberts, 1994; Bernstein et al., 2004). Bar 1 μm. (D) An electron micrograph of a compact human lymphocyte nucleolus showing the condensed chromatin inclusions (chr), several fibrillar centres (fc), dense fibrillar component (df), and the granular component (gc) (see text for details) (reproduced from Schwarzacher and Mosgoeller, 2000). Bar, 0.4 μm.

on the 5' ends of nascent rRNAs (Fig. 1.6C) are believed to be the small subunit processomes (SSU), large ribonucleoprotein particles which consist of about 40 accessory proteins, including several 40S r-proteins, and the U3 snoRNA (Bernstein et al., 2004). The SSU is required for primary rRNA modifications and biogenesis of the 18S rRNA (Bernstein et al., 2004). The first step of rRNA processing includes

pseudouridilation (Ψ) and 2'-O-ribose methylation, at sites selected by snoRNAs (Fig. 1.7) (reviewed in Venema and Tollervey, 1999). Next, the 35S species is trimmed to 32S pre-rRNA via a cleavage at B_0 by the endonuclease Rnt1p, followed by three successive cleavages by unidentified enzymes at A_0, A_1 and A_2 (Fig. 1.7). The last step in this series, the endonucleolytic cleavage at the A_2 site, splits the 35S, generating the 20S and $27SA_2$ pre-rRNAs that will form the 40S and 60S subunits, respectively. The 20S pre-rRNA is exported to the cytoplasm, where it is cleaved at the 3' end, to generate the 18S rRNA.

The $27SA_2$ pre-rRNA follows a much more complicated processing pathway (Venema and Tollervey, 1999). Alternative pathways generate two distinct forms of the 27SB pre-rRNA, $27SB_S$ (short) and $27SB_L$ (long), from $27SA_2$. The pathway leading to the formation of $27SB_S$ is the major pathway. In it, $27SA_2$ pre-rRNA is cleaved at the A_3 site by a RNA-protein complex called RNase MRP. This is followed by digestion of the 5' end to the B_{1S} site by the exonucleases Rat1p and Xrn1p, with the principal activity provided by Rat1p. In the alternate minor pathway $27SA_2$ is processed at the B_{1L} site by an unknown mechanism to yield the $27SB_L$ intermediate.

The further processing of the $27SB_S$ and $27SB_L$ is believed to use an identical pathway giving rise to a common 25S rRNA, but two distinct forms of 5.8S rRNA species, $5.8S_S$ (short) and $5.8S_L$ (long), respectively. The major short form $5.8S_S$ is seven nucleotides shorter at the 5' end than the long form and represents about 80% of the total 5.8S rRNA. The precursors to both of the 5.8S forms are separated from the precursor 25S rRNA by cleavage at the C_2 site in ITS2 by an unknown nuclease. The subsequent 3' processing of 5.8S rRNA is a multistep reaction involving the exosome, a complex of

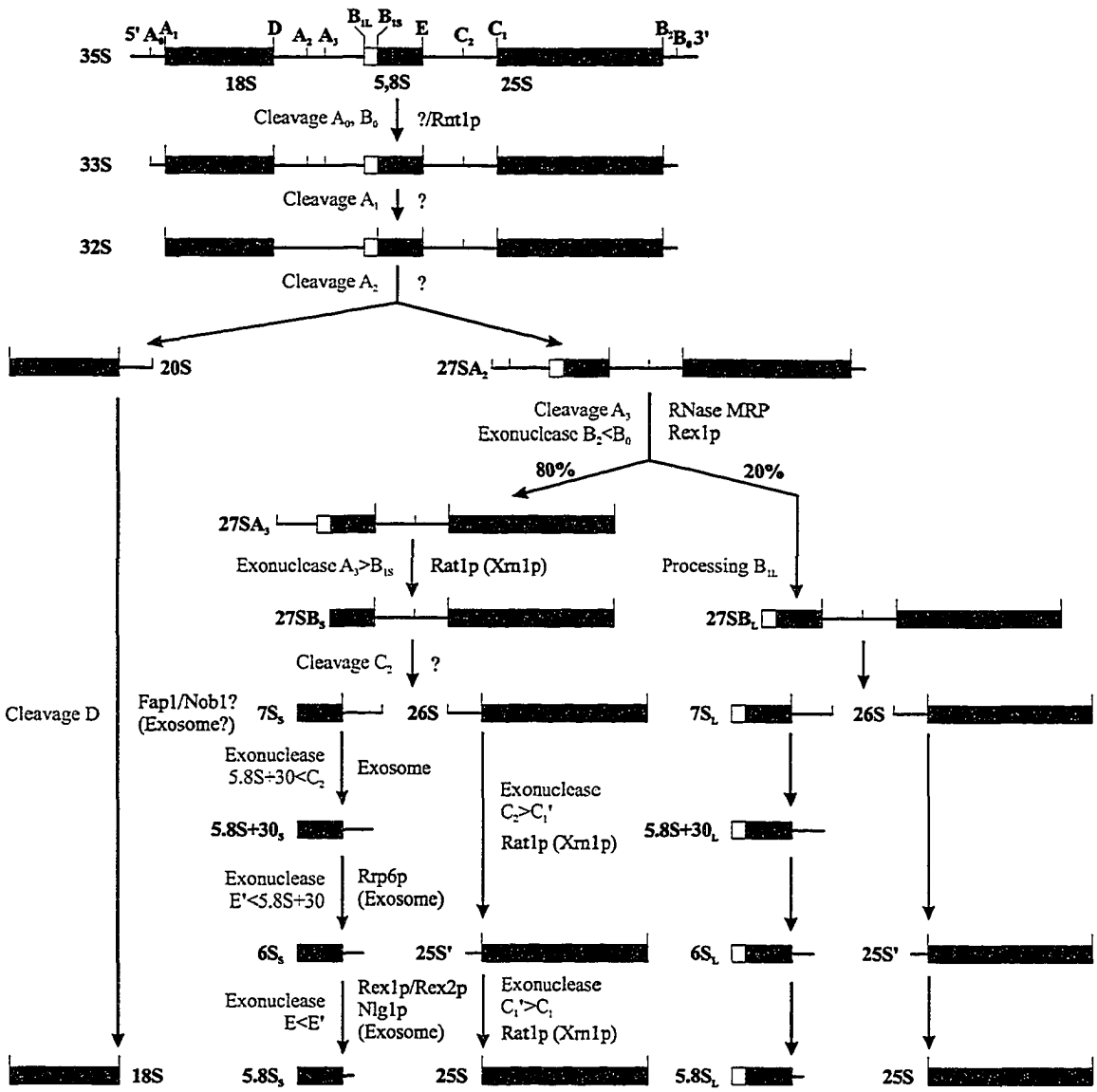

Figure 1.7. The rRNA processing map in *S. cerevisiae*. Top: The structure of pre-rRNA primary transcript with major restriction sites indicated. Bottom: *S. cerevisiae* pre-rRNA processing map with the types of cleavages and the names of cleaved products indicated in blue; known enzymes are indicated in red. See sections 1.3.1 and 1.3.3 for details (Fatica and Tollervey, 2002).

3'→5' exonucleases including Rex1p and Rex2p (reviewed in Fatica and Tollervey, 2002; Kressler et al., 1999b; Venema and Tollervey, 1999). The 3' end of the 25S rRNA is generated by exonuclease digestion by Rex1p from site B_0 to B_2. 5' processing of the 25S requires Rat1p and Xrn1p.

It should be noted that, although the rRNA processing has been the most intensively studied aspect of ribosome biogenesis during the past two decades, nucleases involved in several cleavage steps are yet to be identified and characterized.

1.4 Nucleocytoplasmic transport in ribosome biogenesis

1.4.1 Nucleolus

Ribosome synthesis largely takes place in a specialized nuclear compartment, the nucleolus, which is also the site of rRNA transcription and most ribosome maturation steps (Fig. 1.6A). The nucleolus, visible in the light microscope, was first described in the beginning of the 1800s as a distinct, dense, spherical structure. It contains large loops of DNA emanating from chromosomes, each of which contains a cluster of rRNA genes. Each of these gene clusters constitutes a nucleolar organizer region. Here the rRNA genes are transcribed at a rapid rate, and packaging of the 5' tail of 35S pre-rRNA begins while the transcription is still in progress (Fig. 1.6B, C). As visualized by electron microscopy, the nucleolus, unlike most cytoplasmic organelles, is not bounded by a membrane. It seems to be maintained as a distinct entity by the specific binding of unfinished ribosome precursors one to another, which form a large network. Three partialiy segregated regions can be distinguished: a fibrillar center, which contains DNA

that is not being actively transcribed; a dense fibrillar component, which contains rRNA molecules in the process of transcription; and a granular component, which contains maturing ribosomal precursor particles (Fig. 1.6D) (Dundr and Misteli, 2001).

When the cell approaches mitosis, ribosome biogenesis stops as the nucleolus shrinks, fragments, and disappears. This happens concomitantly with chromosome condensation and a pause in RNA synthesis. When rRNA synthesis restarts at the end of mitosis, tiny nucleoli reappear at the chromosomal loci of the rRNA genes. As the chromosomes decondense, these small nucleoli rapidly grow and fuse together reforming the nucleolus and reestablishing ribosome biogenesis.

1.4.2 Nucleocytoplasmic transport

The genetic material of eukaryotes is surrounded by a nuclear envelope, which acts as a barrier to the free exchange of proteins and nucleic acids between the nucleoplasm and cytoplasm. This barrier provides eukaryotes with several tremendous advantages over prokaryotes. It allows eukaryotes to temporally and spatially separate transcription and translation, which provides an opportunity to alter the RNA transcripts via RNA splicing, giving a single gene the potential to make several different proteins. In addition, spatial separation and selectivity of transport between the nucleoplasm and cytoplasm allows for a faster and more efficient transcriptional response to various environmental cues. This occurs through rapid import of pre-synthesized transcriptional regulators, stored in the cytoplasm. Because of the separation of the transcription and translation sites, nucleocytoplasmic transport is an important part of ribosome biogenesis in eukaryotes.

Transport between the nucleus and the cytoplasm is active, receptor-mediated and selective; it occurs by the concerted action of soluble transport factors and the nuclear pore complex (NPC). Proteins destined for the nucleus carry a nuclear localization signal (NLS) (Dingwall and Laskey, 1991), while substrates to be exported from the nucleus harbor nuclear export signals (NESs) (Fischer et al., 1996; Gerace, 1995). The signals are recognized by a structurally related family of proteins, termed karyopherins (abbreviated as Kaps, but also known as importins or exportins) (Gorlich and Kutay, 1999; Pemberton et al., 1998; Wozniak et al., 1998), that interact with the NPC and the small GTPase Ran to mediate translocation (Fig. 1.8A, B) (Rout et al., 2003). The NPC is a large, octagonally symmetric structure, and its overall architecture is highly conserved from yeast to metazoans (reviewed in Allen et al., 2001; Rout and Aitchison, 2001; Wente, 2000). The yeast NPC contains multiple copies of 30 protein components, termed nucleoporins or Nups (Fig 1.8C). Twelve of these Nups contain characteristic degenerate repeated peptide motifs (GLFG, FXFG, PSFG, or FG) and are thus collectively termed FG-Nups. These nucleoporins provide multiple docking sites for cargo-bearing transporters and are present throughout the NPC, extending from the cytoplasmic filaments to the nuclear basket (Rout et al., 2000). It remains a mystery how the interactions between karyopherins and the NPC mediate vectorial transport; however, karyopherins appear to derive directional cues from both the specific nucleoporins and Ran (reviewed in Harel and Forbes, 2004; Rout and Aitchison, 2001; Rout et al., 2003; Wente, 2000).

Figure 1.8. Nucleocytoplasmic transport. (A) The RanGTP–GDP gradient across the nuclear envelope (NE) provides directional cues and the energy for transport across the nuclear pore complex (NPC). RanGEF (guanosine nucleotide exchange factor) loads Ran with GTP, whereas RanGAP (GTPase activating protein) encourages Ran to hydrolyze GTP. RanGEF strongly binds to chromatin flagging the position of chromatin in the cell, while RanGAP is found largely in the cytoplasm. Thus, the nucleoplasmic Ran is bound mostly to GTP, whereas cytoplasmic Ran is mainly found in its GDP-bound form (Rout et al., 2003). (B) The nuclear transport cycle. In the cytoplasm an importing karyopherin (designated in blue) binds to its NLS-bearing cargo and facilitates its passage through the NPC. On the nucleoplasmic side, RanGTP binds to the karyopherin, causing a conformational change that releases the cargo. In the nucleoplasm, exporting karyopherins bound with RanGTP are loaded with NES-bearing cargos and traverse through the NPC to the cytoplasm. Once the exporting complexes are on the cytoplasmic side, RanGTP hydrolysis is stimulated by RanGAP and the conformational change releases the cargo. RanGDP is then recycled to the nucleoplasm by NTF2 and is reloaded with GTP to begin another cycle (Rout et al., 2003). (C) The nuclear pore complex is the stationary phase of nuclear transport. Each NPC is a large and complex protein structure embedded in the double membrane nuclear envelope, forming a pore for selective protein migration in and out of the nucleus. The NPC contains eight spokes, projecting radially from the wall of the pore membrane and surrounding a central tube called the central transporter. Each spoke is composed of numerous struts and attached to its neighbors by four coaxial rings: an outer spoke-ring in the lumen of the NE adjacent to the pore membrane, a nucleoplasmic ring, a cytoplasmic ring, and an inner spoke-ring surrounding the central transporter. A considerable portion of each spoke traverses the pore membrane and resides in the NE lumen. Together these structures comprise the central core. Peripheral elements project from this core toward the nucleoplasm and cytoplasm. These include: numerous proximal filaments on both faces of the cylindrical central core, whose presence is deduced from the large number of symmetrically disposed filamentous nucleoporins; eight cytoplasmic filaments, attached at the cytoplasmic ring; and nuclear filaments originating at the nuclear ring and conjoining distally to form the nuclear basket, which connects with elements of the nucleoskeleton (reproduced from Rout and Aitchison, 2001).

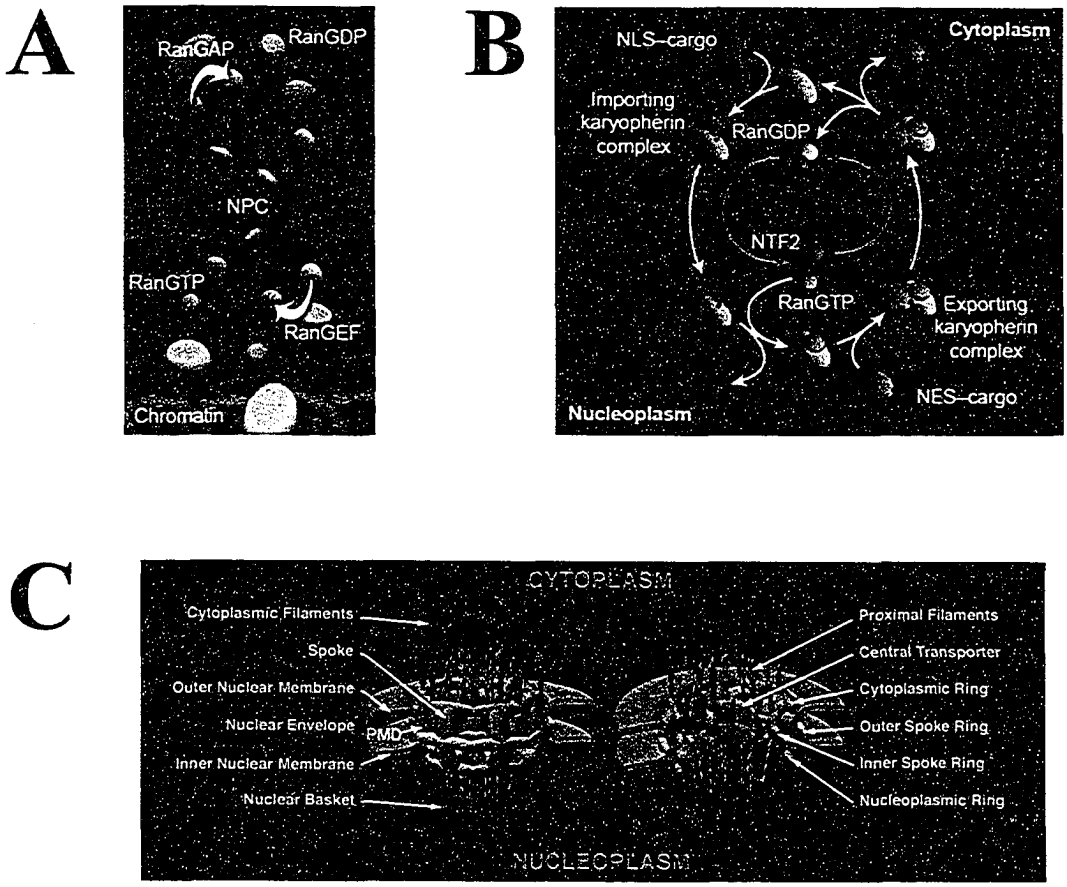

In a rapidly growing cell, the complex process of ribosome biogenesis accounts for a major portion of nucleocytoplasmic transport. Like all mRNAs, mRNAs encoding r-proteins are exported to the cytoplasm, where translation occurs. Once synthesized, r-proteins are imported into the nucleus and assembled into ribosomes in the nucleolus. Although small, r-proteins are imported into the nucleus using conventional nuclear localization signals, utilizing a set of specific karyopherins (Jakel et al., 2002; Rout et al., 1997; Schlenstedt et al., 1997). With approximately 150 pores per nucleus, each pore in a rapidly growing yeast cell must import nearly 1000 r-proteins per minute and simultaneously export about 25 assembled ribosomal subunits per minute (Warner, 1999).

1.4.3 Ribosomal protein import

In *S. cerevisiae*, it is thought that the import burden of this biogenesis program is accomplished largely by the karyopherin Kap123p. Kap123p binds to many different r-proteins including rpL25, rpS1a, rpL8a/b, rpL18a/b, rpL12a/b, rpL32, rpL11a/b, and rpL42a/b, and at least rpL25 requires Kap123p to be efficiently imported into the nucleus (Rout et al., 1997; Schlenstedt et al., 1997). However, deletion of *KAP123* from the yeast genome does not dramatically affect cell growth; thus, it is apparent that there are other ribosomal protein importers in yeast. One such candidate is Kap121p which, among the karyopherin family members, is most similar to Kap123p. Kap121p also binds to several r-proteins in the absence of Kap123p and, when overexpressed, suppresses the rpL25 import defect observed in *kap123Δ* strain (Rout et al., 1997).

All r-proteins are very basic and readily aggregate with cytoplasmic polyanions such as RNA (Warner, 1999). It was shown recently that in human cells the karyopherin Imp9 can effectively prevent such precipitation of r-proteins rpS7 and rpL18a by covering their basic domains (Jakel et al., 2002). It remains to be determined whether the karyopherin performs a chaperone role *per se*, or whether the effect is simply a result of karyopherin binding.

1.4.4 Subunit export

By comparison to import, ribosomal subunit export is less straightforward, because ribosomal subunit assembly and export appear to be temporally and physically coupled. Biogenesis involves a series of consecutive steps. Alteration of any particular step leads to a backlog in both the assembly and export processes. Ribosome subunit

export is also energy dependant, receptor-mediated and not competed by other major export pathways (tRNA, snRNA and mRNA) (Bataille et al., 1990; Mattaj and Englmeier, 1998). It requires a functional Ran cycle and a set of specific nucleoporins (Nup49p, Nic96p and Nsp1p) (Hurt et al., 1999; Stage-Zimmermann et al., 2000).

The exact export pathways and pre-export requirements have yet to be established. However, the available data allow one to predict several possibilities for how ribosomal transport might proceed. For instance pre-ribosomes might acquire active transport signals during assembly and maturation. Alternatively, retention signals on pre-ribosomes may need to be blocked to activate export. Moreover, there could be quality control systems along the entire path to check that the developing pre-ribosomes have correct rRNA processing/modification, ribosome maturation and the acquisition of transport competence. Many of the non-ribosomal proteins found associated with evolving nascent ribosomes could possibly be involved in these control systems (Tschochner and Hurt, 2003).

The analysis of intracellular transport of ribosomes has been greatly facilitated by the development of functional GFP-tagged ribosomal protein reporters, which when incorporated into ribosomal subunits can be detected by fluorescence microscopy in living cells. These in vivo transport/export assays employ both large-subunit (rpL25–GFP and rpL11–GFP) (Gadal et al., 2001b; Hurt et al., 1999; Stage-Zimmermann et al., 2000) and small-subunit reporters (rpS2–GFP) (Grandi et al., 2002; Milkereit et al., 2003). Accumulation of the ribosomal reporters in the nucleolus/nucleoplasm has been observed in several mutants defective in both 60S and 40S ribosome biogenesis (Gadal et al., 2001b; Grandi et al., 2002; Hurt et al., 1999). There are no export receptors/adapters

yet identified that would permit one to physically connect the 40S subunit to any particular karyopherin/export pathway.

1.4.5 60S export pathway

Unlike 40S, the elucidation of the 60S subunit export pathway has been developing rapidly (Fig. 1.9). One of the last r-proteins added to the pre-60S subunit before export from the nucleus is rpL10 which has been previously implicated in subunit joining (Dick et al., 1997; Eisinger et al., 1997; Kressler et al., 1999a). A conserved nonribosomal protein, Nmd3p, acts as an adapter between 60S subunits and the nuclear export pathway mediated by the karyopherin Crm1p (Gadal et al., 2001b; Ho et al., 2000a). Nmd3p directly interacts with rpL10 and when immunoprecipitated from yeast, it yields mature 60S subunits from the cytoplasmic pool (Ho et al., 2000b). Localization studies demonstrate that Nmd3p shuttles between the nucleus and cytoplasm (Gadal et al., 2001b; Ho et al., 2000a). A leptomycin B-sensitive *CRM1* mutant was employed to establish that two Nmd3p nuclear export sequences are specifically recognized by the karyopherin Crm1p, and exported from the nucleus along with the 60S pre-ribosomal subunit, tethered to the Nmd3p through rpL10 (Fig. 1.9) (Gadal et al., 2001b).

Recently, another member of the 60S export pathway has been found. A cytoplasmic GTPase Lsg1p is required along with rpL10, to release Nmd3p from the 60S pre-ribosomal subunit. Release allows Nmd3p to be recycled to the nucleus (Hedges et al., 2005).

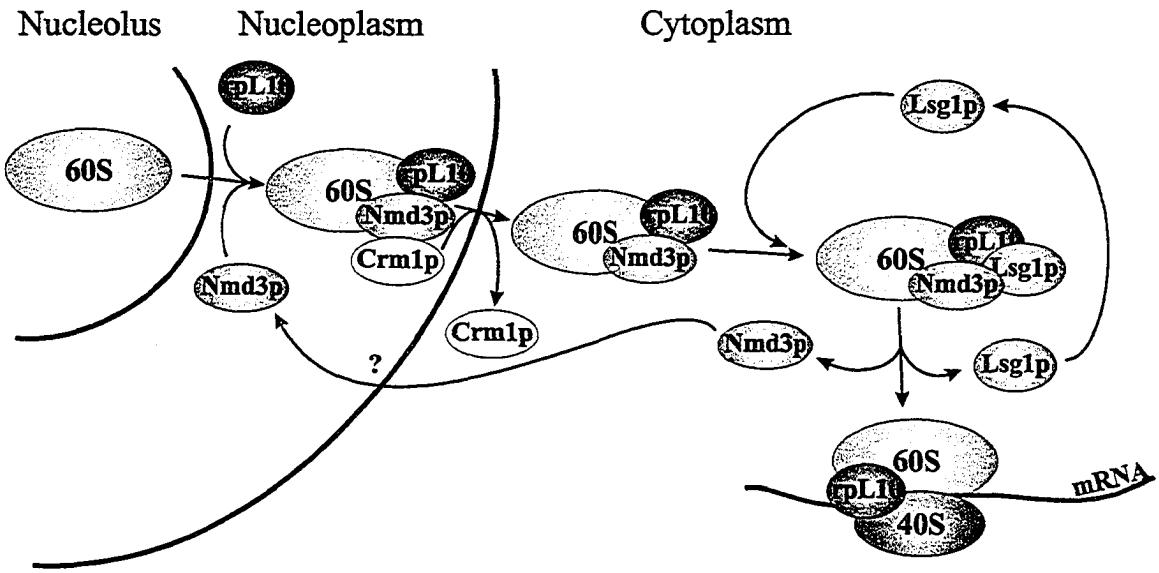

Figure 1.9. The model of 60S subunit export pathway in *S. cerevisiae*. The 60S subunit is exported from the nucleus by the karyopherin, Crm1p which binds the 60S subunit through the late assembling r-protein rpL10 and the ribosome biogenesis factor Nmd3p. See section 1.4.5 for details (adapted from Hedges et al., 2005).

1.5 Ribosome biogenesis regulation

Biogenesis and maintenance of the protein biosynthetic machinery is very costly to a cell. While the rRNA genes of *S. cerevisiae* make up only 10% of the entire genome, the transcription of rRNA by RNA polymerase I represents nearly 60% of the total transcription in a yeast cell (Warner, 1999). Thus, in order to survive, the cell must tightly regulate the synthesis of ribosomes. Indeed, the yeast cell responds to most environmental and intracellular insults by repression of ribosome synthesis. For example, in response to nutritional shortage, the cell ceases ribosome biogenesis when the culture is at 30% of its maximum density (Ju and Warner, 1994). Subsequently, the cell will start to degrade its ribosomes. In addition, cells in stationary phase have fewer than 25% of the ribosomes cells would have in logarithmic phase. Moreover, mild heat

shock or major defects in the secretory pathway lead to a rapid repression of the transcription of both rRNA and the r-protein genes. Excess unassembled r-proteins, left over after repression of ribosome biogenesis pathway, are rapidly degraded with a half-life of 0.5–3.0 minutes (Warner, 1999).

It is also apparent that ribosome biogenesis and cell cycle regulation are tightly connected. Two potent negative regulators of cell cycle Start, Sfp1p and Sch9p, were shown recently to be activators of the r-protein and ribosome biogenesis regulons (Jorgensen et al., 2002; 2004). A model has been proposed in which nutrient control of the critical cell-size threshold at Start is communicated by rates of ribosome production. According to this model the nuclear concentration of Sfp1p responds rapidly to nutrient and stress conditions and is regulated by the Ras/PKA and TOR signaling pathways. In turn, Sfp1p influences the nuclear localization of Fhl1p and Ifh1p, which bind to r-protein gene promoters (Jorgensen et al., 2004, reviewed in Jorgensen and Tyers, 2004).

Additional interactions that shed light on the feedback pathways between the ribosome biogenesis machinery and the cell cycle have been reported. For example, p53, a key cell cycle regulator of human cells, which is important for cell cycle arrest and activates apoptotic genes under stress conditions, is bound to the E3 ubiquitin ligase, Hdm2p, during normal growth conditions. Initial binding takes place in the nucleolus. The complex is then exported to the cytoplasm and targeted for degradation by the proteosome. Degradation by the proteosome maintains p53 at low levels preventing its activation (Sherr and Weber, 2000). R-proteins Rpl11p and Rpl23p have also been shown to bind Hdm2p, completely inhibiting its interaction with p53. Thus, an excess of Rpl11p and Rpl23p stabilizes and activates p53, causing p53-dependent cell cycle arrest

(Dai et al., 2004; Jin et al., 2004; Lohrum et al., 2003). These data suggest that the change of levels of these two r-proteins triggers the response to changing growth conditions in mice and humans.

A role in mitotic exit was found recently for one more component of the yeast ribosome biogenesis machinery, providing yet another link to the cell cycle. The endoribonuclease, RNase MRP, which catalyses pre-rRNA cleavage at the A_3 site, also cleaves *CBL2* mRNA which, in turn, suppresses expression of the major B-type cyclin required for the G2/M transition (Gill et al., 2004).

Interestingly, ribosome biogenesis factors have recently been reported to be linked to DNA replication. For instance, Noc3p depletion inhibits the initiation of DNA replication (Zhang et al., 2002), whereas cells depleted of Yph1p are defective in S phase progression following the initiation of replication (Du and Stillman, 2002). However, their precise roles and molecular mechanisms of action remain unclear (Dez and Tollervey, 2004).

1.6 Valuable experimental approaches to study ribosome biogenesis

From its humble beginnings to modern days, studies of ribosomal function, biogenesis and assembly guide biological science much like Ariadne's thread. In this section I have outlined several major experimental approaches that contributed greatly to our understanding of ribosomal structure and biogenesis.

1.6.1 Sucrose gradient fractionation and rRNA analysis

The earliest breakthroughs in the studies of ribosomal biogenesis were achieved soon after development of sucrose gradient sedimentation analysis in the early 1970s (Udem and Warner, 1972; Warner et al., 1972). All major ribosome precursor particles and associated rRNAs were detected at that time. During the next two decades researchers focused on the most obvious aspect of ribosome biogenesis – the rRNA processing pathway. The wide development of isotope labeling techniques made possible the rapid and precise deciphering of the rRNA processing pathway and stimulated the search for rRNA processing enzymes. Three major methods developed at this point that were essential for the characterization of novel ribosome biogenesis proteins were the Northern blot, primer extension analysis, and metabolic labeling (pulse-chase) analysis. These methods allowed one to precisely locate a step in a pathway at which a protein in question took part, and simultaneously to predict the protein's normal biochemical function. This was particularly valuable when coupled with molecular genetics as specific gene defects were used to provide "snapshots" of otherwise dynamic and undetectable processes. Because mutations affecting ribosome biosynthesis are often lethal, conditional mutants were also generated.

Most of the ribosome biogenesis factors detected during the 1970s and 1980s were enzymes directly involved in rRNA processing and modification. These include the rRNA-modifying enzymes (pseudouridine synthases, 2'-O-methyl transferases), RNA helicases, exo- and endonucleases. Another class of protein *trans*-acting factors identified in 1980s and early 1990s, included proteins found associated with small nucleolar RNAs (snoRNAs). These nucleolar ribonucleoprotein particles turned out to be

also involved in ribosomal biogenesis (reviewed in Gerbi et al., 2001). Since snoRNPs have low complexity, they proved to be relatively easy to analyze (Henras et al., 2004).

1.6.2 Fluorescent microscopy

Although green fluorescent protein (GFP) was first discovered in 1960s (Shimomura, 2005; Shimomura et al., 1962), it did not become commercially available and widely used by the scientific community until the 1990s. The impact of this unusual brightly fluorescent protein capable of being expressed and monitored in live, physiologically normal cells has influenced the field enormously. GFP and related fluorescent proteins have been a very valuable tool for identifying nucleolar proteins and ribosome assembly factors in yeast.

Tagging ribosomal reporter-proteins and proteins involved in ribosome biogenesis has significantly improved our knowledge of the spatial organization of the ribosome biogenesis pathway and has enabled the use of multiple screens designed to search for factors involved in the export of maturing pre-ribosomal particles from the nucleus.

1.6.3 High throughput protein analysis

Recent advances in mass spectrometry and the development of sophisticated multi-step affinity purification techniques, in which a set of pre-ribosomal particles containing associated proteins and pre-rRNAs co-purifies with a protein of interest, have significantly accelerated the search for new ribosome biogenesis factors (Bassler et al., 2001; Grandi et al., 2002; Harnpicharnchai et al., 2001; Nissan et al., 2002; Saveanu et al., 2003; Schafer et al., 2003). One such co-purification procedure can identify some 50

to 500 proteins (Fromont-Racine et al., 2003). These can be tentatively assigned to various stages of the ribosome biogenesis pathway based on their rRNA processing profile, localization, or their association with co-purifying proteins and rRNAs (See Fig. 1.6). Unfortunately, deciphering the huge volumes of information acquired using proteomic-based methods and distinguishing protein contaminants have proven more difficult then initially predicted. Nevertheless, this approach has led to great advances in our knowledge of ribosome biogenesis, doubling the number of known biogenesis factors in five years.

1.7 Focus of this thesis

Due primarily to the ease with which it can be genetically manipulated, the budding yeast *S. cerevisiae* has provided many fundamental insights into eukaryotic ribosome biogenesis over the last three decades. Studies done in this model organism using new molecular, biochemical and genetic approaches, including proteomic/mass spectrometry techniques, enabled the recent rapid identification of ribosome biogenesis factors. Insights gained from the study of ribosome biogenesis in yeast are easily applicable to metazoans and mammals, including humans.

This thesis focuses on the identification and characterization of two novel proteins involved in ribosome biogenesis in *S. cerevisiae*. We show that two previously uncharacterized proteins, Rai1p and Nop53p, are involved in 60S subunit biogenesis, and localize predominantly to the nucleus and the nucleolus, respectively. The product of *RAI1*, (*YGL246c*) is a ribosome biogenesis factor required for efficient rRNA processing and mutants in this gene are deficient in 60S subunit export from the nucleus in a

KAP123 deletion background. The protein encoded by *YPL146c*, which we name *NOP53*, is essential for early stages of 60S biogenesis and 27S rRNA processing.

Chapter 2

Materials and Methods

2.1 Materials

2.1.1 List of chemicals and reagents

Acetone	Acros
30% acrylamide:N,N'-methylene-bis-acrylamide (37.5:1)	Bio-Rad
30% acrylamide:N,N'-methylene-bis-acrylamide (19:1)	Bio-Rad
Adenine sulfate	Acros
Agar	Difco
Agarose, electrophoresis grade	Gibco/BRL
Agarose, GTG	Invitrogen
Albumin, bovine serum (BSA)	Roche
L-amino acids	Aldrich, Acros, Fisher
Ammonium acetate	Fisher
Ammonium persulfate	BDH, Amresco
Ammonium sulfate	Fisher
Ampicillin	Sigma
Aprotinin	Roche, Sigma
Bradford protein assay dye reagent	Bio-Rad
Bromphenol blue	Sigma, BDH
Chloroform	Fisher
CSM (complete synthetic medium)	Q-BIO Gene
Coomassie Brilliant Blue R-250	ICN
Deoxynucleotide triphosphates (dNTPs)	Fermentas
Diethylpirocarbonate (DEPC)	ICN
Dimethyl sulfoxide (DMSO)	Fisher
Dithiothreitol (DTT)	ICN
DNA sheared salmon sperm	Eppendorf
DNase I	Sigma, Roche
Ethylenediaminetetraacetic acid (EDTA)	Fisher, Sigma
Ficoll 400	Amersham
Formamide	Sigma, BDH
Formalin (formaldehyde, 37% v/v)	Fisher
5'-Fluoroorotic acid	Zymo Research
D-Galactose	Acros
Glass beads, acid washed	Sigma
Gluthatione, reduced	Sigma
Gluthatione-sepharose	Amersham
Glycerol	BDH
4-[2-hydroxyethyl]-1-piperazineethanesulphonic acid (HEPES)	Fisher, Roche
Hydrogen peroxide solution, 30% (w/v)	Sigma
Iso-amyl alcohol	Fisher
Isopropyl β-D-thiogalactopyranoside (IPTG)	Vector Biosystems
Leupeptin	Roche
Lithium acetate	Acros
Magnesium chloride	Fisher
β-mercaptoethanol	ICN, BDH

Methanol	Fisher
N,N'-methylenebisacrylamide	Bio-Rad
3-[N-morpholino]propanesulphonic acid (MOPS)	Acros, Sigma
Nonidet P-40 (NP-40)	USB, BDH
Pepstatin A	Fisher, Sigma
Peptone	Difco
Phenol, buffer saturated	Acros, Gibco/BRL
Phenylmetylsulfonylfluoride (PMSF)	Roche
Poly L-lysine (solution of 1 mg/mL)	Sigma
Polyvinylpyrollidone (PVP)	Sigma
Ponceau S	Sigma
Protein A-Sepharose	Amersham
D-Raffinose	Sigma
Sodium dodecyl sulphate (SDS)	Fisher, Sigma
Sodium sulphite	Sigma
Sodium citrate	Fisher
D-Sorbitol	Acros, BDH
Sucrose	Fisher
N,N,N',N'-tetramethylethylethylenediamine (TEMED)	Promega, Gibco/BRL
Trichloracetic acid (TCA)	Fisher, BDH
Tris[hydroxymethyl]aminomethane (Tris)	Roche, Fisher
Triton X-100	Sigma, MP Biomedicals
Tryptone	Difco
Polyoxyethylenesorbitan monolaureate (Tween 20)	Sigma, Fisher
Polyoxyethylenesorbitan monopalmitate (Tween 40)	Sigma, Fisher
Urea	Fisher
5-bromo-4-chloro-3-indolyl-β-D-galactoside (X-gal)	Vector Biosystems
Yeast extract	Difco
Yeast Nitrogen Base without amino acids and ammonium sulphate (YNB)	Difco

2.1.2 List of enzymes

CIAP (calf intestinal alkaline phosphatase)	NEB, Fermentas
DNA ligase, T4	Gibco/BRL, NEB, Roche
DNA polymerase, T4	NEB, BioLabs
Expand DNA polymerase (enzyme blend)	Roche, Fermentas
Klenow fragment of DNA polymerase I, *Escherichia coli*	NEB, Fermentas
Polynucleotide kinase, T4	NEB, Fermentas
RNase A (ribonuclease A), bovine pancreas	Sigma, Roche
Taq DNA polymerase, *Thermus aquaticus*	Roche, Fermentas
Trypsin, mass spectrometry grade	Roche, Promega
Zymolyase 100T	ICN
Zymolyase 20T	ICN

2.1.3 Molecular size standards

1 kb DNA ladder (75-12,216 bp)	Gibco/BRL, Fermentas
Dephosphorylated ΦX174 *Hinf* I DNA markers	Promega
SDS-PAGE Standards, Broad Range (6.5-200 kD)	Bio-Rad

2.1.4 Multicomponent systems

BigDye Terminator Cycle Sequencing Ready Reaction Kit	ABI Prism
Bradford Protein Assay Kit	Bio-Rad
QIAprep MiniPrep Kit	Qiagen
QIAquick Gel Extraction Kit	Qiagen
QIAquick PCR Purification Kit	Qiagen
Promega AMV Reverse Transcriptase Primer Extension System	Promega
Re-Blot Western Blot Recycling Kit	Chemicon

2.1.5 Radiochemicals and detection kits

[^{3}H] uracil	Perkin Elmer
[γ-^{32}P]ATP (3,000 Ci/mmol)	Perkin Elmer
[γ-^{32}P]ATP (6,000 Ci/mmol)	Perkin Elmer
ECL Detection Kit for Immunoblotting	Amersham
Nitrocellulose Hybond ECL	Amersham
Nylon Hybond-XL membrane	Amersham
Immuno-Blot PVDF membrane	Bio-Rad
SuperSignal West Pico Chemiluminescent Substrate Kit for Immunoblotting	Pierce
X-ray film (X-Omat AR and X-Omat X-K1)	Eastman Kodak Company

2.1.6 Plasmids

Plasmids used in this study are listed in the Table 2.1. See section 2.6 for details on construction of the protein expression plasmids.

Source plasmids

pRS314 (CEN/ARS, Amp^{r}, *TRP1*, *lacZp*)	(Sikorski and Hieter, 1989)
pRS316 (CEN/ARS, Amp^{r}, *URA3*, *lacZp*)	(Sikorski and Hieter, 1989)
pRS317 (CEN/ARS, Amp^{r}, *LYS2*, *lacZp*)	(Sikorski and Hieter, 1989)
pRS425 (REP3/FRT, Amp^{r}, *LEU2*, *lacZp*)	(Sikorski and Hieter, 1989)
pYX242 (CEN, Amp^{r}, *GFP*, *LEU2*, *TP1p*)	Novagen, Madison, WI
pKW431 (CEN, Amp^{r}, *URA3*, 2 x *GFP*)	(Stade et al., 1997)
pYEUra3 (CEN/ARS, Amp^{r}, *URA3*, *GALp*)	Clonetech, Palo Alto, CA

Table 2.1 Plasmids used in this study

Name	Genes, auxotrophic markers and *cys*-elements	Derivation
pRS316-KAP123	CEN/ARS, Amp^r, *URA3*, *lacZp*, *KAP123*	pRS316
pRS317-KAP123	CEN/ARS, Amp^r, *LYS2*, *lacZp*, *KAP123*	pRS317
pJA8	CEN/ARS, Amp^r, *URA3*, *lacZp*, *ADE3*, *KAP123*	pRS316-KAP123
rpL2-GFP	CEN, Amp^r, *GFP*, *LEU2*, *TP1p*, *RPL2*	pYX242
rpL3-GFP	CEN, Amp^r, *GFP*, *LEU2*, *TP1p*, *RPL3*	pYX242
rpL25-GFP	CEN, Amp^r, *GFP*, *LEU2*, *TP1p*, *RPL25*	pYX242
Nop1p-GFP	CEN, Amp^r, *GFP*, *LEU2*, *TP1p*, *NOP1*	pYX242
pYGL246C	CEN/ARS, Amp^r, *TRP1*, *lacZp*, *YGL246c*	pRS314
pYGL247W	CEN/ARS, Amp^r, *TRP1*, *lacZp*, *YGL247w*	pRS314
Pde1p-pRS314	CEN/ARS, Amp^r, *TRP1*, *lacZp*, *PDE1*	pRS314
Kap95p-pRS314	CEN/ARS, Amp^r, *TRP1*, *lacZp*, *KAP95*	pRS314
Kap121p-pRS314	CEN/ARS, Amp^r, *TRP1*, *lacZp*, *KAP121*	pRS314
Sxm1p-pRS314	CEN/ARS, Amp^r, *TRP1*, *lacZp*, *SXM1*	pRS314
Nmd5p-pRS314	CEN/ARS, Amp^r, *TRP1*, *lacZp*, *NMD5*	pRS314
Rai1p-GFP	CEN, Amp^r, *URA3*, 2 x *GFP*, *ADHp*, *RAI1*	pKW431 (Stade et al., 1997)
pNmd3p	REP3/FRT, Amp^r, *LEU2*, *lacZp*, *NMD3*	pRS425
pNmd3Δ100	REP3/FRT, Amp^r, *LEU2*, *lacZp*, *NMD3Δ100*	pRS425
prpl10	REP3/FRT, Amp^r, *LEU2*, *lacZp*, *RPL10*	pRS425
pKap121p	REP3/FRT, Amp^r, *LEU2*, *lacZp*, *KAP121*	pRS425
pNmd5p	REP3/FRT, Amp^r, *LEU2*, *lacZp*, *NMD5*	pRS425
[a]Rat1p-GFP	CEN, Amp^r, *URA3*, *GFP*, *RAT1*	pAJ226 (Johnson, 1997)
[a]Nmd3p-NLS-GFP	CEN, Amp^r, *URA3*, *GFP*, NLS^{NMD3}	Nmd3p-NLS-GFP (Ho et al., 2000b)
[a]Nmd3p-NLS/NES-GFP	CEN, Amp^r, *URA3*, *GFP*, NLS^{NMD3}/NES^{NMD3}	Nmd3p-NLS/NES-GFP (Ho et al., 2000b)
pBH1	CEN/ARS, Amp^r, *URA3*, *lacZp*, *NOP53*	pRS316
pBH2	CEN/ARS, Amp^r, *URA3*, *lacZp*, *NOP53-ΔC*	pRS316
pGAL-NOP53	CEN/ARS, Amp^r, *URA3*, *GALp*, *NOP53*	pYEUra3
[b]Nop1p-RFP	CEN, Amp^r, *RFP*, *TRP1*, *NOP1*	pRS314-DsRed-NOP1 (Gadal et al., 2001b)

[a]Kindly provided by A.W. Johnson, University of Texas at Austin, Austin, TX
[b]Kindly provided by O. Gadal, Institute Pasteur, Paris, France

2.1.7 Antibodies

The antibodies used in this study are described in Table 2.2.

Table 2.2 Antibodies used in this study

Primary Antibodies			
Antibody name	Type	Dilution	Description
Anti-mouse IgG	Rb-pc	1:10000	[a]Cappel, Organon Teknika Corp.
Anti-Tcm1p (rpL3)	m-mc	1:1000	[b](Elion et al., 1995)
Anti-GFP	Rb-pc	1:5000	[c](Seedorf et al., 1999)
Anti-Nop1p (D77)	m-mc	1:100	[d](Aris and Blobel, 1988)

Secondary Antibodies			
Antibody name		Dilution	Description
HRP conjugated anti-mouse Ig	dk	1:10000	[e]Amersham Biosciences
HRP conjugated anti-rabbit Ig	dk	1:10000	[e]Amersham Biosciences

rb, rabbit; m, mouse; dk, donkey; pc, polyclonal; mc, monoclonal.
[a]Cappel, Organon Teknika Corp., (West Chester, PA).
[b]Kindly provided by J.L. Woolford (Carnegie Mellon University, Pittsburgh, PA).
[c]Kindly provided by M. Rout (The Rockefeller University, New York, NY).
[d]Kindly provided by G. Blobel (The Rockefeller University, New York, NY).
[e]Amersham Biosciences (Piscataway, NJ).

2.1.8 Oligonucleotides

Oligonucleotides were purchased from IDT (International DNA Technologies, Coralville, IA), Gibco/BRL (Life Technologies Inc., Burlington, ON) or synthesized on an Oligo 1000M DNA Synthesizer (Beckman Coulter, Fullerton, CA).

Table 2.3 Oligonucleotides used in this study

Name	[a]Sequence	Application
5'ETS-A0	GGT CTC TCT GCT GCC GG	Northern blot analysis
5'18S	CAT GGC TTA ATC TTT GAG AC	Northern blot and primer extension assay
D-A_2	GCT CTC ATG CTC TTG CCA	Northern blot analysis
[b]A2-A3	TGT TAC CTC TGG GCC C	Northern blot analysis
[c]A_2-A_3	ATG AAA ACT CCA CAG TG	Northern blot analysis
A_3-B_{1L}	CCA GTT ACG AAA ATT CTT G	Northern blot analysis
5'5.8S	CGC TGC GTT CTT CAT CGA TG	Northern blot and primer extension assay
E-C_2	GGC CAG CAA TTT CAA GTT A	Northern blot analysis
C_2-C_1	GTT CGC CTA GAC GCT CTC	Northern blot analysis
5'25S	CTC CGC TTA TTG ATA TGC	Northern blot and primer extension assay
YPL146C-5'	CGG CTC GAG CTT CCT TTA ATT ATT GAT	pBH1, pBH2 (5' Xho1)
YPL146C-3'	GCC GAG CTC GCC AAC ACA AAT ATG AAC	pBH1 (3' Sac1)
YPL146C aa401-3'	CGG GAG CTC TTA TTC GTC AGA AAA TTT AAT	pBH2 (3' Sac1)
YPL146C-5'	AAA GGA TCC ATG GCT CCA ACT AAT CTA ACC AAG AAA CCA	pGAL-NOP53 (5' BamHI)
YPL146C-3'	AAA CAG CTG GAT AAA CTT CAG GAA TAC ACA GGT GAA AAG	pGAL-NOP53 (3' SalI)
prpL10-5'	AAA CTG CAG CTC TTC ACC GAA TAT CTA CCC	prpL10 (5' PstI)
prpL10-3'	AAA CTG CAG TCA CTA CCC AAC ATG CTG AAC	prpL10 (3' PstI)
pNmd5p-5'	GC TCT AGA CTC GAG ACC ATG GAT ATT ACA GAA TTG TT	pNmd5p construction
pNmd5p-3'	CCG CTC GAG TTA TCT AGA GGC ATT CAT AAT TCC CAT G	pNmd5p construction
RAI1-5'	CCG GAA TTC AAG CTT ATG GGT GTT AGT GCA AAT TTG	*RAI1* deletion
RAI1-3'	CGG GAA TTC TTT CAA AGA TTT TCT CCA CTC	*RAI1* deletion
NOP53-5'	CGT TAA TGA ATC ATT TAT TTA AAA ATG GCT CCA ACT AAT CTA ACC AAG AAA CCA TCT CAA TAA CCT GAC ATA ATC CAA TTC ATC	*NOP53* deletion
NOP53-3'	CTA GAG ATA TCG ACA TGG GAA TGC CCT CTC AAA CTA GAA AAG GGC AGA GAA CGA AAA GAA GCT GAC GGT ATC GAT AAG CTT	*NOP53* deletion

Name	[a]Sequence	Application
SXM1-5'	AGA GAT TCC TTG CAG GTA ATT CTG GAA TTT GTT TCT CAA CAC GGT GAA GCT CAA AAA CTT AAT	*SXM1* deletion
SXM1-3'	AAA AAG AAA CAA CTT TTA TAT TTG TAT ATT AGA GTA TAA ACT GTC GAC GGT ATC GAT AAG CTT	*SXM1* deletion
NMD5-5'	ACC CCG GCT GAT CAA GAA CTA TTC ATG GGA ATT ATG AAT GCC GGT GAA GCT CAA AAA CTT AAT	*NMD5* deletion
NMD5-3'	AGG CAA CAA ACT TTG AGC ATA ATA TCC TCT CTC TTC TAT CTA GTC GAC GGT ATC GAT AAG CTT	*NMD5* deletion
KAP123-5'	GCG CTT GAG TTG CTT CAA GTG CAT G	*KAP123-W303* deletion
KAP123-3'	ACA AGA TGA CCT GAA CTT GCG CGT A	*KAP123-W303* deletion
RAI1-A-5'	TTG ATT GAT GGA GAA CAT ATA TTA TCG AAC GGG TTT AAG GAG TGG AGA AAA TCT TTG AAA ATT GAA GGT AGA GGT GAA GCT	RAI1-A construction
RAI1-A-3'	TAG GTA TAA TAT TTG TTA CCA ATA CGA GTT TCG GAT CAT ACA GGG TTT ATC TCA ATA ATA GTC GAC GGT ATC GAT AAG CTT	RAI1-A construction

[a]Sequences are written 5' to 3'.
[b]This oligonucleotide was used in the Rai1p study.
[c]This oligonucleotide was used in the Nop53p study.

2.1.9 Standard buffers and solutions

Commonly used solutions are described below.

Table 2.4 Standard buffers and solutions

Solution	Composition	Reference
50 x Denhardt's solution	10 mg/mL BSA (bovine serum albumine fraction V), 10mg/mL PVP (polyvinylpyrollidone) and 10 mg/mL Ficoll (made up in DEPC-treated water) (maker)	(Maniatis et al., 1982)
10 x MOPS	200 mM 3-[N-morpholino]-propanesulfonic acid, 50 mM NaAc, 10 mM EDTA; (pH 7.0, adjusted with NaOH)	Qiagen Oligotex Handbook
100 x Solution P	0.4 mg/mL Pepstatin A and 18 mg/mL PMSF	This study
20 x SSC	3 M NaCl, 0.3 M trisodium citrate (pH 7.0) (made up in DEPC-treated water)	(Maniatis et al., 1982)
TE	10 mM Tris-HCl (pH 7.0-8.0, as appropriate), 1 mM EDTA	(Maniatis et al., 1982)
10 x TBE	0.89 M Tris-borate, 0.89 M boric acid, 0.02 M EDTA	(Maniatis et al., 1982)
TBST	(20 mM Tris-HCl (pH 7.5), 150 mM NaCl, 0.05% (w/v) Tween 20)	(Ausubel, 1994)

2.2 Microorganisms and culture conditions

2.2.1 Yeast strains and culture conditions

The *S. cerevisiae* strains used in this study were derivatives of the diploid DF5 strain, unless otherwise specified, and are listed in Table 2.5. Yeast culture media are described in Table 2.6. Liquid cultures were grown in glass tubes or flasks at 30°C with constant agitation. Construction of the *S. cerevisiae* mutant strains is described in the Section 2.2.4. All yeast genetic manipulations were performed according to established procedures (Guthrie and Fink, 1991). Gene knockout marker modules were switched as required using "marker swap" plasmids, as described previously (Cross, 1997).

Table 2.5 ***S. cerevisiae*** **strains**

Strain	Genotype	Derivation
DF5	MAT*a*/MATα *ura3-52/ura3-52 his3Δ200/ his3Δ200 trp1-1/trp1-1 leu2-3,112/leu2-3,112 lys2-801/lys2-801*	
W303	MAT*a*/MATα *ade2-1/ ade2-1 ura3-1/ ura3-1 his3-11,15/ his3-11,15 trp1-1/ trp1-1 leu2-3,112/ leu2-3,112 can1-100/ can1-100*	
kap123Δ	MAT*a ura3-52 his3Δ200 trp1-1 leu2-3,112 lys2-801 kap123::ura3::HIS3*	Marker switch of *kap123::URA3* (Rout et al., 1997)
123SLS[a]	MAT*a ura3-52 his3Δ200 trp1-1 leu2-3,112 lys2-801 ade2 ade3 kap123::ura3::HIS3* +pJA8	This study. Segregant of *kap123Δ* x CH1462 (Kranz and Holm, 1990)
sf17[a]	*ura3-52 his3Δ200 trp1-1 leu2-3,112 lys2-801 ade2 ade3 kap123::ura3::HIS3 rai1-1*	This study, see text
sfA7[a]	*ura3-52 his3Δ200 trp1-1 leu2-3,112 lys2-801 ade2 ade3 kap123::ura3::HIS3 sxm1-1*	This study, see text
sf5[a]	*ura3-52 his3Δ200 trp1-1 leu2-3,112 lys2-801 ade2 ade3 kap123::ura3::HIS3 nmd5-1*	This study, see text
sf21[a]	*ura3-52 his3Δ200 trp1-1 leu2-3,112 lys2-801 ade2 ade3 kap123::ura3::HIS3 kap121-1*	This study, see text
sfA9[a]	*ura3-52 his3Δ200 trp1-1 leu2-3,112 lys2-801 ade2 ade3 kap123::ura3::HIS3 sxm1-2*	This study, see text
KAP123-A[a]	MAT*a ura3-52 his3Δ200 trp1-1 leu2-3,112 lys2-801 KAP123-pA-HIS3-URA3*	See (Rout et al., 1997)
RAI1-A[b]	MAT*a ura3-52 his3Δ200 trp1-1 leu2-3,112 lys2-801 RAI1-pA-spHIS5*	This study, see text
rai1Δ[a]	MAT*a ura3-52 his3Δ200 trp1-1 leu2-3,112 lys2-801 rai1::HIS3*	This study, see text

Strain	Genotype	Derivation
kap123Δ-w303	MAT**a** *ade2-1 ura3-1 his3-11,15 trp1-1 leu2-3,112 can1-100 kap123::kanMX*	This study, see text (W303 derivative)
kap121-34[c]	MAT**a** *ura3-52 his3Δ200 trp1-1 leu2-3,112 lys2-801 kap121::ura::HIS3* +p*kap121-34*	See (Leslie et al., 2002)
sxm1Δ	MAT**a** *ura3-52 his3Δ200 trp1-1 leu2-3,112 lys2-801 sxm1::his3::TRP1*	This study, see text
nmd5Δ[b]	MAT**α** *ura3-52 his3Δ200 trp1-1 leu2-3,112 lys2-801 nmd5::HIS3*	This study, see text
kap95-14[a]	*ura3-52 his3Δ200 trp1-1 leu2-3,112 lys2-801 kap95::HIS3* +p*kap95-14*	See (Leslie et al., 2002)
rai1Δ/sxm1Δ	*ura3-52 his3Δ200 trp1-1 leu2-3,112 lys2-801 rai1::HIS3 sxm1::his3::TRP1*	This study, segregant of sporulated *rai1Δ/sxm1Δ*
rai1Δ/nmd5Δ	*ura3-52 his3Δ200 trp1-1 leu2-3,112 lys2-801 rai1::HIS3 nmd5::his3::TRP1*	This study, segregant of sporulated *rai1Δ/nmd5Δ*
rai1Δ/kap121ts	*ura3-52 his3Δ200 trp1-1 leu2-3,112 lys2-801 rai1::HIS3 kap121::ura3::trp1::LEU2* +p*kap121-34*	This study, see text
rai1Δ/kap123Δ	*ura3-52 his3Δ200 trp1-1 leu2-3,112 lys2-801 rai1::HIS3 kap123::ura3:: TRP1*	This study, see text
rat1-1[d]	MAT**a** *ura3-52 his3Δ200 trp1Δ63 leu2Δ1 rat1-1*	See (Johnson, 1997)
rai1Δ/rat1-1	*ura3-52 his3Δ200 trp1-1 leu2-3,112 rai1::HIS3 rat1-1* +Rai1p-GFP	This study, segregant of sporulated *rai1Δ/rat1-1*
sxm1Δ/nmd5Δ	MAT**α** *ura3-52 his3Δ200 trp1-1 leu2-3,112 lys2-801 nmd5::HIS3 sxm1::his3::TRP1*	This study, segregant of sporulated *sxm1Δ/nmd5Δ*
sxm1Δ/kap123Δ	MAT**a** *ura3-52 his3Δ200 trp1-1 leu2-3,112 lys2-801 sxm1::his3::TRP1 kap123::ura3::HIS3*	This study, segregant of sporulated *sxm1Δ/kap123Δ*
nmd5Δ/kap123Δ	MAT**a** *ura3-52 his3Δ200 trp1-1 leu2-3,112 lys2-801 nmd5::HIS3 kap123::ura3::TRP1*	This study, see text
kap123Δ/kap121ts	MAT**a** *ura3-52 his3Δ200 trp1-1 leu2-3,112 lys2-801 kap121::ura::HIS3 kap123::ura* +p*kap121-34*	This study, see text
rai1Δ/rai1-1	*ura3-52/ura3-52 his3Δ200/his3Δ200 trp1-1/trp1-1 leu2-3,112/leu2-3,112 lys2-801/lys2-801 ADE2/ade2 ADE3/ade3 KAP123/kap123::ura3::HIS3 rai1::HIS3/rai1-1*	This study, see text
rai1-1/kap123Δ	*ura3-52/ura3-52 his3Δ200/his3Δ200 trp1-1/trp1-1 leu2-3,112/leu2-3,112 lys2-801/lys2-801 ade2/ADE2 ade3/ADE3 kap123::ura3::HIS3/kap123::ura3 rai1-1/RAI1*	This study, see text
nop53Δ	MAT**α** *ura3-52 his3Δ200 trp1-1 leu2-3,112 lys2-801 nop53::HIS3*	This study, see text
NOP53-GFP	MAT**a** *ura3-52 his3Δ200 trp1-1 leu2-3,112 lys2-801 NOP53-GFP-spHIS5* +Nop1p-RFP	This study, see text
NOP53-A	MAT**α** *ura3-52 his3Δ200 trp1-1 leu2-3,112 lys2-801 NOP53-pA-spHIS5*	This study, see text
nop53-FL	MAT**α** *ura3-52 his3Δ200 trp1-1 leu2-3,112 lys2-801 nop53::spHIS5* +pBH1	This study, see text
nop53-ΔC	MAT**α** *ura3-52 his3Δ200 trp1-1 leu2-3,112 lys2-801 nop53::spHIS5* +pBH2	This study, see text

[a]Constructed by J.D. Aitchison.
[b]Constructed by R. Baker.
[c]Constructed by B. Grill.
[d]Kindly provided by A.W. Johnson, University of Texas at Austin, Austin, TX.

Table 2.6 Yeast culture media

Medium[a]	Composition
YEPD[b, c]	1% yeast extract, 2% peptone, 2% glucose
YEPA[b, c]	1% yeast extract, 2% peptone, 2% sodium acetate
Sporulation medium	0.1% yeast extract, 1% potassium acetate, 0.05% glucose, 2 mg/mL uracil, 4 mg/mL histidine, 12 mg/mL leucine
Sporulation supplemented[d]	0.1% yeast extract, 1% potassium acetate, 0.05% glucose, 0.1 x amino acid CSM dropout powder
CSM[d, e]	0.17% yeast nitrogen base without amino acids and ammonium sulfate, 0.5% ammonium sulfate, 1 x amino acid CSM dropout powder, 2% glucose
FOA medium[d, f] (Boeke et al., 1987)	1% 5'-fluoroorotic acid, 12 mg/L uracil, 0.17% yeast nitrogen base without amino acids and ammonium sulfate, 0.5% ammonium sulfate, 1 x amino acid CSM-URA dropout powder, 2% agar, 2% glucose

[a]All media except for FOA were made according to the instructions in Guthrie et al., 1991 (Guthrie and Fink, 1991)
[b]For solid media agar was added to 2%.
[c]Stock solutions of carbon sources were autoclaved separately and added after media autoclaving.
[d]Amino acid complete synthetic medium (CSM) dropout powders (Q-BIO Gene Inc., Irvine, CA), lacking amino acids as required, were used to maintain auxotrophic selective pressure.
[e]For solid media one pellet per L of sodium hydroxide and agar to a final concentration of 2% were added.
[f]5'-fluoroorotic acid and uracil were dissolved in 200 mL of preheated to 50°C water, filter-sterilized and added to the medium after autoclaving.

2.2.2 Bacterial strains and culture conditions

E. coli strains and culture media used in this study are described in Tables 2.6 and 2.7 respectively. Bacteria were grown at 37°C unless stated otherwise. Cultures of 5 mL or less were grown in culture tubes in a rotary shaker at 250 rpm.

Table 2.7 *E. coli* strains

Strain	Genotype	Reference/source
DH5α	F⁻ φ80d*lacZ*ΔM15 Δ(*lacZYA-argF*)U169 *deoR recA1 endA1 hsdR17*(r_K^-, m_K^+) *phoA supE44* λ⁻ *thi-1 gyrA96 relA1*	Gibco/BRL
TG1	K12Δ(*lac-pro*) *supE thi hsd*Δ5/F' *tra*Δ36 *proA*$^+$B$^+$ *lacIq laczΔM15*	Amersham-Pharmacia
BRL-DE3	F⁻ *ompT hsd*S_B(r_B^-, m_B^-) *gal dcm lon* (*srl-recA*) *306::Tn10*(DE3)	Novagen

Table 2.8 Bacterial culture media

Medium	Composition	Reference
2 x YT[a]	1.6% tryptone, 1% yeast extract, 0.5% NaCl	Pharmacia GST Gene Fusion System Protocol, 2nd Edition
LB[a, b]	1% tryptone, 0.5% yeast extract, 1% NaCl (pH 7.5)	(Maniatis et al., 1982)
SOB	2% tryptone, 0.5% yeast extract, 10 mM NaCl, 2.5 mM KCl	(Maniatis et al., 1982)
SOC	SOB + (10 mM $MgCl_2$, 10 mM $MgSO_4$, 0.36% glucose)[c]	(Maniatis et al., 1982)

[a]Ampicillin was added to 100 μg/mL for plasmid selection, as necessary.
[b]For solid media, agar was added to 1.5%.
[c]Added after autoclaving.

2.2.3 Mating, sporulation and tetrad dissection of yeast

All yeast genetic manipulations were performed according to established procedures (Fink et al., 1990; Guthrie and Fink, 1991). Prior to mating, yeast strains were grown overnight on solid selective media. For mating, haploid strains of different mating types were mixed on YEPD solid media and incubated overnight at 30°C. Diploids were selected by restreaking crosses onto solid CSM lacking amino acids as needed. Alternatively, after 4 hours of mating on rich medium, several mating cells (diploids) were selected using a dissection microscope, and grown overnight separately to obtain diploid colonies.

For sporulation, diploid cells were grown in 2 mL of liquid rich or selective medium overnight at 30°C, washed in water, and transferred into 2 mL of YEPA for 6 h. Cells were then washed in water and incubated in 2 mL of sporulation medium, supplemented with appropriate CSM as needed, for 3-10 days. To dissect tetrads, 30 μL of sporulated cell culture were washed with water and digested with Zymolyase 100T for 20 to 30 min. The tetrads were dissected using a dissection microscope (Eclipse E400, Nikon Inc.) and grown for 3 to 6 days at 30°C or at room temperature, as needed.

2.2.4 Construction of mutant strains of *S. cerevisiae*

Deletion of the *RAI1* ORF was accomplished by integrative transformation of diploid DF5 cells. A PCR-synthesized *HIS3* marker containing short flanking sequences of identity to the upstream and downstream regions of the *RAI1* ORF was generated using the oligonucleotides RAI1-5' and RAI1-3' (Table 2.3). Transformants were selected on CSM plates lacking histidine (CSM-His plates), sporulated and tetrads were dissected to obtain a haploid *rai1Δ* strain. *nop53Δ*, *sxm1Δ*, *nmd5Δ* and *kap123Δ-w303* strains were obtained in a similar manner, using the following oligonucleotides: NOP53-5', NOP53-3', SXM1-5', SXM1-3', NMD5-5', NMD5-3', KAP123-5', KAP123-3' (Table 2.3).

RAI1-A cells expressing a chromosomal fusion of the gene encoding the IgG binding domain (amino acids 44 through 271) of *Staphylococcus aureus* protein A (pA) appended, in-frame, to the 3' end of *RAI1* were generated as described previously (Aitchison et al., 1995a; 1996). Essentially, the primers RAI1-A-5' and RAI1-A-3', and the template plasmid pProtA-spHis5 (Aitchison et al., 1995a) were used to generate a PCR product containing a C-terminal fusion which places the region encoding protein A at the 3' end of *RAI1*, followed by *S. pombe HIS5*. This PCR product was then transformed into diploid DF5 cells as for disruption. His+ transformants were selected and probed for protein A expression by western blotting.

The NOP53-GFP strain was generated by appending the coding sequence of *Aequoria victoria* green fluorescent protein (GFP) at the 3' end of *NOP53* resulting in the in-frame fusion of GFP to the C-terminus of Nop53p, essentially as described for protein A chimeras (Dilworth et al., 2001).

The 123SLS strain was constructed by introducing the pJA8 plasmid into a segregant from a cross of *kap123Δ* and CH1462 strains (Kranz and Holm, 1990). Strains sf17, sfA7, sf5, sf21 and sfA9 were derived from the 123SLS strain, and were obtained from the *KAP123* synthetic fitness screen (Section 2.11).

The *nop53-FL* and *nop53-ΔC* strains are isogenic with the *nop53Δ* strain except that they harbor plasmids pBH1 and pBH2, respectively. All other double mutant strains were obtained using standard yeast genetic manipulations (Section 2.2.3) and switching auxotrophic selection markers as required (Cross, 1997).

2.3 Introduction of DNA into microorganisms

DNA was introduced into microorganisms via chemical transformation or electroporation, and transformants were identified by antibiotic or auxotrphic marker selection. Electroporation was performed in microelectroporation cuvettes (width 0.15-0.2 cm) using MicroPulser (Bio-Rad Laboratories, Hercules CA).

2.3.1 Chemical transformation of *E. coli*

Plasmid DNA was introduced into transformation-competent DH5α cells (Table 2.7) following the manufacturer's specifications (Gibco/BRL). Generally, 1 to 2 μL of a ligation reaction or 0.25 μg of plasmid DNA was added to 25 μL of cells. The mixture was incubated on ice for 30 min, subjected to heat shock at 37°C for 20 sec and then returned to ice for 2 min. 1 mL of LB (Table 2.8) was added, and the cells were incubated in a rotary shaker at 37°C for 45 min. Cells were spread onto LB agar plates containing ampicillin (Table 2.8) for antibiotic selection. When necessary, 75 μL of 2%

X-gal in DMF was spread onto plates prior to plating cells. Plates were incubated at 37°C for ~16 h for colony formation.

2.3.2 Electroporation of *E. coli*

Electroporation was used for high efficiency transformation of DH5α cells with plasmid DNA (Cosloy and Oishi, 1973). Cells were made electrocompetent following a method suggested by Gibco/BRL. Essentially, cells were grown overnight in 10 mL of SOB medium (Table 2.8). 0.5 mL of this overnight culture was added to 500 mL of SOB, and cells were grown to an OD_{600} (optical density at a wavelength [λ] of 600 nm) of 0.5. Cells were harvested by centrifugation at 2,600 x *g*, and washed twice with 500 mL of ice-cold 10% (v/v) glycerol. Cells were resuspended in a minimal amount of 10% (v/v) glycerol, aliquoted, frozen in a dry ice/ethanol bath and stored at -80°C. For transformation, 1 μL of a ligation reaction was added to 20 μL of cells, which were suspended between the electrodes of an ice-cold electroporation cuvette. Cells were subjected to electroporation with an electrical pulse of 395 V (amplified to ~2.4 kV) at a capacitance of 2 μF and a resistance of 4 kΩ. Cells were immediately added to 1 mL of SOC medium (Table 2.8), incubated in a rotary shaker at 37°C for 45 min and plated as described in section 2.3.1.

2.3.3 Electroporation of *S. cerevisiae*

Yeast cells were made electrocompetent essentially following the method of Delmore et al., 1989 (Delorme, 1989). Briefly, cells were grown overnight in 5 mL of rich or selective liquid media, added to 50 mL of fresh medium, and grown to an OD_{600}

of 0.5 to 0.8. Cells were harvested by centrifugation, washed twice with water and resuspended in TE (pH 7.5) (Table 2.4) containing 10 mM lithium acetate. The suspension was mixed gently for 45 min at 30°C. 1 M dithiothreitol (DTT) was added to the cells to a final concentration of 20 mM and the cells were incubated as before for 15 min. Following this incubation, the cells were washed twice with 1 mL of ice-cold water, and twice with ice-cold 1 M sorbitol. 0.5-1 μg of plasmid DNA, or 100-200 ng of linearized DNA were mixed with 40 μL of electrocompetent yeast cells, and cells were pulsed in a prechilled 0.2 cm disposable Gene Pulser (Bio-Rad) electroporation cuvette at 2.25 kV/cm, 25 μF, 200 Ω, in a Bio-Rad MicroPulser apparatus. The pulsed cells were resuspended in 200 μL of ice-cold 1 M sorbitol and plated onto appropriate selective medium at 30°C. The colonies of transformed cells were generally visible within 3-5 days.

2.4 Isolation of DNA and RNA from microorganisms

2.4.1 Plasmid DNA isolation from bacteria

Single bacterial colonies were inoculated into 2 mL of LB (Table 2.8) containing ampicillin and grown overnight. Plasmid DNA was isolated from 1.5 mL of culture by alkaline lysis method (Maniatis et al., 1982) or by using a QIAprep Miniprep Kit (Qiagen).

For the alkaline lysis method, cells were harvested by microcentrifugation and resuspended in 100 μL of 50 mM glucose, 25 mM Tris-HCl (pH 8.0), 10 mM EDTA. To denature DNA, samples were gently mixed by inversion with 200 μL of 0.2 M NaOH

containing 1% SDS and incubated on ice for 5 min. To renature plasmid DNA and precipitate proteins, 150 µL of potassium acetate solution (3 M K^+, 5 M CH_3COO^-) was added, and samples were incubated on ice for 5 min. The precipitate was pelleted by microcentrifugation for 5 min. Residual proteins were removed from the supernatant by extraction with phenol/chloroform/isoamyl alcohol (25:24:1), and DNA was precipitated by the addition of ethanol as described in Section 2.5.7. DNA was dissolved in 40 µL of TE (pH 8.0) (Table 2.4) containing 20 µg RNase A/mL.

Plasmid DNA isolation using the QIAprep Miniprep Kit was performed according to the manufacturer's instructions. This method employs essentially the same principles as the alkaline lysis method, except that after precipitation of proteins with potassium acetate solution, plasmid DNA is adsorbed onto a silica-gel matrix in a high-salt environment. Chaotrophic salts are passed over the column to remove contaminating proteins, residual salts are removed, and plasmid DNA is eluted in 50 µL of water.

2.4.2 Chromosomal DNA isolation from yeast

Chromosomal DNA was isolated from yeast using a rapid isolation procedure described in Ausubel et al., 1994 (Ausubel, 1994). Yeast cells were grown overnight in 10 mL of YEPD. Cells were harvested by centrifugation and washed twice with 10 mL of water. Cells were transferred to a 1.5 mL microcentrifuge tube and washed once with breakage buffer (10 mM Tris-HCl (pH 8.0) 100 mM NaCl, 1 mM EDTA, 2% (w/v) Triton X-100, 1% SDS). Cells were mixed with 200 µL each of breakage buffer, glass beads and phenol/chloroform/isoamyl alcohol (25:24:1) and mixed rapidly using a vortex mixer for 3 min at 4°C to simultaneously break yeast cells and separate nucleic acids

from proteins. 200 µL of TE (pH 8.0) were added, tubes were mixed briefly using vortex and the aqueous and organic layers were separated by centrifugation for 5 min. DNA was purified and precipitated from the aqueous solution as described in Section 2.5.7 and resuspended in 100 µL of TE (pH 8.0) containing 20 µg/mL RNase A. DNA was dissolved by heating at 37°C for 1 h, and DNA was quantified spectrophotometrically by measuring the OD_{260} (1 OD_{260} = 50 µg DNA).

2.4.3 Plasmid DNA isolation from yeast

Recessive defects in genes of mutant yeast strains were rescued by complementation with a plasmid genomic library. To recover plasmids from complemented strains, the procedure described in Section 2.4.2 was used, except that yeast cells were grown in CSM selective medium instead of YEPD, and isolated nucleic acids were dissolved in 20 µL of water instead of TE (pH 8.0). Isolated plasmid DNA was amplified by transformation of *E. coli* by electroporation (Section 2.3.2), followed by plasmid DNA isolation (Section 2.4.1).

2.4.4 RNA isolation from yeast

Total yeast RNA was isolated by the hot-phenol technique (Ausubel, 1994). Yeast cultures were grown in 50 mL of appropriate medium to an OD_{600} of ~0.8. Cells were harvested by centrifugation at 1,500 x *g*, at 4°C, and washed once in 5 mL of water. Cells were resuspended in 2 mL of buffer containing 10 mM Tris-HCl (pH 7.5), 10 mM EDTA and 0.5% SDS, mixed with 2 mL of phenol, pre-heated to 65°C, and mixed vigorously using a vortex to simultaneously break yeast cells and separate nucleic acids

from proteins. The mixture was incubated at 65°C for 1 h with occasional vortexing, then stored on ice for 5 min, and subjected to centrifugation for 5 min at 16,000 x *g*, 4°C, to separate the phases. The aqueous phase was transferred to a clean tube and 2 mL of phenol (pre-heated to 65°C) were added. The tube was mixed vigorously using a vortex and the phase separation procedure repeated. The phenol washes were repeated until the aqueous phase appeared to be clear. The aqueous phase was then mixed with 2 mL of chloroform, mixed by vortex and the phases separated by centrifugation. RNA was precipitated essentially the same as described for DNA in Section 2.5.7, except that the sample was incubated at -20°C was done overnight. The samples were then pelleted, supernatants aspirated and the pellets dried in rotary vacuum desicator Savant Speed Vac SC 210A (GMI). The dry pellets were dissolved in 200 µL of DEPC-treated water (autoclaved 0.1% (v/v) di-ethylpirocarbonate solution) and stored at -80°C. The quality of RNA was estimated by examining the ratio between sample absorbance at wavelengths 260 and 280.

2.5 Standard DNA manipulation

Unless otherwise stated, reactions were in 1.6 mL microcentrifuge tubes, and microcentrifugation was done at 16,000 x *g*.

2.5.1 Amplification of DNA by the polymerase chain reaction (PCR)

PCR was used either to introduce restriction endonuclease sites within a DNA molecule or to facilitate the construction of hybrid DNA molecules. PCR conditions (including primer design, cycling conditions and reaction components) were according to

standard procedures (reactions were performed in 0.6 mL microcentrifuge tubes typically containing 5 U of Taq DNA polymerase, 0.1 μg of template DNA, 20 to 100 pmol of each primer, 50 mM of each dNTP in 100 μL of reaction buffer. Reactions were cycled in a Robocycler 40 (Stratagene) according to the cycle conditions suggested by the PCR enzyme system manufacturer.

2.5.2 Restriction endonuclease digestion

DNA was digested according to the restriction enzyme manufacturer's instructions. For diagnostic and preparative digests, 0.5 to 1 μg and 2 to 3 μg of DNA, respectively, were digested for 3 to 16 h. Double digests were done according to the instructions supplied by enzyme manufacturers (NEB, Fermentas).

2.5.3 Construction of blunt-ended DNA fragments

The ends of DNA fragments with 5' overhangs were made blunt using the Klenow fragment of *E. coli* DNA polymerase I according to the instructions of the manufacturer (NEB). Reactions contained 2 to 3 μg of DNA, 5 U of enzyme, 33 μM of each dNTP and 1 x digestion buffer or 1 x DNA polymerase I buffer. Reactions were incubated for 15 min at room temperature, and DNA fragments were analyzed by agarose gel electrophoresis (Section 2.5.5).

2.5.4 Dephosphorylation and phosphorylation of 5' ends

Prior to ligation, the 5' ends of linear plasmid DNA molecules were usually dephosphorylated to prevent intramolecular ligations. Essentially, after plasmid

digestion, reactions were mixed with 5 U of CIAP and incubated for 15 min at 37°C. Also prior to ligation, the 5' termini of DNA molecules amplified by PCR were phosphorylated, essentially by mixing reactions with 10 U of T4 polynucleotide kinase, ATP and PNK buffer (to 10 mM and 1 x respectively) and incubation at 37°C for 1 h. Dephosphorylation and phosphorylation reactions were terminated by agarose gel electrophoresis of the sample (Section 2.5.5).

2.5.5 Separation of DNA fragments by agarose gel electrophoresis

DNA fragments in solution were added to 0.2 volumes of 6 x sample dye (30% glycerol (w/v), 0.25% bromphenol blue, 0.25% xylene cyanole) (Maniatis et al., 1982) and separated on agarose gels in 1 x TBE containing 0.5 μg ethidium bromide/mL. Fragments were separated on 1% agarose gels, and DNA was visualized using an Ultra-Violet Transilluminator Model 3-3006 (Photodyne).

2.5.6 Purification of DNA fragments from agarose gels

DNA fragments were isolated from agarose gels using a QIAQuick Gel Extraction Kit (Qiagen) according to the manufacturer's instructions. Essentially, the gel fragment containing the DNA of interest is dissolved, the DNA is adsorbed to a silica-gel matrix, contaminants are removed by washing and the DNA is eluted in 30 μL of 10 mM Tris-HCl (pH 8.5).

Alternatively, DNA was isolated from agarose gels by electroelution using a unidirectional eluter (Model UEA, International Biotechnologies) according to the specifications of the manufacturer. Essentially, the eluter was filled with 0.5 x TBE, a

gel fragment containing the DNA of interest was placed in the slot of the platform, and 80 μL of 7.5 M ammonium acetate containing 0.25% bromophenol blue was placed in the V-channel collection tube. DNA was transferred from the gel fragment to the salt solution by electrophoresis at 100 V for 15 to 45 min. 350 μL of the salt/DNA mixture was removed from the V-channel, the DNA was precipitated by the addition of ethanol and linear polyacrylamide (Section 2.5.7), and dissolved in 10 μL of water.

2.5.7 Purification and concentration of DNA from solution

The QIAQuick PCR Purification Kit was used according to the specifications of Qiagen to concentrate DNA and remove contaminants (small oligonucleotides, salt, dyes, ethidium bromide, triphosphates and protein). Essentially, DNA (100 bp to 10 kbp) is adsorbed to a silica-gel matrix, contaminants are removed by washing, and DNA is eluted in 30 μL of Tris-HCl (pH 8.5).

Alternatively, DNA was purified by extraction against phenol/chloroform/isoamyl alcohol and precipitation with ethanol (Ausubel, 1994). Essentially, DNA in 0.1 to 0.4 mL of aqueous solution was mixed by vortex with an equal volume of phenol/chloroform/isoamyl alcohol (25:24:1) for 10 sec, and the organic and aqueous phases were separated by microcentrifugation for 1 min. If a white precipitate was observed, at the interface of the phases, the extraction was repeated. The aqueous layer was then extracted against an equal volume of chloroform/isoamyl alcohol (24:1), and DNA was precipitated by adding 0.1 volume of 3 M sodium acetate and 2 to 2.5 volumes (calculated after salt addition) of ice-cold absolute ethanol and incubated at -20°C for 30 min. The precipitate was pelleted by microcentrifugation for 15 min, and salts were

removed by washing the pellet in 70% ethanol. The pellet was dried in rotary vacuum desicator Savant Speed Vac SC 210A (GMI) and dissolved in a minimal volume of water or TE (pH 8.0). If the DNA solution contained a high concentration of salt (between 0.3 and 0.5 M), no additional salt was added to the precipitation reaction. Also, if the DNA concentration was very low, 5 μL of 0.25% linear polyacrylamide was added to the precipitation reaction as a carrier.

2.5.8 Construction of hybrid DNA molecules by ligation

DNA fragments to be ligated were usually obtained by restriction enzyme digestion (Section 2.5.2). Prior to ligation, the 5' ends of the plasmid DNA molecules were dephosphorylated to prevent intramolecular ligation and, if necessary, the 5' ends of the insert DNA fragments were phosphorylated (Section 2.5.4). Then, if necessary, DNA fragments were made blunt by filling in 5' overhangs (Section 2.5.3). DNA fragments to be ligated were purified by agarose gel electrophoresis (Sections 2.5.5 and 2.5.6), combined and treated with DNA ligase in the presence of 1 mM ATP and ligase buffer according to the instructions of the manufacturer. The molar ratio of plasmid to insert DNA molecules was typically between 1:3 and 1:5, with final DNA concentration of about 20 ng/μL. Reactions were incubated at 16°C for 16 h in the cases of ligation of blunt fragments or at room temperature for 3 to 16 h for all other ligations. 1 to 2 μL of ligation reaction was introduced into *E. coli* (Sections 2.3.1 and 2.3.2). Transformants were identified by antibiotic selection, and positives were identified by restriction digestion.

2.6 Construction of plasmids for gene expression

Plasmids used in this study are listed in the Table 2.1. The source plasmids are listed in the section 2.1.6.

The *KAP123* gene was isolated as genomic 6.85 kb XhoI-XbaI fragment from a *S. cerevisiae* phagemid library (87021, ATCC) and cloned into the *SalI* and *XhoI* sites of pRS316 or pRS317 (Sikorski and Hieter, 1989) to yield pRS316-KAP123 or pRS317-KAP123, respectively. The *ADE3* gene (nt 8136-11677 on chromosome VI) was amplified by PCR from yeast genomic DNA to generate a PCR product with *SacI* linkers, which was subsequently cloned into the *SacI* site of pRS316-KAP123 to yield the pJA8 plasmid (done by John Aitchison).

The *RPL2*, *RPL3*, *RPL25* and *NOP1* ORFs were amplified by PCR from yeast genomic DNA and cloned into the *EcoRI* and *HindIII* sites of pYX242, which contains the in-frame coding sequence for *Aequoria victoria* green fluorescent protein (GFP) (Rosenblum et al., 1998). The resulting recombinant plasmids were termed rpL2-GFP, rpL3-GFP, rpL25-GFP and Nop1p-GFP, respectively (done by Benjamin Timney).

The *RAI1*, *YGL247W*, *PDE1*, *KAP95*, *KAP121*, *SXM1* and *NMD5* ORFs where amplified by PCR from yeast genomic DNA and cloned into the *PstI* and *SacI* sites of pRS314, and the resulting recombinant plasmids were termed pYGL246C, pYGL247W, Pde1p-pRS314, Kap95p-pRS314, Kap121p-pRS314, Sxm1p-pRS314, and Nmd5p-pRS314 (Sikorski and Hieter, 1989), respectively (done by Rosanna Baker).

The *RAI1* ORF was amplified by PCR from yeast genomic DNA and cloned into the *EcoRI* and *HindIII* sites of p12-GFP2-NLS (pKW431; a gift from K. Weis, University of California, San Francisco, CA) (Stade et al., 1997), which resulted in the replacement

of the cNLS sequence with the *RAI1* coding sequence, in frame with a mutant NES (p12) followed by two GFP coding sequences. The resulting recombinant plasmid was termed Rai1p-GFP (done by Rosanna Baker).

Multicopy plasmids pNmd3p, prpL10, pKap121p, pNmd5p and pNmd3Δ100, were constructed by PCR amplification of respective gene, including 250 nucleotides upstream of the initiation codon, or in the case of pNmd3Δ100 including 250 nucleotides upstream but lacking the 3' 300 coding nucleotides. *NMD3*, *RPL10*, and *NMD3*Δ100 fragments were then ligated into the *PstI* site of pRS425, while *KAP121* and *NMD5* fragments were ligated into the *XhoI* site (pNmd3p and pNmd3Δ100 plasmids were constructed by Marcello Marelli).

pBH1 and pBH2 were constructed using two PCR products corresponding to both full-length *NOP53* gene (pBH1) and a mutant version lacking nucleotides 1201-1368 encoding the C-terminal amino acids 401-456, which contains a heptad repeat of the leucine zipper motif (aa 402-434) and a (pBH2, *NOP53-ΔC*) (done by Brendan Halloran). PCR products were generated using oligonucleotides YPL146C-5', YPL146C-3' and YPL146C aa401-3'. PCR products were digested with SacI and XhoI and then ligated into these restriction sites of pRS316.

pGAL-NOP53 was obtained by subcloning a PCR product corresponding to full-length *YPL146c* into the BamHI/SalI sites of pYEUra3 (Clonetech, Palo Alto, CA). The PCR product was obtained using oligonucleotides YPL146C-5' and YPL146C-3'.

Rat1p-GFP (pAJ226) (Johnson, 1997), Nmd3p-NLS-GFP (GFP-NLS) and Nmd3p-NLS/NES-GFP (GFP-NLS+NES) (Ho et al., 2000b) were gifts from A.W. Johnson, University of Texas at Austin, Austin, TX. The Nop1p-RFP plasmid

(containing Nop1p fused to red fluorescent protein (RFP)) was kindly provided by O. Gadal, Institute Pasteur, Paris, France.

2.7 DNA and RNA analysis

All buffers and solutions used for RNA manipulations or storage were made-up in DEPC-treated water (de-ionized water treated for 2-4 h with di-ethylpirocarbonate at a concentration of 0.1% (v/v), and subsequently autoclaved).

2.7.1 DNA sequencing

DNA sequencing was performed by dideoxynucleotide chain-termination method (Sanger et al., 1977) using fluorescently labeled DNA. Sequencing reactions were performed on plasmid DNA using the BigDye Terminator Cycle Sequencing Ready Reaction Kit (ABI Prism) following the 0.5 x reaction protocol. Thermal cycle sequencing was performed in a RoboCycler 40 equipped with a Hot Top. Reactions consisted of 2 min denaturation at 96°C followed by 25 cycles of 96°C, 50°C and 60°C for 46 sec, 51 sec and 4 min, respectively. Fluorescently labeled DNA was precipitated and analyzed by capillary electrophoresis in a 310 Genetic Analyzer (ABI Prism).

2.7.2 Separation of RNA fragments by formaldehyde agarose gel electrophoresis

Separation of RNA fragments by formaldehyde agarose gel electrophoresis was performed using the modified protocol from Oligotex Handbook (May 2002, Appendix G) (Qiagen). RNA fragments in solution were added to 0.2 volume of 5 x loading buffer (0.16% (v/v) saturated bromphenol blue solution, 4 mM EDTA (pH 8.0), 7.2% (v/v)

formalin (2.66% formaldehide), 20% (w/v) glycerol, 30.84% (v/v) formamide, 40% (v/v) of 10 x MOPS), incubated for 3-5 min at 65°C, chilled on ice, and loaded onto equilibrated formaldehyde agarose gel. The gel contained 1.4% agarose, 1 x MOPS, 15% (v/v) formalin and 0.1 μg ethidium bromide per mL, and was equilibrated in the gel running buffer (1 x MOPS, 2% (v/v) formalin) for at least 30 min prior to running. The gel was run at 5-7 V/cm until the dye front reached the edge of the gel.

2.7.3 Labeling of DNA probes for primer extension and northern blot analysis

Probes used in primer extension assay and northern blot analysis are listed in Table 2.3. The probes were radiolabeled using T4 polynucleotide kinase (PNK) (Fermentas Inc., Hanover, MD) which catalyzes the transfer of the terminal phosphate of ATP to 5' hydroxyl termini of polynucleotides. A typical labeling reaction contained 10 pmol of oligonucleotide, 20 pmol [γ-^{32}P]ATP (3,000 Ci/mmol, or 6,000 Ci/mmol) (Perkin Elmer, Boston, MA), 1.5 U PNK, and 3 μL of 10 x PNK buffer. The reaction volume was brought to 30 μL with DEPC-treated water, thoroughly mixed and incubated at 37°C for 45 min. The reaction was terminated by heating at 65°C for 20 min, stored at -20°C, and used for primer extension and northern blot analysis without any further manipulations.

2.7.4 Northern blot analysis

RNA was isolated by the hot-phenol technique (Section 2.4.4) (Ausubel, 1994). Separation of RNA fragments was performed by formaldehyde agarose gel electrophoresis, a modified protocol from Qiagen Oligotex Handbook (Section 2.7.2).

The analysis of rRNA by northern hybridization was performed as described previously (Ausubel, 1994; Iouk et al., 2001). After the electrophoretic separation of RNA samples was complete, the gels were rinsed in DEPC-treated water and soaked with nylon Hybond-XL membranes (Amersham Pharmacia Biotech, Buckinghamshire, England) in 10 x SSC (Table 2.4). RNA was transferred to the nylon membranes by capillary action in 5 x SSC for ~18 h. After transfer the membranes were soaked in 3 x SSC, air-dried and exposed to 1,200 μJ of light in a UV Stratalinker 2400 (λ = 254 nm) (Stratagene, La Jolla, CA) to immobilize the RNA.

Probes used to identify various rRNA species are listed in the Table 2.3. Unless otherwise stated, all steps were conducted at 37°C. After crosslinking, the membranes were incubated in hybridization buffer (5 x SSC, 5 x Denhardt's solution (Table 2.4), 50 μg/mL of heat-denatured sheared salmon sperm DNA (Eppendorf, Hamburg, Germany), 1% SDS) in heat-sealed plastic pouches for 4 h to block the membrane and reduce nonspecific binding. The buffer was discarded and the blots were incubated in hybridization buffer containing 0.10-0.15 pmol/mL of heat-denatured radiolabeled probe for at least 18 h. Blots were washed twice for 1 min in 5 x SSC, twice for 2 min in 2 x SSC, 0.1% SDS, and twice for 15 min in 1 x SSC, 0.1% SDS. The counts were monitored with a Geiger counter, and the washes were shortened if the counts were under 50 cpm. The blots were exposed to X-Omat AR film (Kodak) for 6 to 48 h with an intensifying screen (Kodak) at -80°C.

2.7.5 Primer extension assay

Primer extension was done using Promega AMV Reverse Transcriptase Primer Extension System (Promega Corporation) using the 5'18S, 5'5.8S, 5'25S primers (Table 2.3). The primers were labeled as described in Section 2.7.3. DNA markers were labeled essentially as described in Section 2.7.3, except that the reaction composition was 250 ng (5 µL) dephosphorylated ΦX174 *Hinf* I DNA markers, 1 x PNK buffer, 30 µCi (3 µL) [γ-^{32}P]ATP (3,000 Ci/mmol) (Perkin Elmer, Boston, MA), 10 U PNK (10 U/µL). RNA was isolated by the hot-phenol technique (Section 2.4.4) (Ausubel, 1994). Primer extension reactions were performed as suggested in the AMV Reverse Transcriptase Primer Extension System Technical Bulletin provided by the manufacturer. Briefly, 15 ng of labeled primers were annealed to 5 µg of RNA for 20 min at 58°C, cooled for 10 min at room temperature and mixed with the AMV reverse transcriptase reaction mix. The reverse transcriptase reactions were held for 30 min at 42°C and were terminated by heating to 90°C for 10 min. Gel analysis of the primer extension products were performed on a 50 cm x 30 cm denaturing polyacrylamide gel (sequencing gel) containing 6% acrylamide (19:1 acrylamide/N,N'-methylene-bis-acrylamide), 7M urea and 1 x TBE buffer (Table 2.4) (Ausubel, 1994). The gels were equilibrated by running in 1 x TBE buffer for 45 min before loading, and the primer extension products were separated by electrophoresis for 150 to 200 min at 1000 V and 50 mAmp. The gels were placed on Whatman paper (3M), covered with a thin plastic wrap and dried on a vacuum gel drier (Model 583, Bio-Rad). Dried gels were exposed to X-Omat AR film (Kodak) for 18 to 96 h with an intensifying screen (Kodak) at -80°C.

2.7.6 Metabolic labeling (Pulse-chase)

Metabolic labeling was performed as described previously (Tollervey et al., 1991). *nop53Δ* and wild-type strains harboring the pRS316 plasmid were grown in 8 ml of CSM-Ura medium to an OD_{600}=0.4. The cells were concentrated to 4 ml cultures and labeled by the addition of 200 μCi of [^{3}H] uracil (Perkin Elmer, Boston, MA). After 1 min, an excess of unlabeled uracil (0.4 ml of 3 mg/ml) was added and 1 ml aliquots were removed after continued incubation for 1, 5, 15 or 30 min. Total RNA was isolated from each sample using hot phenol as described (Schmitt et al., 1990) and 50,000 cpm of labeled RNA derived from each strain were resolved by electrophoresis on a 1.3% agarose gel. Labeled species were transferred to the nylon membranes (Amersham) by capillary action (see Section 2.7.4) and detected by exposure to X-Omat AR film (Kodak).

To monitor the effects of Nop53p depletion, *nop53Δ* cells harboring pGAL-NOP53, pre-grown in CSM-Ura medium with 2% galactose as a carbon source, were incubated for additional 14 hrs in CSM-Ura medium containing either 2% glucose or 2% galactose as the carbon source. Cells were concentrated, labeled and RNA was isolated as described above.

2.8 Protein analysis and manipulation

2.8.1 Precipitation of protein

To precipitate proteins from solution, trichloroacetic acid (TCA) was added to a final concentration of 10% (w/v), and samples were incubated on ice for 30 min.

Precipitates were collected by centrifugation at 16,000 x *g* for 30 min at 4°C. The resulting pellet was washed twice with 1 mL of 80% (v/v) ice-cold acetone and dried in a rotary vacuum desicator Savant Speed Vac SC 210A (GMI).

2.8.2 Determination of protein concentration

The concentration of protein in solution was determined by the Bradford method, using the Bio-Rad protein assay dye reagent. To create a standard curve, 1 mL of reagent was added to each of ten 100 µL aliquots of solution containing from 0 to 20 µg of BSA. Samples were mixed briefly by vortex and incubated at room temperature for 10 min. Absorbance at 595 nm was measured for each sample and plotted against protein concentration. Dilutions of samples to be assayed were prepared and measured in the same way as for standards and the protein concentrations were estimated from samples with absorbances in the linear range of the curve of standards.

2.8.3 Affinity purifications from yeast whole-cell lysates

Affinity purifications from yeast whole-cell lysates were performed as described previously (Dilworth et al., 2001; Marelli et al., 1998). The whole-cell extracts were prepared as described in Section 2.9.1, and incubated overnight with 50 µL of IgG-Sepharose beads (Pharmacia) which had been preequilibrated in wash buffer, (20 mM Na_2HPO_4 (pH 7.5), 150 mM NaCl, 0.1 mM $MgCl_2$, 0.1% Tween 20 and 1 x solution P) (Table 2.3). After incubation in cell extracts, IgG-Sepharose beads were pelleted and washed ten times by resuspending the pellet in 1 mL of wash buffer and re-pelleting. Bound proteins were eluted in wash buffer containing either 0.2 M or 1 M $MgCl_2$ and

precipitated with TCA (see Section 2.8.1). Copurified proteins were resolved by SDS-PAGE (see Section 2.8.5) and visualized by Coomassie blue or silver-staining (see Section 2.8.6) (Shevchenko et al., 1996). Bands of interest were excised from the gel, subjected to in-gel trypsin digestion, and identified by mass spectrometry (see Section 2.8.8) (Hayashi et al., 2001).

2.8.4 Nop53p-pA affinity purification

Nop53p-pA and associated proteins were isolated from the nuclear fraction by affinity purification. Nuclei were isolated from 4 L of mid-logarithmically growing yeast as described in Section 2.9.2 (Rout and Kilmartin, 1990; Strambio-de-Castillia et al., 1995). Nuclei were pelleted, resuspended in 10 mL of 50 mM Tris-HCl (pH 8.0), 250 mM NaCl, 0.1 mM $MgCl_2$, 1 x solution P (Table 2.4) and treated with 20 µg DNase I per mL on ice for 15 min prior to passage through a prechilled French pressure cell (3 times at 1000 Ψ). The resulting lysate was clarified by centrifugation (27,000 x *g* for 15 min) and Nop53p-pA was isolated using IgG-Sepharose beads (Pharmacia Biotech) essentially as described (Aitchison et al., 1996; Sydorskyy et al., 2003). Beads were washed ten times with 1 mL of wash buffer (50 mM Tris-HCl (pH 8.0), 150 mM NaCl, 0.1 mM $MgCl_2$, 1 x solution P). Bound proteins were eluted with wash buffer containing increasing concentrations of $MgCl_2$ (0.05 M – 4 M). Proteins in the eluted fractions were precipitated with TCA (Section 2.8.1), resolved by SDS-PAGE (Section 2.8.5) and visualized by Coomassie blue staining (Section 2.8.6). Bands of interest were excised from the gel and subjected to in-gel digestion with trypsin (Section 2.8.8). Proteins were identified mass spectrometry (See section 2.8.8) (Eng et al., 1994).

2.8.5 Electrophoretic separation of proteins

Proteins were separated by SDS-PAGE, by the method of Laemmli as described by Ausubel et al., 1994 (Ausubel, 1994). Proteins were dissolved in a buffer containing 0.5 M Tris base, 6.5% SDS, 15% glycerol, 0.1 M DTT and 0.125% bromophenol blue and separated by electrophoresis on discontinuous slab gels. Stacking gels contained 4% acrylamide/N,N'-methylene-bis-acrylamide (30:0.8), 60 mM Tris-HCl (pH 6.8), 0.1% (v/v) TEMED, 0.1% ammonium persulphate. Resolving gels contained between 7 and 15% acrylamide/N,N'-methylene-bis-acrylamide (30:0.8), 370 mM Tris-HCl (pH 8.8), 0.1% SDS, 0.1% (v/v) TEMED, 0.042% ammonium persulphate. Electrophoresis was in SDS-PAGE running buffer (50 mM Tris-HCl (pH 8.8), 0.4 M glycine, 0.1% SDS).

2.8.6 Detection of proteins by gel staining

Proteins in polyacrylamide gels were visualized by staining with 0.1% Coomassie Brilliant Blue R-250, 10% (v/v) acetic acid and 35% (v/v) methanol for 1 h. Unbound dye was removed by incubating gels in 10% (v/v) acetic acid, 35% (v/v) methanol. Gels were dried on a vacuum gel drier (Model 583, Bio-Rad).

Alternatively, proteins in polyacrylamide gels were visualized by silver staining (Shevchenko et al., 1996). The proteins in the gels were fixed by incubation in 50% (v/v) methanol and 10% (v/v) acetic acid for 30 min, quickly rinsed in 50% (v/v) methanol and washed three times for 20 min in water. The gels then were sensitized by incubating for 90 sec in freshly made 0.2 g $Na_2S_2O_3 \cdot H_2O$/L, washed three times for 30 sec each in water and incubated for 30 min in 0.2 g $AgNO_3$/L. Further, the gels were washed three times

for 60 sec in water and developed by incubating up to 10 min in a solution containing 60 g Na_2CO_3/L, 0.5 mL formaldehyde/L, and 4 mg $Na_2S_2O_3 \cdot H_2O$/L. Development of the bands was stopped by the addition of 6% acetic acid, incubation for 10 min and immersion into water. Bands of interest were excised, subjected to in-gel trypsin digestion and identified by mass spectrometry (Section 2.8.8).

2.8.7 Detection of proteins by immunoblotting

Specific immuno-reactive protein bands were detected by western blotting, as follows. Proteins separated by SDS-PAGE were transferred to nitrocellulose membranes for 3 h at 400 mAmp on ice or for 16 h at 100 mAmp at room temperature in transfer buffer (20 mM Tris base, 150 mM glycine, 20% (v/v) methanol) (Burnette, 1981; Matsudaira, 1987) in a Trans-Blot tank transfer system with electrodes (Bio-Rad). Proteins bound to nitrocellulose were visualized by staining with 0.1% Ponceau S in 1% TCA for 2 to 3 min and destained in water. To prevent non-specific binding of antibodies, blots were incubated with gentle agitation in blocking buffer (TBST (Table 2.4) containing 1% skim milk powder) for 1 h. Blots were then incubated for 1 h with primary antiserum in blocking buffer and then with the appropriate HRP-labeled secondary antibody in TBST for 30 min (Table 2.2). After each antibody incubation, unbound antibodies were removed by washing blots three times for 10 min each in TBST. Antigen-antibody complexes were detected by incubating the blot with 1:1 mixture of the SuperSignal West Pico Chemiluminescent Substrate detection reagents (Pierce, Rockford, IL), according to manufacturer's instructions. The blots were then exposed to Kodak X-Omat X-K1 film.

Blots could be re-probed using a Re-Blot western blot recycling kit (Chemicon). Blots were rinsed with water, incubated with antibody stripping solution for 10-15 min, and washed three times in TBST for 5 min each. Proteins were then detected as described above.

2.8.8 Protein in-gel digestion and sequencing

After separation by SDS-PAGE and detection by gel staining (see Sections 2.8.5, 2.8.6) the proteins of interest were subjected to in-gel digestion essentially as described previously (Shevchenko et al., 1996). The excised fragments of polyacrylamide gel containing protein bands of interest were dehydrated for 10 min in acetonitrile, and acetonitrile was removed for 10 min in vacuum centrifuge. Dry polyacrylamide gel fragments were reswollen by addition of 10 mM DTT and 100 mM NH_4HCO_3 solution in which the proteins were reduced for 1 h at 56°C. DTT containing solution was replaced with the same volume of 55 mM iodacetamide and 100 mM NH_4HCO_3 solution, and incubated for 15 min in the dark with occasional vortexing. The gel fragments were washed in 100 mM NH_4HCO_3 solution for 10 min and dehydrated in acetonitrile twice. Dried gel fragments were swollen in digestion buffer containing 50 mM NH_4HCO_3, 5 mM $CaCl_2$ and 12.5 ng/μL for 45 min at 0°C. Proteins were digested overnight at 37°C. Polypeptides were extracted with one change of 20 mM NH_4HCO_3 and three changes of 5% formic acid in 50% acetonitrile for 20 min each. Supernatants containing polypeptides were collected and dried in vacuum centrifuge until the desired volume was reached.

The polypeptides were identified by microcapillary high-performance-liquid-choromatography (HPLC) tandem mass spectrometry, and comparison of peptide tandem mass spectra to sequences in a non-redundant protein database as previously described (done by Eugene Yi) (Eng et al., 1994).

2.8.9 Overlay blot assay

The experiment was performed essentially as described in Aitchison et al., 1996 (Aitchison et al., 1996). Polypeptides from 80S and 60S ribosomal fractions were separated by SDS-PAGE and transferred to nitrocellulose. Nitrocellulose membranes were blocked with transport buffer (20 mM Hepes (pH 7.5), 110 mM KOAc, 2 mM $MgCl_2$, 0.1% (v/v) Tween 20, 0.2 mM PMSF, 2 μg of leupeptin/mL, 2 μg of aprotinin/mL, and 0.4 μg of pepstatin A/mL) and probed with a cytosolic fraction isolated from yeast expressing Kap123p-pA as described previously (see Section 2.9; Aitchison et al., 1996 (Aitchison et al., 1996)). Binding of Kap123p-pA was detected with HRP-conjugated donkey anti-rabbit antibodies and SuperSignal West Pico Chemiluminescent Substrate (Pierce, Rockford, IL), essentially as described in Section 2.8.7.

2.9 Subcellular fractionation of yeast

2.9.1 Preparation of whole cell lysates

Yeast lysates were prepared by glass bead disruption. 200 μL of cells were pelleted from freshly grown culture by centrifugation at 200 x *g*, washed three times with 10 mL of water and transferred to a 1.6 mL microcentrifuge tube. Cells were washed

with 1 mL ice-cold disruption buffer (25 mM Tris-HCl (pH 7.5), 0.1 mM EDTA, 100 mM KCl, 1 mM DTT, 0.1% (v/v) Triton X-100, 10% (w/v) glycerol, and 1 x solution P (Table 2.4)) and resuspended in 200 µL of disruption buffer. A volume of glass beads was added to reach the bottom of the meniscus, and the mixture was mixed vigorously by vortex at 4°C for 5 min to disrupt the cells. 100 µL of disruption buffer was added, and glass beads were pelleted by centrifugation for 20 sec. The lysate was recovered and clarified by microcentrifugation at 16,000 x *g* for 20 min at 4°C.

Alternatively, yeast whole-cell lysates were prepared by cell disruption in the French pressure chamber (Dilworth et al., 2001; Marelli et al., 1998). Strains expressing appropriate protein A chimeras were grown in 500 mL of YEPD at 30°C to an OD_{600} of ~0.8, or in 500 mL of CSM-Leu medium for the strain expressing *nmd3Δ100* in Rai1p-pA background. All subsequent steps were conducted at 4°C unless otherwise stated. Cells were collected by centrifugation, resuspended in 15 mL lysis buffer (50 mM Tris-HCl (pH 8.0), 150 mM NaCl, 0.1 mM $MgCl_2$, 0.2 mM PMSF, 1 x solution P) and lysed by passing the cells (at 1000ψ) through a prechilled French pressure chamber three times. The lysates were diluted with an equal volume of lysis buffer containing 40% (v/v) DMSO, and 2% (v/v) Triton X-100. The lysates were cleared by centrifugation at 11,300 x *g* for 15 min followed by centrifugation at 311,000 x *g* for 45 min. The cleared supernatants were further used for immunoprecipitations from yeast whole-cell lysates (Section 2.8.3).

2.9.2 Isolation of nuclei

Nuclei were prepared by the method of Rout and Kilmartin (Kipper et al., 2002; Rout and Kilmartin, 1990) with minor modifications. Cell cultures (4 liters) were harvested at an OD_{600} of 0.7 - 0.8, washed twice with water and pretreated in ice-cold buffer containing 100 mM Tris-Cl (pH 9.5) and 10 mM DTT, after which cells were washed with 1 M Sorbitol and incubated for 3 hours at 30°C with gentle shaking in 1 M sorbitol containing 1% zymolyase 20T (ICN Biomedicals), 1% mutanase (Sigma) and 10% glusulase (NEN). Cells were pelleted at 2,000 x *g* for 5 min, washed in 1.1 M sorbitol and resuspended in 1.1 M sorbitol containing 1 x solution P. Spheroplasts were loaded on a 10 ml 7.5% Ficoll 400/1.1 M sorbitol cushion and pelleted at 4,000 x *g* for 20 min in a Beckman JS13.1 rotor at 4°C. The sorbitol and Ficoll layers were removed, cell pellets were resuspended in 8% polyvinylpyrollidone (PVP) containing 2 mM DTT, 0.025% Triton X-100 and 1 x solution P. The samples were homogenized using a Polytron (Brinkman Instruments) and the lysates were loaded onto a cushion containing 0.6 M sucrose, 8% PVP and 1 x solution P. Cytoplasmic supernatants were collected after centrifugation at 14,200 x *g* for 20 min in a Beckman JS13.1 rotor at 4°C, and were used for quantification of cytoplasmic 60S particles by sucrose gradient centrifugation (Section 2.9.3), and to asses the presence of rpL3 by western blotting. The pellet was washed by resuspending in a volume of buffer (10 mM Bis-Tris (pH 6.5), 1 mM $MgCl_2$, 1 x solution P) equal to that of the pellet and the suspension was centrifuged at 27,200 x *g* for 15 min in a Beckman JA25.5 rotor at 4°C, to yield a nuclear fraction. The nuclear fractions were also used for quantification of cytoplasmic 60S particles, and to asses the presence of rpL3 by western blotting.

2.9.3 Polysome and ribosome analysis by linear sucrose gradient centrifugation

For polysome preparations, yeast cultures were grown to an OD_{600} of 0.6, treated with cycloheximide (100 µg per mL of culture) and harvested by centrifugation. The cells were disrupted by glass-bead lysis, essentially as described previously (Section 2.9.1) (Foiani et al., 1991; Kressler et al., 1997), except that the buffer in which the cells were washed and disrupted contained 10 mM Tris-HCl (pH 7.4), 100 mM NaCl, 30 mM $MgCl_2$, 50 µg cycloheximide/mL, and was made up in DEPC-treated water (Section 2.7). The cells were disrupted by vortexing cells with glass beads 10-16 times for 15 sec, with 30 sec cooling on ice after each vortexing. Cellular debris was removed by three subsequent microcentrifugations, 2000 x *g*, 5,000 x *g* and 16,000 x *g* for 5 min at 4°C each. For each sample, 200 A_{260} units of cell lysate supernatants were loaded onto a 36-mL linear 7 to 42% sucrose gradient and centrifuged for 6-8 hours at 141,000 x *g* in a Beckman SW28 rotor at 4°C. Sucrose gradient fractions were analyzed by continuous monitoring at 254 nm with a UV monitor (Pharmacia LKB UV-M II).

Dissociated ribosomal subunits were analyzed as described above except that extracts were prepared in buffer containing 10 mM Tris-HCl (pH 7.4), 100 mM NaCl and 30 mM EDTA. In addition, sucrose gradients also contained 30 mM EDTA instead of $MgCl_2$ (Sabatini et al., 1966). Appropriate fractions from the Section 2.9.2 were used to quantify 60S particles in the cytoplasm and the nucleus. Aliquots of these fractions were mixed with appropriate buffer to obtain a final concentration of 10 mM Tris-HCl (pH 7.4), 100 mM NaCl, 30 mM EDTA, and separated by linear sucrose gradient centrifugation to obtain two absorbance peaks, corresponding to 40S and 60S ribosomal

subunits, when monitored at wavelength 254 nm. The amount of 60S subunits was estimated from the height of the absorbance peaks representing 60S subunits.

2.10 Microscopy

Cells expressing GFP- or RFP-tagged (DsRed) proteins were grown overnight in selective medium, diluted into fresh medium and grown for an additional 4 h before direct visualization by fluorescent microscopy. For experiments requiring galactose induction, cells were grown overnight in medium containing 2% raffinose, diluted into fresh medium containing 2% raffinose and grown for an additional 4 h before the addition of galactose to 2%. Plasmids expressing the GFP and RFP chimeras are listed in the Table 2.1. See section 2.2.4 for details on construction of the strains expressing chromosomal fusions of the gene encoding GFP, and section 2.6 for details on construction of the plasmids expressing the GFP chimeras. A heated microscope slide tray was used when visualizing temperature sensitive mutants. The GFP or RFP chimeras were visualized using either a Zeiss Axioskop 2 (Carl Zeiss, Inc.) and a Spot camera (Diagnostic Instruments Inc.), or a confocal microscope (LSM 510 NLO; Carl Zeiss, Inc.). Further processing of images was performed using Adobe® Photoshop® 6.0 (Adobe Systems Inc.).

2.11 *KAP123* synthetic fitness screen

2.11.1 Isolation of synthetic fitness mutants

A colony sectoring assay was used to isolate *KAP123* synthetic fitness mutants as described previously (Aitchison et al., 1995b; Bender and Pringle, 1991; Kranz and Holm, 1990). The haploid strain 123SLS, harboring pJA8 (Table 2.1), was UV mutagenized (14 mJ/cm^2) on YPD plates with a Stratalinker (Stratagene, La Jolla, CA) to a viability of 15%. Approximately 200,000 colonies were screened to identify red, nonsectoring (sec$^-$) mutants after extended (5-8 days) growth on YPD at 30°C. The red phenotype appears in the cells lacking Ade2p and expressing functional Ade3p. 35 sec$^-$ strains were identified, of which 33 were Ura$^+$ and failed to grow on media containing 5'-FOA. The Ura$^+$ cells were inviable on 5'-FOA because the product of *URA3* converts 5'-FOA to 5'-fluorouracil, which is toxic to the cells. Therefore, only Ura$^-$ cells can grow on 5'-FOA-containing media. The sec$^+$ phenotype and the ability to grow on 5'-FOA (Boeke et al., 1987) could be restored to 30 mutants by transformation with the plasmid pRS317-KAP123, but not with pRS317 alone. The diploids derived from backcrosses with the parent strain were sporulated and tetrads were dissected. The resulting haploids showed a 2:2 segregation of the mutant phenotype suggesting a single mutation was responsible for the sec$^-$ phenotype. These 30 strains were chosen for complementation studies [Aitchison, 1995; Nehrbass 1996; Marelli 1998] (done in parts by John Aitchison, Rosanna Baker and Adriana Antunz-de-Mayolo).

2.11.2 Complementation of synthetic fitness mutants

The strains chosen for complementation were transformed with an *S. cerevisiae* genomic DNA library cloned into the vector, pSB32 (provided by J. Rine, University of California, Berkeley, CA; (Aitchison et al., 1995b)). Leu^+ transformants were screened to identify the sectoring (sec^+) colonies, which were then transferred to 5'-FOA containing media (Boeke et al., 1987) to confirm that they had regained ability to lose the pJA8 covering plasmid. The cDNA library plasmids were purified from the sec^+ strains which were able to grow on 5'-FOA (see Section 2.4.3) and amplified by shuttling into the *E. coli* strain DH5α (see Section 2.3.1). In order to confirm complementation the genomic DNA library plasmids were reintroduced into the mutant from which they were isolated and the complementing fragments of DNA were sequenced. To determine the gene affected in a synthetic fitness mutant, the genes within the complementing fragments of genomic DNA were amplified by PCR and subcloned individually into a pRS314 plasmid (CEN-TRP). The resulting plasmids were transformed into the corresponding mutant to identify the complementing gene. Transformants were restreaked onto CSM solid medium lacking Trp and subjected to plasmid shuffling by replica plating to medium containing 5'-FOA.

2.12 Computer-aided DNA and protein sequence analyses

Query protein and DNA sequences were compared to sequences from the (SGD) Saccharomyces Genome Database (http://seq.yeastgenome.org/cgi-bin/nph-blast2sgd) or National Centre for Biotechnology Information (NCBI) protein and nucleic acids sequence databases (http://www.ncbi.nlm.nih.gov/BLAST/) using the BLAST and

BLAST2 algorithms (Altschul et al., 1997; Schaffer et al., 2001). All other DNA sequence analyses were done using the DNA Star software package (DNAStar Inc., Madison, WI) and IDT SciTools applications available on the International DNA Technologies (IDT) site (http://www.idtdna.com/SciTools/SciTools.aspx). Cytoscape 2.0 software was used to visualize protein and genetic interactions (http://www.cytoscape.org/). The structural prediction service Robetta (Chivian et al., 2003) was used to predict protein folding and the domain structure of query proteins. Additional information on protein and genetic interactions was obtained by searching NCBI National Library of Medicine (NLM) PubMed service (http://www.ncbi.nlm.nih.gov/entrez/query.fcgi) and BioKnowledge Library (http://proteome.com/) (Biobase Biological Databases, Beverly, MA).

Chapter 3

Intersection of the Kap123p-mediated nuclear import and ribosome export pathways

The data presented in this chapter have previously been published as "Intersection of the Kap123p-mediated nuclear import and ribosome export pathways" (Yaroslav Sydorskyy, David J. Dilworth, Eugene C. Yi, David R. Goodlett, Richard W. Wozniak and John D. Aitchison. 2003. Mol. Cell. Biol. 23:2042-2054).

3.1 Overview

A genetic screen was used to identify genes that interact with the major ribosomal protein nuclear import factor, β-karyopherin *KAP123*. Through this analysis we found three other karyopherins, Pse1p/Kap121p, Sxm1p/Kap108p, and Nmd5p/Kap119p. We propose that, in the absence of Kap123p, these karyopherins are able to substitute for Kap123p in the import of ribosomal proteins into the nucleus.

In addition to the karyopherins, we identified Rai1p, a novel protein implicated in rRNA processing. Rai1p is also not essential, but deletion of the *RAI1* gene is deleterious to cell growth and causes defects in rRNA processing, which lead to an imbalance in the 60S:40S ratio and the accumulation of halfmers, 40S subunits assembled on polysomes that are unable to form functional ribosomes. Rai1p localizes predominantly to the nucleus, where it physically interacts with Rat1p and pre-60S ribosomal subunits. Analysis of the *rai1/kap123* double mutant strain suggests that the observed genetic interaction results from an inability to efficiently export pre-60S subunits from the nucleus, which arises from a combination of compromised Kap123p-mediated nuclear import of the essential 60S ribosomal subunit export factor, Nmd3p, and a *rai1Δ*-induced decrease in the overall ribosome biogenesis efficiency.

3.2 *KAP123* synthetic fitness screen

Kap123p plays an integral role in ribosome biogenesis by importing ribosomal proteins into the nucleus prior to their incorporation into assembling pre-ribosomal particles (Rout et al., 1997; Schlenstedt et al., 1997). To investigate how cells compensate for the loss of Kap123p, and its interaction with other components of the

ribosome assembly pathways, we have isolated mutants that, in combination with the *kap123* null mutant, exhibit a synthetic fitness defect. A previously developed screen (Aitchison et al., 1995b; Bender and Pringle, 1991; Kranz and Holm, 1990) was used to address this point (see section 2.11 for details). The genes encoding the β-karyopherins Sxm1p/Kap108p, Nmd5p/Kap119p and Pse1p/Kap121p complemented mutant strains sfA7 and sfA9, sf5 and sf21, respectively, suggesting that the nuclear import pathways mediated by these karyopherins overlap with those mediated by Kap123p (Fig. 3.1A). Indeed, genetic and functional interactions have previously been reported between *KAP123* and *KAP121* (Rout et al., 1997; Seedorf and Silver, 1997). Furthermore, Sxm1p/Kap108p interacts with ribosomal proteins, suggesting a role in importing this class of proteins (Rosenblum et al., 1998). Such functional redundancy between multiple members of this family is underscored by the fact that each of these synthetic fitness mutants was viable, displaying synergistic fitness defects but not synthetic lethality at 30°C. To confirm these results, we constructed strains harboring double knockouts of genes encoding *Sxm1p/Kap108p*, *Nmd5p/Kap119p* and *Kap123p* in all three combinations, along with a *kap123Δ/kap121ts* double mutant strain. All of these strains were viable; but their growth rates were dramatically reduced (performed by Rosanna Baker).

Interestingly, the sf17 mutant was not complemented by a gene encoding a karyopherin, but rather by the gene *YGL246C/RAI1* (Fig. 3.1B). Rai1p stabilizes and augments the function of Rat1p (Xue et al., 2000), a 5'-exonuclease required for the trimming of the $27A_3$ precursor rRNA to the 27SBs and degradation of excised pre-rRNA

Figure 3.1. *KAP123* interacts genetically with several karyopherins and *YGL246C/RAI1*. (A) Summary of genetic interactions uncovered by the *KAP123* synthetic fitness screen. (B) top: the chromosomal region contained in the sf17 rescuing plasmid is indicated by the dashed box. ORFs are indicated above. bottom: plasmids containing candidate genes (*RAI1*, *YGL247W*, *PDE1*) and genes encoding several karyopherins (*SXM1/KAP108, NMD5/KAP119, KAP95, KAP121*) were analyzed using a plasmid shuffling assay in sf17 cells. Note only cells transformed with *YGL246C/RAI1*, were able to grow in the absence of pJA8 assayed by growth on 5'-FOA. (C) top: cells lacking the *RAI1* ORF were viable in a *kap123Δ* background but exhibited a synthetic fitness interaction with *KAP123*. bottom: the reduced growth rate of *rai1Δ* cells was complemented by plasmids encoding either Rai1p or Rai1p-GFP. (D) Sequencing of the *RAI1* ORF in the sf17 mutant revealed an A→T transversion at position 443, which introduced the nonsense mutation shown. (E) Structural prediction analysis using Robetta (http://robetta.bakerlab.org/) indicated that Rai1p is an evolutionarily conserved eukaryotic protein. However, none of the putative Rai1p orthologs have been characterized sufficiently to draw any definitive conclusions from this structural analysis. top: basic secondary structure elements detected by DISOPRED (Jones and Ward, 2003) and PsiPred (Jones, 1999) prediction methods (http://robetta.bakerlab.org/documents/) are represented in black, red and blue stripes (disordered strands, alpha helices, beta strands, respectively). Based on these structural elements two hypothetical domans were detected using Robetta. However, the program was unable to relate these structural elements to any characterized domains. middle: the Blast alignment of Rai1p orthologs. Similar sequences are shaded grey. bottom: top ten putative Rai1p orthologs.

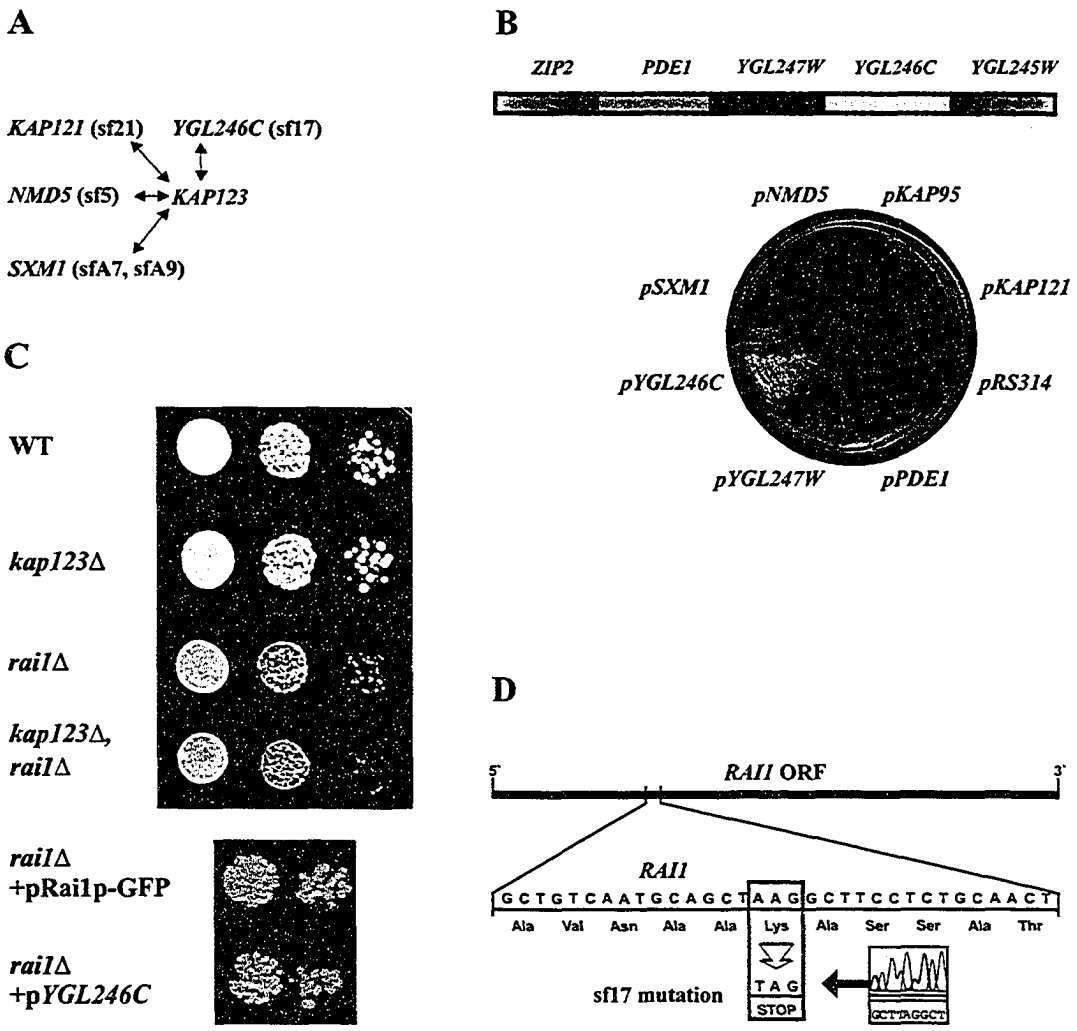

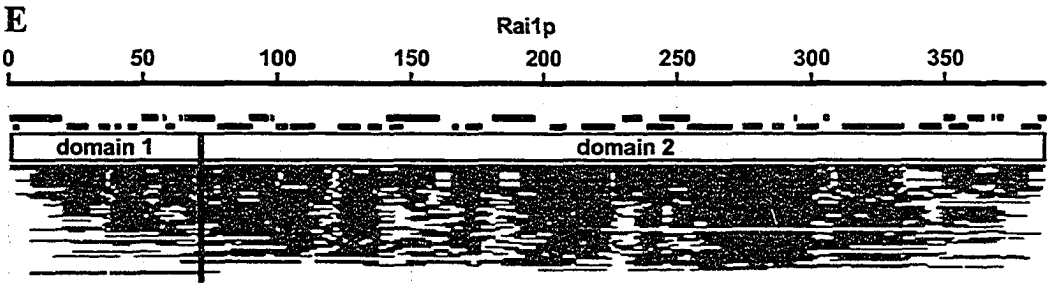

NCBI taxon. ID	Species	PSI-Blast E value	Description
33169	Eremothecium gossypii	1.00E-104	AFR263Cp
229533	Gibberella zeae	1.00E-100	hypothetical protein FG07345.1
10090	Mus musculus	3.00E-98	hypothetical protein
10116	Rattus norvegicus	2.00E-97	similar to DOM-3 homolog Z
237561	Candida albicans	8.00E-96	hypothetical protein CaO19.13610
9606	Homo sapiens	2.00E-95	HLA class III protein Dom3z
5141	Neurospora crassa	6.00E-95	hypothetical protein AL451015
227321	Aspergillus nidulans	2.00E-94	hypothetical protein AN6514.2
3702	Arabidopsis thaliana	2.00E-77	glycine-rich protein
7227	Drosophila melanogaster	2.00E-76	CG9125-PA

spacer fragments during 60S ribosomal subunit biogenesis (Lafontaine and Tollervey, 1995; Venema and Tollervey, 1995). In agreement with the original report on Rai1p (Xue et al., 2000), deletion of *YGL246C* was not lethal, but compromised cell growth. Moreover, these cells showed no specific temperature sensitivity, growing at all temperatures tested (16°C, 23°C, 30°C or 37°C). This generalized growth defect was complemented by reintroduction of a plasmid encoding Rai1p or a gene fusion encoding a Rai1p-GFP chimera (Fig. 3.1C). Furthermore, diploid cells resulting from a cross of *rai1Δ* cells with sf17 cells displayed a similar growth defect as the haploid strains, suggesting that the mutation in sf17 was indeed allelic to *RAI1*. This mutation was termed *rai1-1*. To evaluate the specificity of the *rai1/kap123*genetic interaction, double mutant strains containing *rai1Δ/sxm1Δ, rai1Δ/nmd5Δ* and *rai1Δ/kap121ts* were compared to cells containing single deletions of each gene, and the *rai1-1/kap123Δ* and *rai1Δ/kap123Δ* strains. In contrast to the dramatic growth defect associated with the *rai1Δ/kap123Δ* double deletion, *rai1Δ/sxm1Δ, rai1Δ/nmd5Δ* and *rai1Δ/kap121ts* cells grew only slightly more slowly than *rai1Δ* cells (Fig. 3.1C and data not shown). Direct DNA sequencing of the PCR-amplified *rai1* gene in sf17 cells revealed an A→T transversion at position 443 resulting in a nonsense mutation of lysine 147 that generates an expressed product predicted to contain the amino-terminal one-third of Rai1p (Fig. 3.1D). Interestingly, this mutation seemed more detrimental to cells than complete loss of Rai1p, as the *rai1Δ/kap123Δ* strain was not as defective in growth as the *rai1-1/kap123Δ* strain (Fig. 3.1B, C).

Structural prediction analysis of the Rai1p sequence using Robetta (http://robetta.bakerlab.org/) indicated that this is an evolutionarily conserved eukaryotic

protein (Fig. 3.1E). None of the putative Rai1p orthologs have been characterized previously (http://robetta.bakerlab.org/results.jsp?id=4489&p=1). The Ginzu Domain Prediction program found two hypothetical domains. However, because none of the proteins similar to Rai1p had been characterized biochemically or structurally, functional or 3-dimensional structural predictions were not pursued.

3.3 Rai1p is a nuclear protein

Because of Kap123p's well established role in nucleocytoplasmic transport, we first investigated whether the localization of Rai1p was dependent on Kap123p. Rai1p was therefore C-terminally tagged with GFP and localized by fluorescence microscopy. In wild-type cells, Rai1p-GFP localized primarily to the nucleus but also revealed a distinct cytoplasmic pool (Fig. 3.3A). Surprisingly, we detected no change in the Rai1p-GFP nuclear signal in the single knockouts of *KAP123*, *SXM1/KAP108*, *NMD5/KAP119*, or cells carrying temperature sensitive mutations of Kap121p (*kap121-34*) or Kap95p (*kap95-14*) (Fig. 3.3B). Furthermore, despite numerous attempts, including immunoaffinity purification, overlay and solution binding assays, we failed to detect a physical interaction between Rai1p and Kap123p. Together, these data suggest that Rai1p is not imported into the nucleus by Kap123p and do not support the hypothesis that the genetic interaction reflects a physical interaction between Rai1p and Kap123p.

3.4 Rai1p interacts with Rat1p in assembling 60S ribosomal subunits

To determine the physical interactions made by Rai1p, a Rai1p-proteinA chimera was generated and affinity purified from whole cell lysates using IgG Sepharose. These

experiments yielded a single major protein of approximately 120 kDa, which was identified as Rat1p by tandem mass spectrometry of excised gel slices (Fig. 3.2A). This is in agreement with the data from Johnson's group, which also established a physical interaction between Rai1p and Rat1p (Xue et al., 2000). In those studies, *rai1Δ* strains were shown to accumulate 27A3 precursors, and Rat1p activity was more robust in the presence of interacting Rai1p, suggesting that Rai1p and Rat1p function together in the trimming of the rRNA species to the 27SBs precursor (Fig. (Xue et al., 2000). In agreement with this function for Rai1p, *rai1Δ* and *rat1-1* are synthetically lethal (Fig. 3.2B). Interestingly, we also noted that Rai1p-GFP was mislocalized to the cytoplasm in

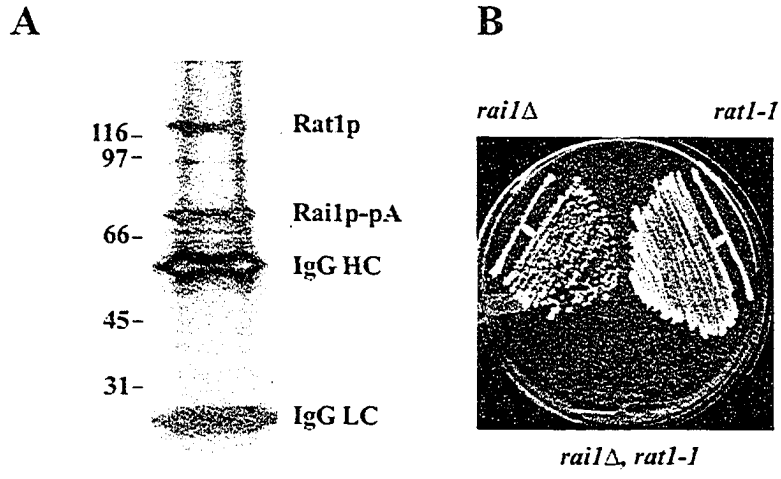

Figure 3.2. Rai1p interacts with Rat1p physically and genetically. (A) Immunoaffinity purification of Rai1p-pA from yeast whole cell lysates yielded stoichiometric amounts of Rat1p. Eluted proteins were resolved by SDS-PAGE and visualized by silver staining. The co-purifying band at ~120 kDa was identified as Rat1p by tandem mass spectromery. (B) *rai1Δ/rat1-1* cells, relieved of the *URA3*-based Rai1p-GFP plasmid by growth on media containing 5-FOA were unable to form colonies at all temperatures tested demonstrating synthetic lethality between these alleles. Shown is the plate incubated at 23°C, with the parental haploid controls, *rai1Δ* and *rat1-1*.

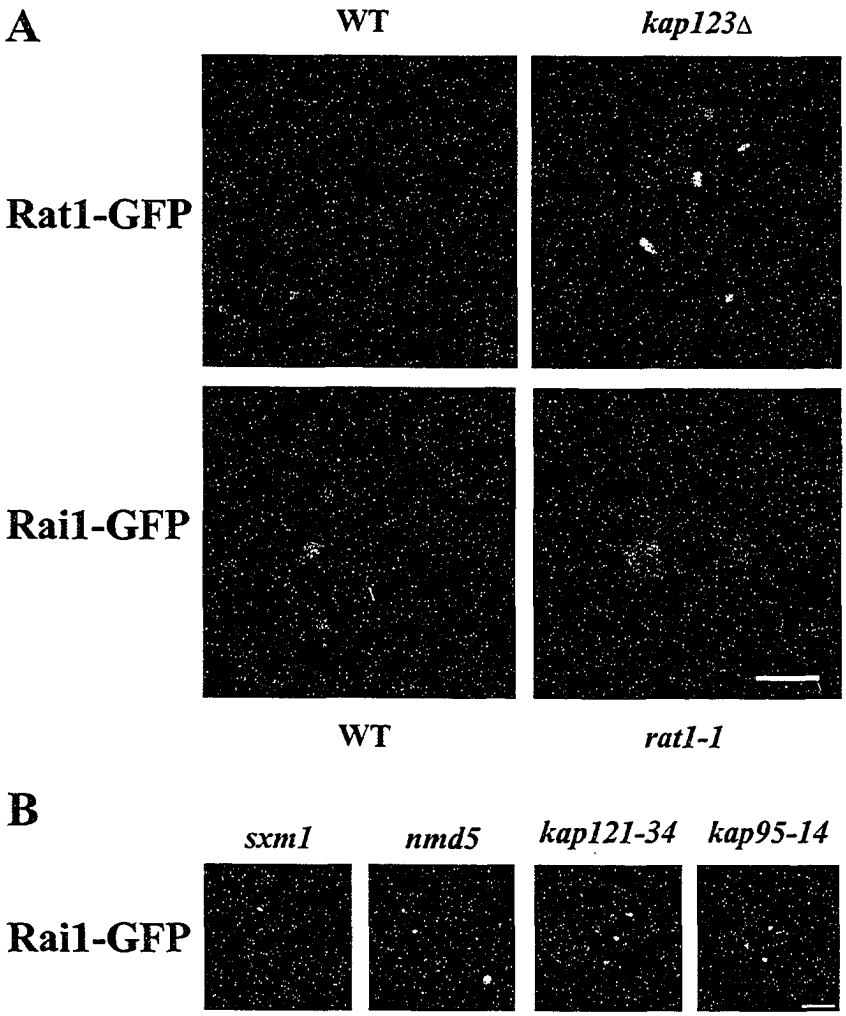

Figure 3.3. The localization of Rai1p-GFP to the nucleus is dependent on functional Rat1p. (A) Rai1p-GFP expressed in wild-type cells, detected by fluorescence microscopy in live cells, was predominantly nuclear, with a distinct cytoplasmic pool (bottom left). In contrast, when expressed in *rat1-1* cells, although grown at permissive temperatures, Rai1p-GFP was not concentrated in the nucleus revealing a predominantly cytoplasmic signal. By comparison, Rat1-GFP remained nuclear/nucleolar when expressed in wild-type or *kap123Δ* cells. Bar, 5 μm. (B) The nuclear localization of Rai1-GFP did not change in *sxm1Δ*, *nmd5Δ*, *kap121-34* or *kap95-14* mutant strains. Bar, 5 μm.

rat1-1 cells (Fig. 3.3). One scenario to explain this interesting result would be that in the absence of a fully functional Rat1p, Rai1p is no longer effectively tethered to Rat1p in the nucleus and has become free to move within the nucleoplasm, and perhaps, exit the nucleus.

One potential mechanism for this movement and exit may be through an interaction with assembling ribosomes. We therefore tested for such an interaction. Ribosomes, polysomes and ribosomal subunits were resolved by linear sucrose gradient centrifugation from a Rai1p-pA expressing strain (RAI1-A) and fractions from the gradient were probed for Rai1p-pA. Under these conditions, Rai1p-pA was found only in the load fraction (Fig. 3.4A). This suggested that if Rai1p interacts with ribosomal particles, it is either not stable under these conditions or occurs below the level of detection. We therefore sought to increase the concentration of 60S subunits in the nucleus by inhibiting 60S subunit export. To accomplish this, a mutant version of Nmd3p was expressed in RAI1-A cells. Nmd3p was previously identified as an adaptor protein that, through its binding to both the 60S subunit protein rpL10, and the karyopherin Crm1p, mediates the Ran-GTP-dependent export of the pre-60S particle from the nucleus (Gadal et al., 2001b; Ho et al., 2000b). It has also been shown that deletion of the C-terminal 100 amino acid residues of Nmd3p inhibits ribosomal subunit export in a dominant negative fashion (Ho et al., 2000b). Thus, polysomes were fractionated from RAI1-A cells expressing *nmd3Δ100* from a plasmid and the presence of Rai1p-pA in each fraction was determined by western blotting. A monoclonal antibody to rpL3 (TCM1) was used to identify the 60S, 80S and polysome fractions. Under these conditions, Rai1p-pA was detected in association with 60S and 90S (precursor) subunits

(Fig. 3.4B), but not with 40S subunits or polysome fractions. Moreover, affinity purification of Rai1p-pA from lysates derived from cells expressing *nmd3Δ100* also showed association of the 60S subunit marker protein rpL3 with the Rai1p chimera (Fig. 3.4C). Further examination of this Rai1p-pA immunopurified fraction by mass spectrometry demonstrated that several ribosomal proteins associated with Rai1p-pA under these conditions. This included 22 60S ribosomal subunit proteins and 8 (early associating) 40S subunit proteins from a total of 33 identifications (Fig. 3.4C). In addition to Rat1p, also associated with the fraction were Las1p and Grc3p (Doseff and Arndt, 1995; El-Moghazy et al., 2000); however, the potential roles of these proteins in ribosome assembly remain to be investigated.

The number of 60S subunit proteins identified by mass spectrometry suggests that pre-60S particles associate with Rai1p. The source of the relatively few 40S proteins identified is unclear. In proteomic approaches to identify components of purified subunit precursors, small numbers of ribosomal proteins from other subunits are commonly detected. In our study, this may be because Rai1p can interact with the 60S particles as well as 90S particles. Alternatively, as suggested by Harnipicharnchai et al. (2001) some 40S subunit proteins may associate with 60S precursor particles. Interestingly, six of the eight small subunit proteins identified here were also identified in association with 66S precursor particles by Harnipicharnchai et al. (2001).

3.5 Ribosome assembly defects in *rai1/kap123* cells

Together, the above data support and extend previous studies demonstrating a role for Rai1p in 60S ribosomal subunit biogenesis; however, they fail to explain the specific

Figure 3.4. Rai1p interacts with 60S ribosomal subunits. (A) Ribosomes, polysomes and ribosomal subunits were resolved by linear sucrose gradient centrifugation from a Rai1p-pA expressing strain. Rai1p-pA was detected only in the top fractions of the gradient as determined by immunoblotting of the collected fractions to detect the protein A tag. Detection of rpL3 served as an internal control to identify 60S particles. The top panel shows the corresponding polysome profile detected by spectrophotometry (OD 254 nm) of the fractionated sucrose gradient. (B) pre-60S ribosomal subunits were accumulated in the nucleus by the expression of a plasmid encoding the *nmd3Δ100* mutant allele in RAI1-A cells. Under these conditions, Rai1p-pA co-fractionated with the 60S ribosomal subunit on sucrose gradients. (C) top: Rai1p-pA immunopurifications were performed from wild-type cells and cells expressing *nmd3Δ100*. Proteins bound to Rai1p-pA were eluted with $MgCl_2$ at the concentrations shown. The resulting fractions were immunoblotted to reveal the 60S marker rpL3 which remained associated with Rai1p-pA in cells expressing *nmd3Δ100*. bottom: Rai1p-pA co-purified with a number of 60S ribosomal subunit proteins isolated from cells expressing the *nmd3Δ100* allele. Proteins contained within the 1M $MgCl_2$ elution fraction were sequenced by tandem mass spectrometry leading to the identification of 22 large and 8 small subunit proteins from a total of 33 identifications. Only proteins identified by two or more unique polypeptide matches were considered significant.

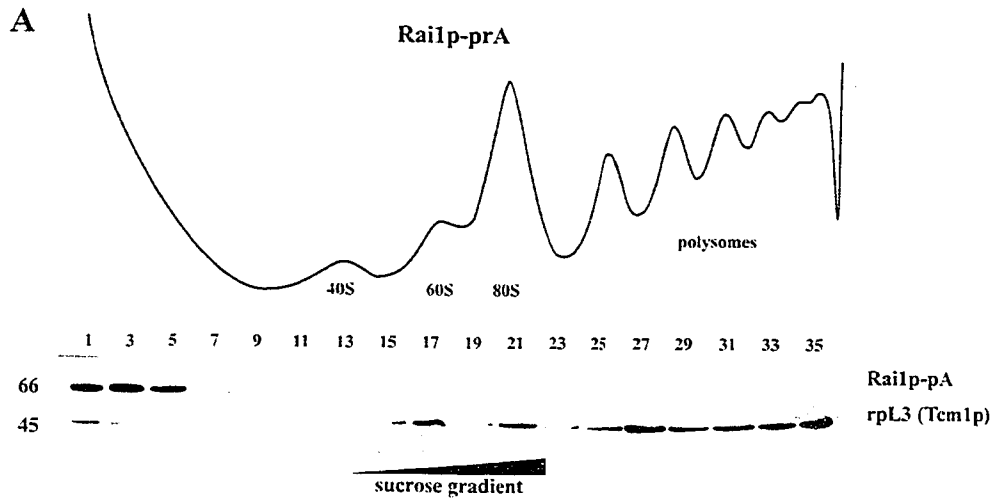

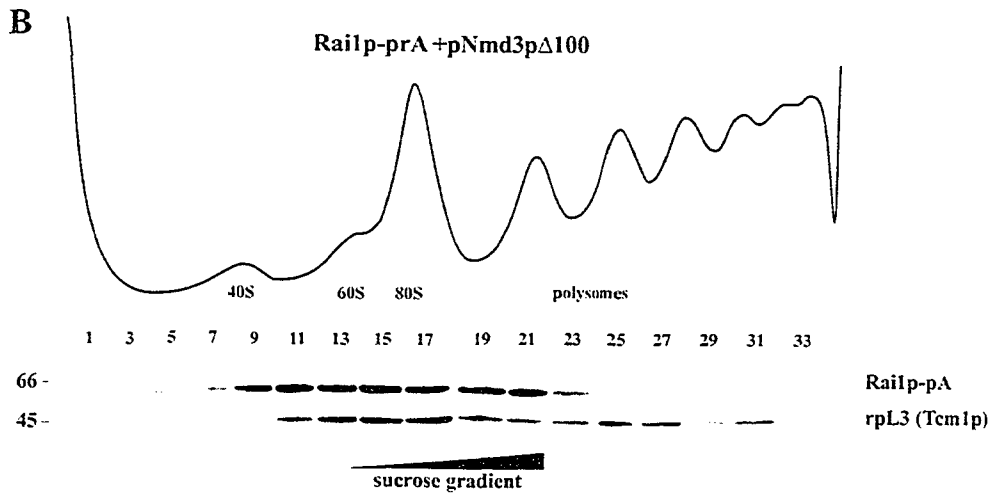

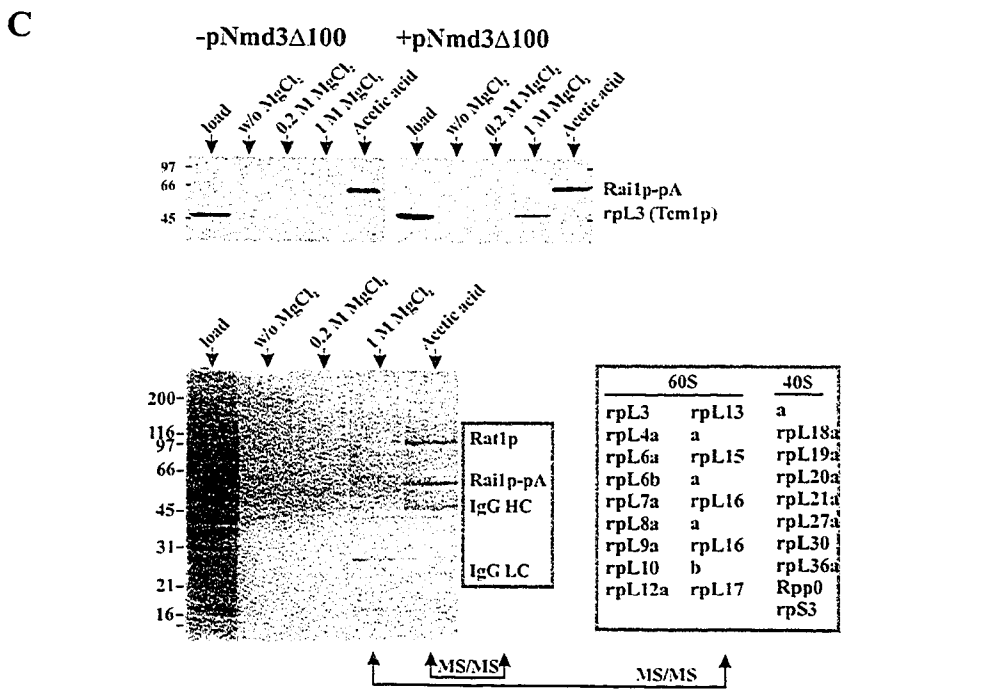

genetic interaction observed between *rai1* and *kap123*. Northern blotting of rRNA was used to identify precursors that accumulate in *rai1* and *kap123* strains (Fig. 3.5). As expected, *rai1* strains accumulated 35S, and 27S rRNA species ($27SA_2$, $27SA_3$). Interestingly, these precursors accumulated to a greater extent in sf17 and *kap123Δ/rai1Δ* cells. In addition, *rai1Δ*, sf17 and *kap123Δ/rai1Δ* cells accumulated 7S precursors and a fragment that corresponds to A_3-E. The A_3-E fragment is proposed to accumulate if the precise order of processing is disrupted (Kufel et al., 2002) and may require Rat1p and/or Rai1p for trimming to 5.8S. On the other hand, the presence of 7S precursors suggests

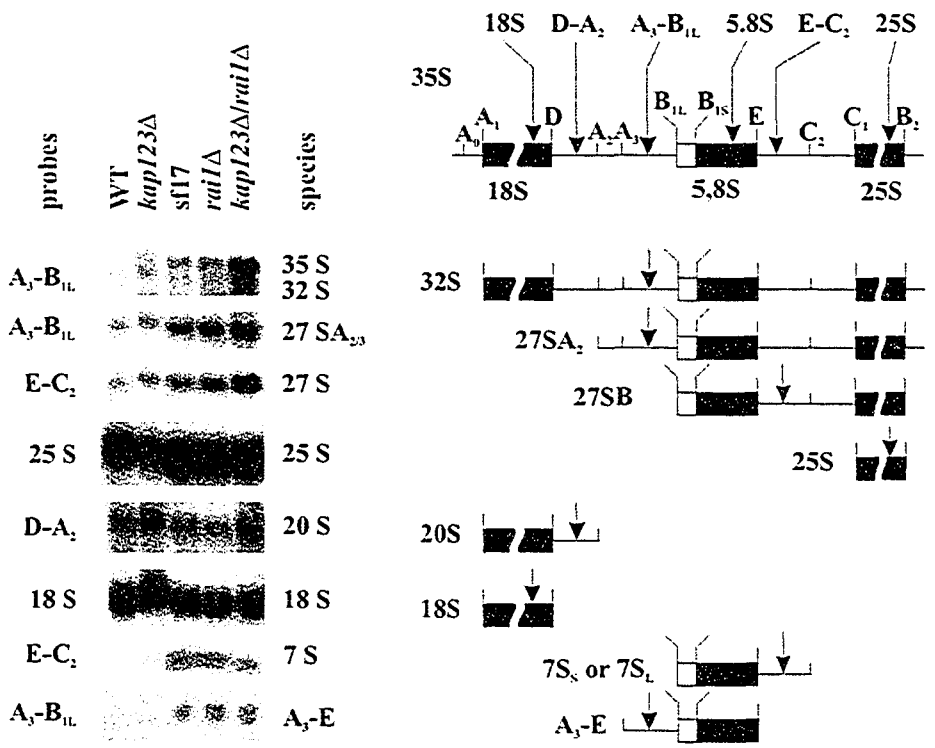

Figure 3.5. Northern Analysis of rRNA processing. Normal rRNA processing is disrupted in strains lacking Rai1p and Kap123p. Equal quantities of total RNA from each strain were separated on a 1% agarose gel, or a 10% TBE-Urea gel in the case of short fragments and hybridized with the oligonucleotide probes listed in the Table 2.3. The position of each probe and the RNA species they are designed to detect are shown at the right.

that exosome function is compromised in the absence of Rai1p, but remains intact in the absence of Kap123p. Interestingly, there was also a detectable increase in the 20S signal in cells lacking Kap123p, suggesting a weak 40S biogenesis defect. Together, these data suggest that the loss of Kap123p marginally alters both the 60S and 40S biogenesis pathways. However, because the rRNA processing defect in *rai1Δ* cells was not dramatically exacerbated or altered by the additional loss of Kap123p it is not likely that the genetic interaction between *kap123* and *rai1* is due to a catastrophic block in either the 40S or 60S assembly pathway.

The ribosome and polysome profiles from each relevant strain were also examined (Fig. 3.6). In agreement with the results of northern blotting analysis, *rai1Δ* cells also had a paucity of assembled 60S subunits. This was revealed by an overall decrease in the mature 60S:40S subunit ratio and by the accumulation of halfmers, small shoulders on 80S and polysome peaks, which result from kinetically stalled 40S subunits that have threaded onto mRNA but are unable to initiate translation due to a lack of cytoplasmic 60S subunits. In contrast, cells lacking Kap123p showed relatively normal polysome profiles. Interestingly, free 40S subunits and halfmers did not accumulate to the same extent in *kap123Δ/rai1Δ* cells as they did in *rai1Δ* cells suggesting that the 60S:40S subunit ratio was somehow normalized in *kap123Δ/rai1Δ* cells. This 'normalizing' effect of *KAP123* deletion was confirmed by analysis of the 60S:40S subunit ratios after sucrose density gradient centrifugation under low Mg^{2+} conditions (Fig. 3.6E). Nevertheless, *kap123Δ/rai1Δ* cells, like *rai1Δ* cells, showed a dramatic decrease in the total ribosomal content (Fig. 3.6). These data are consistent with the loss

Figure 3.6. Deletion of *RAI1* results in a specific 60S subunit assembly defect, while a *kap123Δ/rai1Δ* double mutant exhibits a decrease in the total ribosomal content. Polysome profiles for WT (A), *kap123Δ* (B), *rai1Δ* (C) and *kap123Δ/rai1Δ* (D) cells were obtained by fractionation of cell lysate supernatants on 7% - 42% sucrose gradients and monitoring the (OD 254 nm). The peaks corresponding to 40S, 60S, 80S and polysomes are indicated. Because the same amount of sample (as detected by OD_{260} nm) was loaded in each case, the peak heights are sensitive indicators of the levels of each subunit. The *rai1Δ* strain (C) exhibits a deficit of 60S particles as indicated by the reduction in free 60S subunits and the appearance of halfmers; in contrast, the ratio of 40S:60S particles was normalized in the double mutant *kap123Δ/rai1Δ*; halfmers were reduced, and there was a net decrease in the free subunit concentration. (E) 60S:40S subunit ratios were analysed in WT, *rai1Δ* and *kap123Δ/rai1Δ* strains by sucrose density gradient centrifugation under conditions of low Mg^{2+} concentration. Under these contitions assembled ribosomes separate into 40S and 60S subunits.

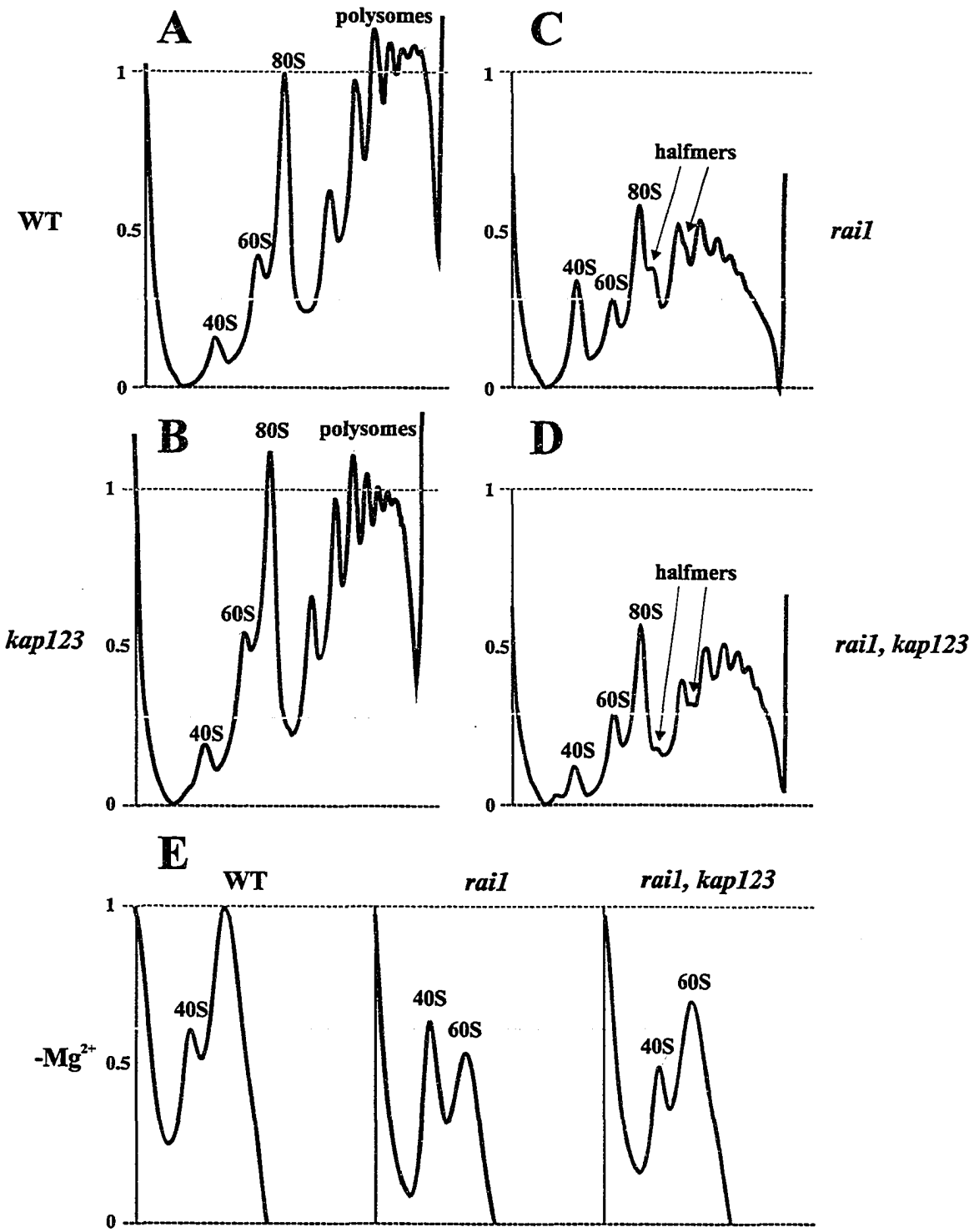

of Kap123p leading to an overall decrease in ribosome biogenesis efficiency, which is not specific to either subunit, but is upstream of Rai1p activity. Because Kap123p interacts with many early and late assembling ribosomal proteins, the observed epistasis likely reflects Kap123p's role in the import of many proteins required for optimal ribosome assembly, perhaps including early assembly factors.

3.6 60S subunit export is impaired in *rai1/kap123* cells

To further investigate this specific *rai1Δ/kap123Δ* genetic interaction, we examined the localization of GFP fusions of three large subunit ribosomal proteins. It has been shown previously that carboxy-terminal GFP tags of some 60S ribosomal subunit proteins are faithfully integrated into functional ribosomes (Hurt et al., 1999; Stage-Zimmermann et al., 2000); thus, plasmids encoding C-terminal GFP chimeras of rpL2, rpL3 and rpL25, were used. When expressed in wild-type cells, as shown for rpL2, each chimera cofractionated with 60S subunits in 7% - 42% sucrose gradients and yielded diffuse cytosolic GFP signals, thereby indicating that these fusions were integrated into 60S subunits (Fig. 3.7A). While GFP-chimera reporters showed normal cytoplasmic distributions in *rai1Δ* or *kap123Δ* cells, double null *kap123Δ/rai1Δ* strains exhibited a striking nuclear accumulation of the GFP signals from each 60S subunit reporter (Fig. 3.7B). A subset of *kap123Δ/rai1Δ* cells revealed an accumulation of the ribosomal-GFP reporters in the nucleolus, similar to the fluorescent signal from Nop1-GFP (Fig. 3.7B). The ratio of nuclear to cytoplasmic "60S" particles was quantified by isolating nuclei and comparing the abundance of 60S particles in the nuclear and cytoplasmic fractions by sucrose density gradient centrifugation under low Mg^{2+}

conditions (Fig. 3.8A). In addition, the presence of rpL3 in the nuclear and cytoplasmic fractions was assayed by western blotting (Fig. 3.8B). Taken together, these data suggest that the reporter proteins accumulated in the nucleus are assembled into pre-60S particles. Thus, *kap123Δ/rai1Δ* cells exhibit a 60S, post-assembly, nuclear export block that was not observed in cells harboring either mutation alone.

3.7 *NMD3* is a multicopy suppressor of sf17

The data presented above suggest that the genetic interaction between *kap123Δ* and *rai1Δ* is manifested at the late stages of 60S assembly. Because the only known role for Kap123p is in nuclear import, we hypothesized that an essential factor required for driving the export process was not imported efficiently in *kap123Δ* cells and that, in the absence of Rai1p, this factor becomes limiting. To investigate this possibility, sf17 cells were transformed with multicopy plasmids encoding two essential proteins required late in the 60S subunit assembly and export, Nmd3p (Eisinger et al., 1997; Ho et al., 2000b) and rpL10p (Gadal et al., 2001b), as well as the karyopherins Kap121p and Nmd5p. Interestingly, overexpression of *NMD3*, but not *RPL10*, *KAP121* or *NMD5*, was sufficient to rescue both the sectoring phenotype (Fig. 3.9A) and the FOA-sensitivity of sf17 cells (Fig. 3.9B).

To determine if the nuclear localization of Nmd3p was altered as a result of the loss of Kap123p, we assayed Nmd3p nuclear import in *kap123Δ* cells. Nmd3p is known to have both NLS and NES sequences (Gadal et al., 2001b; Ho et al., 2000b), which direct the shuttling of Nmd3p between the two compartments. Galactose-inducible GFP

Figure 3.7. Cells lacking both Kap123p and Rai1p are defective in 60S subunit export. (A) The faithful integration of GFP reporters into ribosomal particles was confirmed by sucrose gradient centrifugation and subsequent immunoblotting against GFP-tagged reporters and endogenous rpL3/Tcm1p as an internal control. Shown is the profile for rpL2-GFP which is present in 60S, 80S and polysome fractions, but not the 40S peak. rpL3-GFP and rpL25-GFP profiles were similar (data not shown). (B) The localization of ribosomal-GFP reporters and Nop1-GFP was determined by direct fluorescent microscopy of live cells. The fluorescent signals from ribosomal reporters were detectable throughout the cytosol in WT, *kap123Δ* and *rai1Δ* cells, but appeared to accumulate in the nucleus and in some cases in the nucleolus in *kap123Δ/rai1Δ* cells. Bar, 5 μm.

A

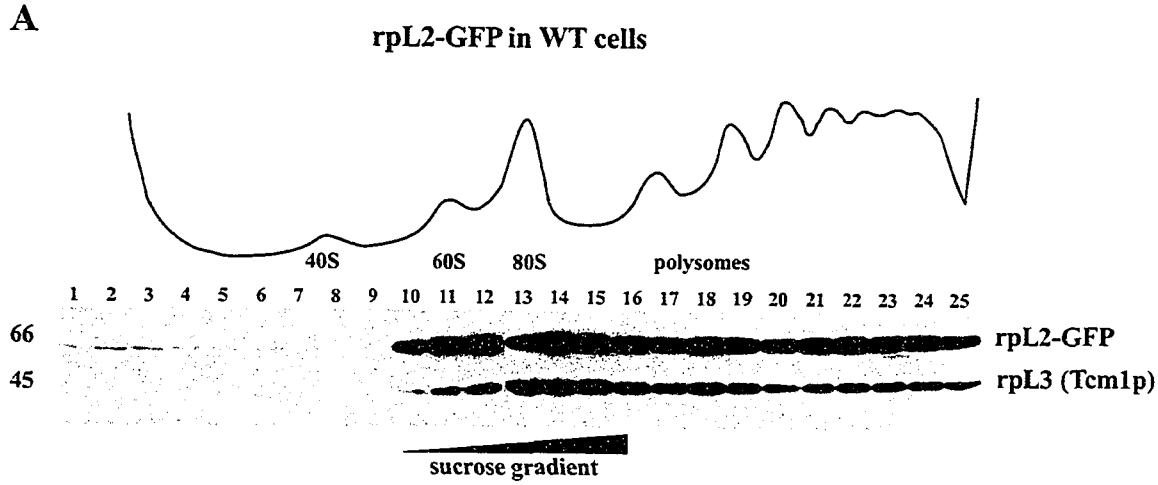

B

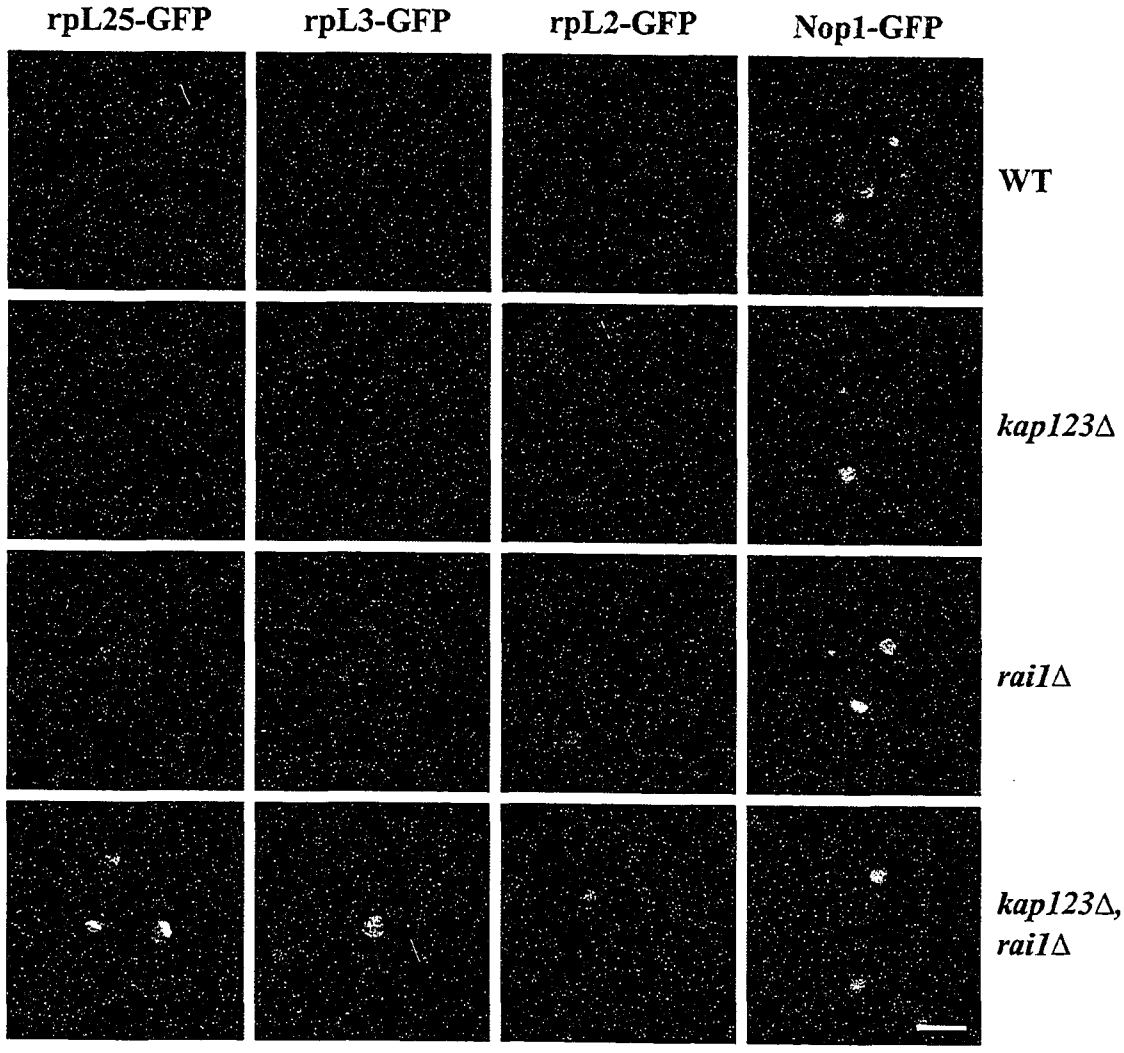

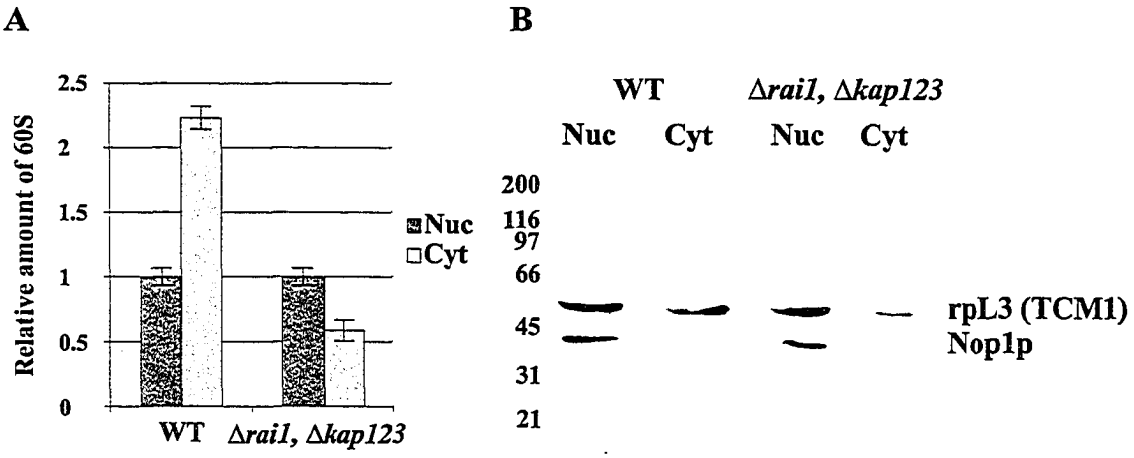

Figure 3.8. *kap123Δ/rail1Δ* strain accumulates assembled 60S subunits in the nucleus. (A) Nuclear and cytoplasmic fractions were isolated from WT and *kap123Δ/rail1Δ* cells and 60S components from each subcellular fraction were separated by further fractionation by sucrose gradient centrifugation under conditions of low Mg^{2+} concentration. Shown is a histogram of the amount of nuclear and cytoplasmic 60S subunits, quantified by OD_{254}. Data were normalized to the amount of 60S subunits in the nucleus. (B) Nuclear and cytoplasmic fractions at a 5:1 cellular equivalent load ratio were resolved by SDS-PAGE and probed with monoclonal anti-rpL3 (Tcm1p), as a marker for 60S subunits, and polyclonal anti-Nop1p antibodies, as a control. Results indicate a significant reduction in the levels of rpL3 in the cytoplasm of *kap123Δ/rail1Δ* strains, reflecting a block in 60S subunit export.

chimeras, containing either the NLS of Nmd3p or both the NLS and NES of Nmd3p (Nmd3-NLS-GFP and Nmd3-NLS/NES-GFP), were expressed in *kap123* and *kap95* mutant strains (Ho et al., 2000b). As shown in Fig. 3.9C, Nmd3-NLS-GFP was nuclear in wild-type cells, but mislocalized to the cytoplasm in *kap123Δ* cells. In contrast, the reporter remained nuclear in *kap95* cells, even after temperature shifts that have been shown to mislocalize cNLS reporters (Leslie et al., 2002).

These results suggest that, in addition to the previously reported role in the import of several ribosomal proteins, Kap123p also imports Nmd3p, an essential late acting assembly/export factor. The presence of a fraction of cells with some nuclear staining

Figure 3.9. Nmd3p links Kap123p to Rai1p. (A) Expression of *NMD3* restores sectoring to sf17 cells. sf17 cells were transformed with the plasmids shown and plated on YPD to assay sectoring. Only pNmd3p restored sectoring. (B) The sf17 strain (*kap123Δ/rai1-1*) or wild-type cells were transformed with a plasmid expressing *NMD3* or vector alone (pRS425). Growth of these strains on YPD (left) or 5'-FOA (right) revealed that the increased Nmd3p expression, due to the introduction of *NMD3* on a multicopy plasmid, rescued the growth defect associated with sf17 cells (*kap123Δ/rai1-1*). (C) GFP chimeras containing the Nmd3p NLS (aa 387-435) (Ho et al., 2000b) or the NLS plus an NES (aa 387-518) were localized in wild-type (W303), W303-derived *kap123Δ* or *kap95-14* mutant cells. The *kap123Δ* strain failed to localize the Nmd3p-NLS-GFP reporter to the nucleus, suggesting that Kap123p is required for efficient import of Nmd3p. The localization of GFP chimeras did not change in *kap95-14* mutant, indicating that Nmd3p NLS is specific to Kap123p. Bar, 5 μm.

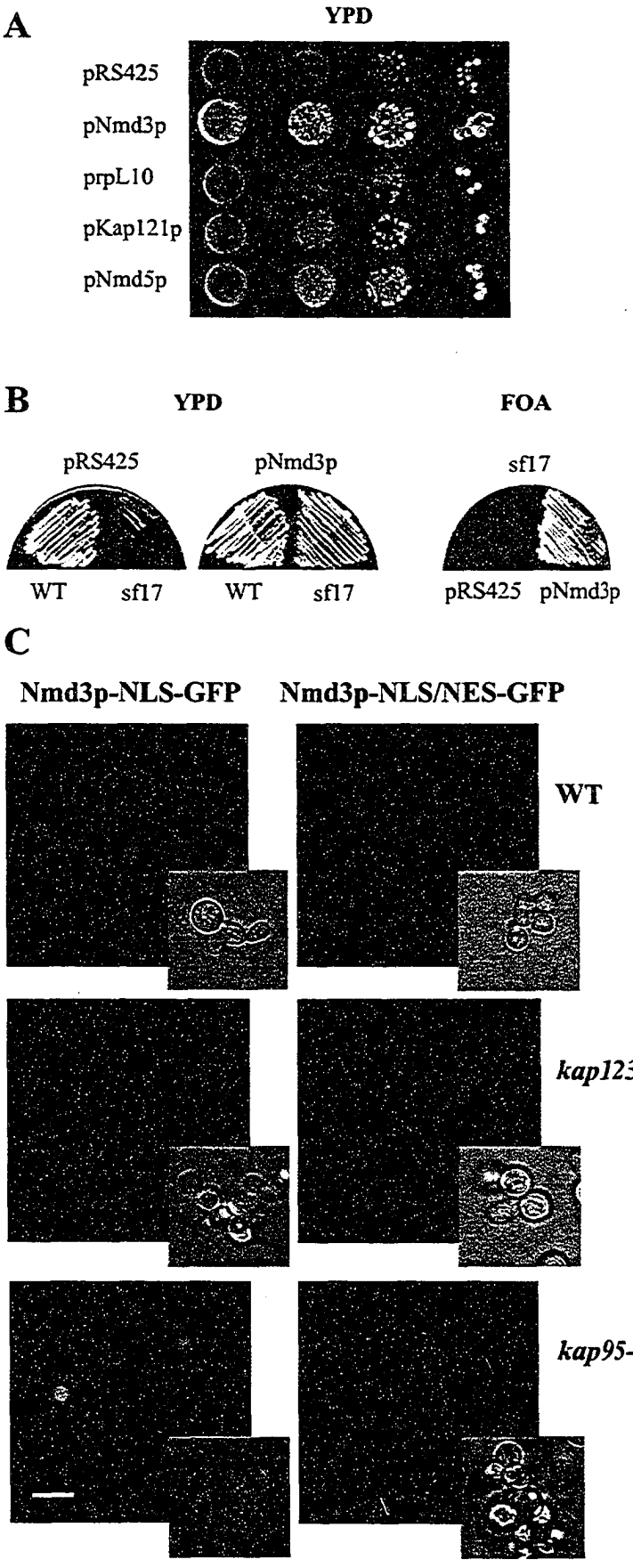

along with cytoplasmic staining in the *kap123Δ* background, suggests that Nmd3p, like other essential Kap123p cargoes, can enter the nucleus by alternate means, albeit with reduced efficiency. Under normal conditions, the import defect associated with the loss of Kap123p alone does not appear to significantly compromise ribosome biogenesis. However, in the absence of Rai1p, the limited nuclear quantities of late acting factors such as Nmd3p are not sufficient to support efficient export, leading to the accumulation of partly assembled 60S subunits in the nucleus and a growth defect that greatly exceeds that observed for either deletion alone.

3.8 Discussion

In this chapter I describe the identification and characterization of the gene *RAI1*, and its encoded ribosome biogenesis factor Rai1p. I also identify a genetic interaction between *RAI1* and the gene encoding karyopherin *KAP123* and propose a mechanism to explain the nature of this genetic interaction.

3.8.1 *KAP123* synthetic fitness screen

We used a synthetic fitness genetic screen to identify components that support Kap123p function and when mutated, render cells dependent on the presence of Kap123p. Not surprisingly, this screen yielded several karyopherins: Kap121p, Sxm1p/Kap108p and Nmd5p/Kap119p. Indeed, Kap121p has previously been shown to compensate for the loss of Kap123p likely by importing several ribosomal proteins in its absence (Rout et al., 1997; Schlenstedt et al., 1997). In addition, Sxm1p/Kap108p has previously been shown to interact physically with the ribosomal proteins rpL11A/B,

rpL25, and rpL31A/B (Rosenblum et al., 1997) and overproduction of this karyopherin suppresses a *kap121ts* mutant phenotype (Pemberton et al., 1998; Seedorf and Silver, 1997) suggesting further complementarity between Kap123p, Kap121p and Sxm1p/Kap108p. Moreover, the high degree of similarity between Sxm1p/Kap108p and Nmd5p/Kap119p (Albertini et al., 1998) and the identification of *NMD5* as genetically interacting with *KAP123* suggest a similar and likely overlapping function for this karyopherin. Interestingly, the use of several karyopherins to import different ribosomal proteins by yeast cells seems to be conserved in metazoans. Numerous vertebrate karyopherins, including Karyopherin β/Importin β, Kap β2/Transportin, RanBP5, RanBP7 and Importin 11 have been implicated in ribosomal protein import (Gorlich and Kutay, 1999). Furthermore, a metazoan Kap123p orthologue, Importin β4, has recently been characterized (Jakel et al., 2002). Thus, data from different systems suggest that ribosomal protein import and assembly make use of a variety of import (and export) karyopherins and that their functional overlap may permit the loss of individual factors. However, it remains unclear to what extent these karyopherins functionally overlap under normal conditions and whether this multiple redundancy is exploited by cells to globally control the transport of classes of different molecules.

3.8.2 Characterization of genetic interaction between *RAI1* and *KAP123*

Beyond redundant import pathways, the genetic screen revealed an interaction between the ribosome assembly factor *RAI1* and *KAP123*. In an attempt to understand the molecular basis for this interaction, we investigated how the loss of both proteins specifically affected the process of ribosome biogenesis. As shown previously, cells

lacking Rai1p revealed a 60S assembly defect, accumulating 27S rRNA and halfmers in polysome profiles. Remarkably, the loss of Kap123p had little affect on ribosome assembly or export as we detected no obvious rRNA accumulation or ribosomal subunit export defects in cells lacking Kap123p, but cells lacking both Rai1p and Kap123p displayed a more complex phenotype. These cells showed a moderate augmentation of the 27S rRNA defect, normalization of the 60S:40S ratio, an overall decrease in the number of ribosomes and an accumulation of assembled pre-60S subunits in the nucleus. Furthermore, although other karyopherins import ribosomal proteins, the genetic interaction between Rai1p and Kap123p was specific: out of the five yeast kaps tested, including all those known to import ribosomal proteins, only *KAP123* was able to rescue sf17 cells and only *kap123/rai1* mutants displayed pre-60S ribosomal subunit export defects. Together these data suggest that, in these cells, the 60S biogenesis program was attenuated at a late, post-assembly, pre-export step.

3.8.3 Elucidating the nature of *KAP123/RAI1* genetic interaction

It is evident that cells lacking Rai1p are defective in 60S assembly, but why should the additional loss of Kap123p, the only known function of which is in nuclear import, specifically cause an export defect? Consider ribosome assembly as a simple series of chemical reactions; the removal of products at each step contributes to the progression of the entire pathway. Alternatively, the failure to remove products at any step causes the accumulation of intermediates. Thus, considering that Rai1p interacts physically with Rat1p, a late acting exonuclease, and that Rai1p was detected associated with assembled pre-60S subunits, we hypothesized that protein(s) required at the late

stages of biogenesis are not imported efficiently in *kap123* strains, and that in combination with a mutation in *RAI1*, products downstream of Rai1p function were not efficiently processed to the next step, leading to the accumulation of (partially) assembled subunits. Thus we speculate that the specific genetic interaction observed between *KAP123* and *RAI1* is due to a reduced efficiency of 60S subunit assembly, contributed by a lack of Rai1p function, as well as an inability to import critical ribosomal assembly and export factors. Here we show that one such factor is Nmd3p. Overexpression of *NMD3* rescued the slow growth phenotype observed in sf17 (*rai1-1/kap123Δ*), *rai1Δ/kap123Δ* and *rai1Δ* cells (data not shown) and direct visualization of GFP chimeras containing either Nmd3p NLS or Nmd3p NLS/NES demonstrated that efficient Nmd3p import into the nucleus requires Kap123p. While the mislocalization of Nmd3p is evident in *kap123* cells, deletion of *NMD3* is lethal. Thus, it is likely that other factors can also import Nmd3p in the absence of Kap123p. Furthermore, it is also likely that inefficient import of other factors contribute to the genetic interaction observed here. One such candidate is rpL10, also a late acting assembly/export factor for 60S subunits imported by Kap123p (Gadal et al., 2001b). Nevertheless, because *NMD3*, but not *RPL10*, expression is sufficient to suppress the growth defects associated with *rai1/kap123* cells, it is apparent that Nmd3p mislocalization is a primary cause of the *rai1/kap123* genetic interaction.

Surprisingly, among the mutants assayed, only *rat1-1* cells mislocalized Rai1p-GFP from the nucleus to the cytoplasm. Considering the tight *in vitro* binding between Rat1p and Rai1p (Xue et al., 2000), we propose that the steady state localization of Rai1p to the nucleus is a result of its interaction with Rat1p. Furthermore, it is interesting to speculate that Rai1p may be used by Rat1p to tether the assembling subunit, but that in

the absence of a functional Rat1p, Rai1p may exit the nucleus with the ribosomal subunit. It has previously been shown that loss of active Rat1p can be complemented by directing Xrn1p, a normally cytoplasmic exonuclease, to the nucleus (Johnson, 1997). It is not yet known if quality control mechanisms exist to prevent incompletely assembled ribosomal subunits from exiting the nucleus, but it seems possible that under conditions in which Rai1p becomes cytoplasmic, the subsequent maturation of unprocessed rRNA could occur in the cytoplasm, under the direction of Xrn1p. It will be interesting to determine if the function of Xrn1p is also augmented by Rai1p and if the export defect observed here also results from an active quality control mechanism.

The synthetic fitness screen employed here revealed a complex genetic interaction between *KAP123*, a nuclear import factor, and *RAI1*, a ribosome biogenesis factor, which manifests itself in a ribosome subunit export defect. The data support a model in which a cause of the defect is an inability to import sufficient quantities of the essential export factor Nmd3p to overcome the loss of Rai1p (Fig. 3.10). The findings presented here underscore the integration of ribosome assembly and nucleo-cytoplasmic exchange; however, a good understanding of the entanglement between these two pathways demands further identification and characterization of ribosome assembly factors and an understanding of their relationships with the nuclear import/export apparatus.

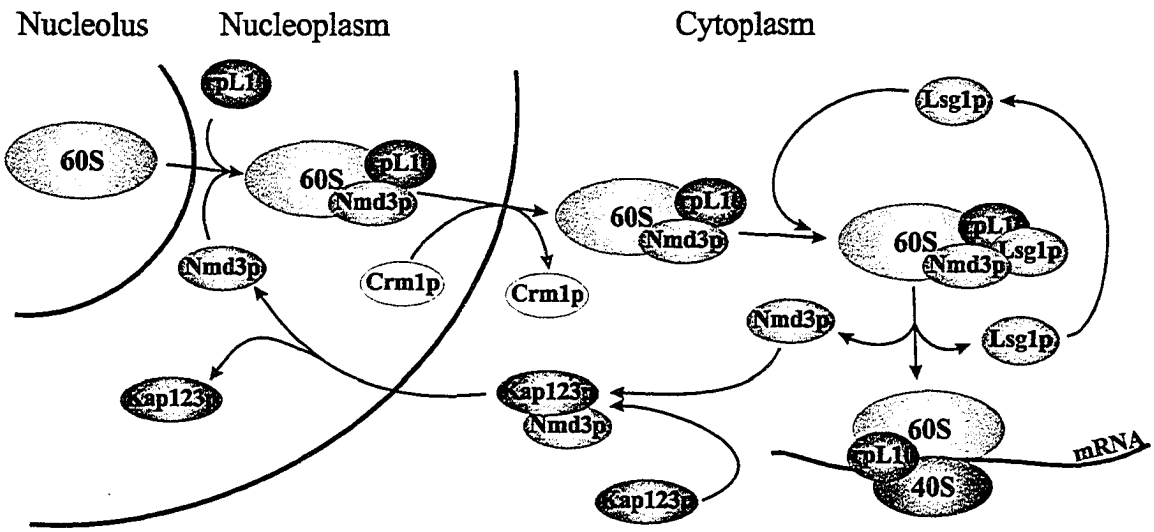

Figure 3.10. The model of the 60S subunit export pathway in *S. cerevisiae* explaining the role of Kap123p in the recycling of Nmd3p. See section 3.8.3 for discussion.

Chapter 4

Nop53p is a novel nucleolar 60S ribosomal subunit biogenesis protein

The data presented in this chapter have previously been published as "Nop53p is a novel nucleolar 60S ribosomal subunit biogenesis protein" (Yaroslav Sydorskyy, David J. Dilworth, Brendan Halloran, Eugene C. Yi, Taras Makhnevych, Richard W. Wozniak and John D. Aitchison. 2005. Biochem. J. 23:2042-2054).

4.1 Overview

In this chapter I describe the identification and characterization of a novel *S. cerevisiae* ribosome biogenesis factor which we have named Nop53p (Ypl146p). Using a set of classical genetic, protein biochemistry and RNA analysis methods we demonstrate a crucial role for Nop53p in 60S subunit biogenesis. Specifically, Nop53p physically interacts with the rRNA processing factors Cbf5p and Nop2p when immunopurified from a nuclear fraction, and cofractionates with pre-60S particles on sucrose gradients. Deletion or mutations within *NOP53* cause dramatic growth defects and display significant 60S subunit deficiencies, and an imbalance in the 60S:40S ratio, as revealed by polysome profiling. A lack of functional Nop53p also causes defects in progression beyond the 27S stage of 25S rRNA maturation during 60S biogenesis, as detected by metabolic labeling, primer extension and northern analysis.

4.2 Deletion of *NOP53* results in a severe growth defect

The protein encoded by the ORF YPL146c was initially identified by proteomic analysis of a highly enriched subcellular fraction of yeast NPCs (Aitchison et al., 1995b). In that screen for potential nucleoporins, Ypl146p was localized primarily to a portion of the nucleus, which was reminiscent of a nucleolar signal, suggesting that Ypl146p was not a nucleoporin, but likely a contaminant of the NPC fraction. Based on further characterization of Ypl146p including its localization, function, and predicted molecular mass, we have named Ypl146p, Nop53p.

Analysis of the Nop53p sequence indicated that the protein is well-conserved from yeast to humans (Fig. 4.1A). Nop53p was subjected to structural prediction analysis

using Robetta (Chivian et al., 2003) which predicted the presence of a large central coiled coil domain that matched several proteins containing this signature structure of myosin heavy chain (http://robetta.bakerlab.org/results.jsp?id=4479&p=1). Proteins with this signature tend to play structural roles. Interestingly, the C-terminal region (amino acid residues ~380-450) did not conform to this family, but contained the highest primary sequence similarity to a putative human orthologue (Glioma tumor suppressor candidate region 2; GTSCR2). Modeling of this domain predicted a leucine zipper motif (amino acid residues 402-434), which we targeted during characterization (see below).

In order to examine the function of Nop53p in vivo, we created a null mutant by targeted gene disruption. In contrast to a previous finding from a yeast high-throughput study (Winzeler et al., 1999), the resulting haploid null mutants were viable, exhibiting growth at all temperatures tested. However, the growth rate of the null mutant was severely impaired, indicating that while not essential for cell survival on rich medium, Nop53p is critical for normal growth and its loss renders cells extremely unfit (Fig. 4.1B). Indeed, log-phase *nop53Δ* cells growing in liquid rich medium exhibited an 8-fold increase in doubling time relative to wild-type cells (12 hours for *nop53Δ* cells compared to 90 min for wild-type cells). This generalized growth defect observed in the *nop53Δ* strain was completely rescued after introduction of a plasmid expressing wild-type *NOP53* under the control of its endogenous promoter (Fig. 4.1B). Moreover, C-terminally tagged protein A and GFP versions of Nop53p chimeras, integrated into the *NOP53* locus, also grew at wild-type rates (Fig. 4.1B) indicating functional complementation by the tagged versions of Nop53p used in this study. In order to create a strain with a less severe growth defect, we also deleted the C-terminal region of

Figure 4.1. Nop53p is a non-essential protein that localizes to the nucleolus. (A) Structural prediction analysis using Robetta (http://robetta.bakerlab.org/) indicated that Nop53p is a well-conserved from yeast to humans. Shown are the Blast alignments from the Ginzu program that predicted the presence of a large central coiled-coil domain that matched several proteins containing this signature structure of myosin heavy chain (middle, grey). Ten proteins with the highest Blast scores are listed beneath (bottom). Basic secondary structure elements were detected by SEG (Wootton and Federhen, 1996), COILS (Lupas et al., 1991), DISOPRED (Jones and Ward, 2003), PsiPred (Jones, 1999), Target99 (Karplus et al., 1998) and JUFO (http://www.jens-meiler.de/) prediction methods. Low complexity strands are represented in light-grey, coiled–coils in dark-grey, disordered strands in black, alpha helices and beta strands in red and blue, respectively (top). (B) Cells lacking the *NOP53* ORF (*nop53Δ*) are viable but exhibited a strongly reduced growth rate compared to wild-type (WT) cells on rich media. Strains expressing genomically encoded GFP or protein A chimeras of Nop53p showed growth rates similar to those of wild type cells, indicating that these fusion proteins are functional. The *nop53-ΔC* strain, expressing a truncation mutant of *NOP53* lacking C-terminal 56 amino acids, also showed a growth defect, but it was less dramatic than that of the *NOP53* knockout. Introduction of a plasmid expressing wild-type *NOP53* under the control of its endogenous promoter was able to rescue the slow growth phenotype of the *nop53Δ* strain. (C) Double labeling fluorescence micrographs of live cells expressing Nop53p-GFP and the nucleolar marker Nop1p-RFP. Note the colocalization of Nop53p-GFP with the Nop1p-RFP. Bar, 5 μm.

A

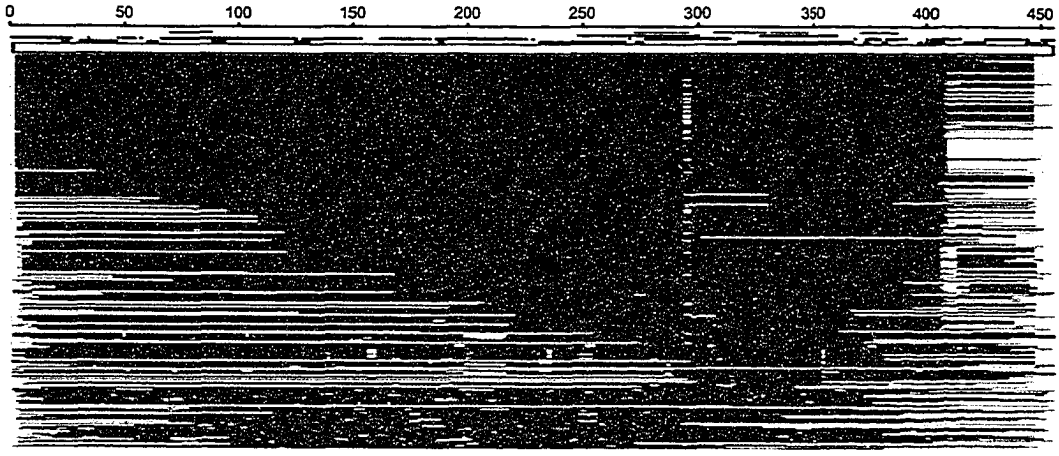

NCBI taxon. ID	Species	PSI-Blast E value	Description
10090	Mus musculus	2.00E-60	Myosin heavy chain IIB
9031	Gallus gallus	3.00E-60	Myosin heavy chain, fast skeletal muscle
10116	Rattus norvegicus	1.00E-59	Similar to myosin heavy chain 2b
9823	Sus scrofa	1.00E-59	Myosin heavy chain 2b
10118	Rattus sp.	5.00E-59	Myosin heavy chain
7962	Cyprinus carpio	5.00E-59	Myosin heavy chain, fast skeletal muscle
8400	Rana catesbeiana	8.00E-59	Myosin heavy chain
9913	Bos taurus	1.00E-58	Myosin, heavy polypeptide 1, skeletal muscle
9796	Equus caballus	1.00E-58	Myosin heavy chain 2a
9606	Homo sapiens	1.00E-58	Myosin, heavy polypeptide 1, skeletal muscle

B

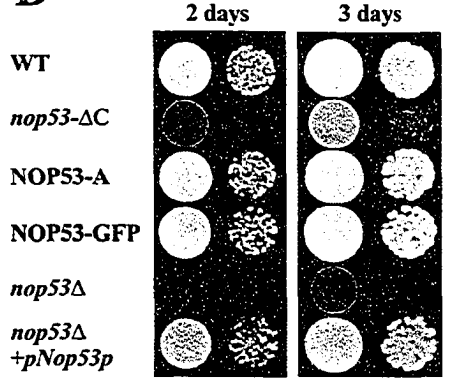

C

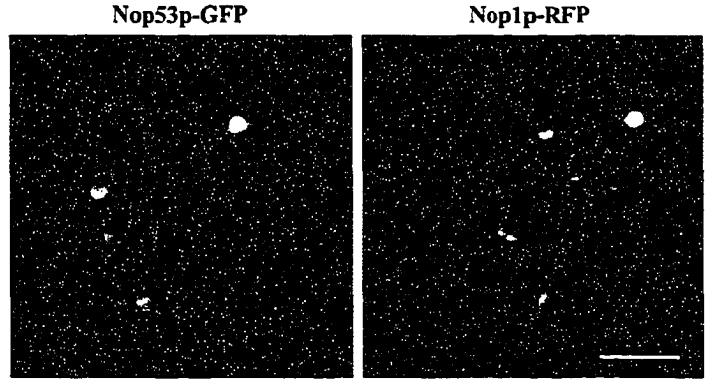

Nop53p which contains the predicted leucine zipper and is the region of highest identity with the human protein, GTSCR2. Indeed, deletion of the C-terminal 56 amino acids of Nop53p (*nop53-ΔC*) yielded a phenotype intermediate between that of the wild-type and *nop53Δ* strains in terms of growth (Fig. 4.1B) and other aspects of Nop53p function (see below).

To monitor the localization of Nop53p in live cells, Nop53p-GFP was observed by fluorescence microscopy. In agreement with our preliminary analysis (Rout et al., 2000) Nop53p-GFP was localized predominantly to the nucleolus as detected by colocalization with the nucleolar protein Nop1p-RFP (Fig. 4.1C). However, it should be noted that Nop53p-GFP was not exclusively nucleolar. By comparison to Nop1p-RFP, Nop53p-GFP showed a significant nucleoplasmic signal suggesting that the protein may perform part of its function outside the confines of the nucleolus.

To gain insight into the function of Nop53p, we attempted to identify proteins with which it physically interacts (performed by David Dilworth). To do this, nuclei were isolated from strains producing a Nop53-protein A (Nop53p-pA) chimera as the only version of Nop53p in the cell. Nuclei were lysed, the extract was incubated with IgG Sepharose, and associated proteins were eluted from the resin with a gradient of $MgCl_2$. Proteins from each fraction were separated by SDS-PAGE and identified by tandem mass spectrometry of excised gel slices (Fig. 4.2) (Sydorskyy et al., 2003). In addition to Nop53p, four prominent bands above the 31 kDa protein marker were identified: Cbf5p, Nop2p, Fpr3p and Fpr4p. All four proteins have been localized to the nucleolus and have been implicated in ribosomal biogenesis. Fpr3p and Fpr4p are members of the FKBP (FK506-binding protein) family, and are predicted to have peptidyl-prolyl cis-trans isomerase activity (Dolinski et al., 1997; Shan et al., 1994). Cbf5p is an essential protein, and is proposed to function in snoRNA-guided uridine to pseudouridine conversions in rRNA (Cadwell et al., 1997; Lafontaine et al., 1998). Nop2p is also essential, is implicated in 60S ribosomal subunit maturation, and is

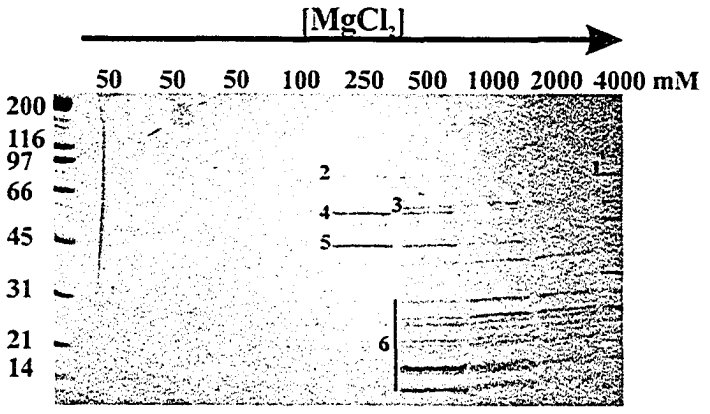

Figure 4.2. Nop53p physically interacts with rRNA processing factors involved in pre-60S ribosomal subunit biogenesis. Nop53p was immunopurified from a nuclear fraction prepared from cells expressing a Nop53p-pA chimera. Proteins bound to Nop53p-pA were eluted with $MgCl_2$ at increasing concentrations and analyzed by SDS-PAGE followed by Coomassie blue staining. The $MgCl_2$ concentrations are noted above each lane. Molecular mass standards are shown at left. Proteins corresponding to the numbered bands were identified by tandem mass spectrometry of excised gel slices. Bands 1 through 5 were identified as Nop53p, Nop2p, Cbf5p, Fpr3p and Fpr4p, respectively. Proteins that migrated below the 31kDa marker (band 6) were excised together and contained numerous 40S and 60S ribosomal subunit proteins.

proposed to have RNA m(5)C-methyltransferase activity (Hong et al., 1997; King and Redman, 2002). In addition to these four ribosome biogenesis factors, mass spectrometry also identified several ribosomal proteins that migrated below the 31 kDa protein marker. Together, these data suggest that Nop53p associates with assembling ribosomal precursors.

To further investigate this possibility, we examined whether Nop53p was directly associated with ribosomes. For these experiments, whole cell lysates were made from cells expressing Nop53p-pA and separated into ribosomal subunits, mature 80S ribosomes and polysomes by sucrose density gradient centrifugation. The gradient was fractionated and simultaneously monitored by recording the OD_{254} (Fig. 4.3A). Proteins

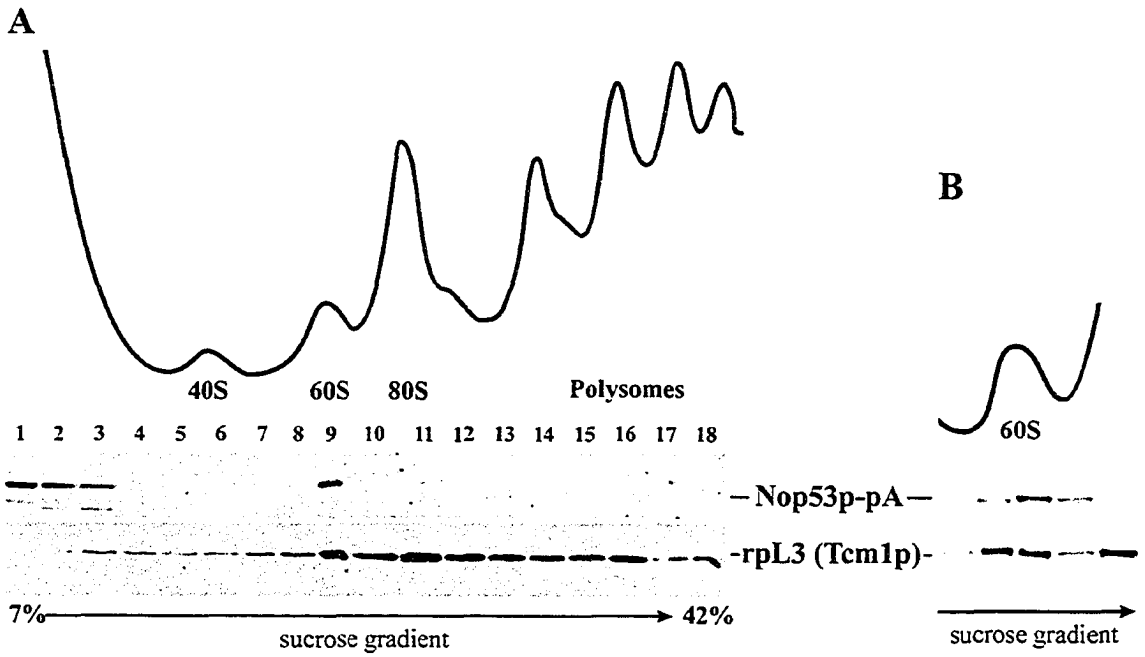

Figure 4.3. Nop53p cofractionates with 60S ribosomal subunits. (A) Yeast lysates from cells expressing Nop53p-pA were fractionated on a linear 5-42% sucrose gradient and monitored by OD_{254} to identify ribosomal fractions (upper trace). Peak fractions are labeled. Fractions derived from the gradient were analyzed by western blotting (lower panel) using monoclonal antibodies against rpL3 (Tcm1p) to detect 60S-containing fractions and rabbit IgG to detect Nop53p-pA. Note that Nop53p-pA cofractionated with the 60S ribosomal subunit peak but not with 40S subunits, assembled 80S ribosomes or polysomes. (B) Further resolution of the 60S region of the gradient. Shown is the relevant region of a sucrose gradient similar to that shown in A, but subjected to longer centrifugation. Note that the peaks of rpL3 (Tcm1p) and Nop53p-pA do not precisely coincide.

in each fraction were analyzed by western blotting using rabbit IgG to detect Nop53p-pA and the monoclonal antibody, anti-Tcm1p (see Table 2.2), directed against the 60S subunit protein rpL3p. Nop53p-pA was detected in the load fraction and associated with unassembled 60S subunits, but was absent from fractions containing 40S subunits, 90S precursors, 80S mature ribosomes and polysomes. Moreover, upon further resolution of the 60S region of the sucrose gradient (Fig. 4.3B), it became apparent that Nop53p associates only with a subset of free 60S subunits. These data suggest that Nop53p

associates with immature 60S subunits after processing of 90S precursors to precursors of the small and large subunits, but is not retained upon its further maturation and assembly into functional 80S ribosomes. These data are consistent with the mass-spectrometric identification of Nop53p (Ypl146p) among several proteins associated with the 60S pre-ribosomal particle (Bassler et al., 2001; Nissan et al., 2002; Saveanu et al., 2003).

4.3 Nop53p is involved in 60S pre-ribosome biogenesis and rRNA processing

To investigate a potential role of Nop53p in ribosome biogenesis, ribosome profiles were obtained from wild-type and *nop53Δ* strains. *nop53Δ* cells showed a dramatic paucity of assembled 60S subunits, revealed by a significant decrease in the mature 60S:40S subunit ratio and by the low 80S and polysome peaks (Fig. 4.4). Wild-type cells displayed a typical distribution of 40S, 60S, and 80S particles and polysomes. By comparison, the profiles from *nop53Δ* cells suggested dramatic defects in 60S biogenesis. The 60S:40S ratio was much lower than that found in wild-type cells, and the abundance of 80S ribosomes and polysomes was dramatically decreased. In addition, shoulders on the 80S and polysome peaks were evident in the profiles. This feature is indicative of halfmers, or stalled 40S subunits that accumulate due to a lack of 60S subunits available to complete ribosome assembly. Profiles from *nop53ΔC* cells exhibited similar features including an imbalance in the 60S:40S ratio, reduced ribosomes and polysomes and the presence of halfmers, albeit, not as dramatically as exhibited by cells completely lacking Nop53p. Importantly, the profiles were normal in haploid cells

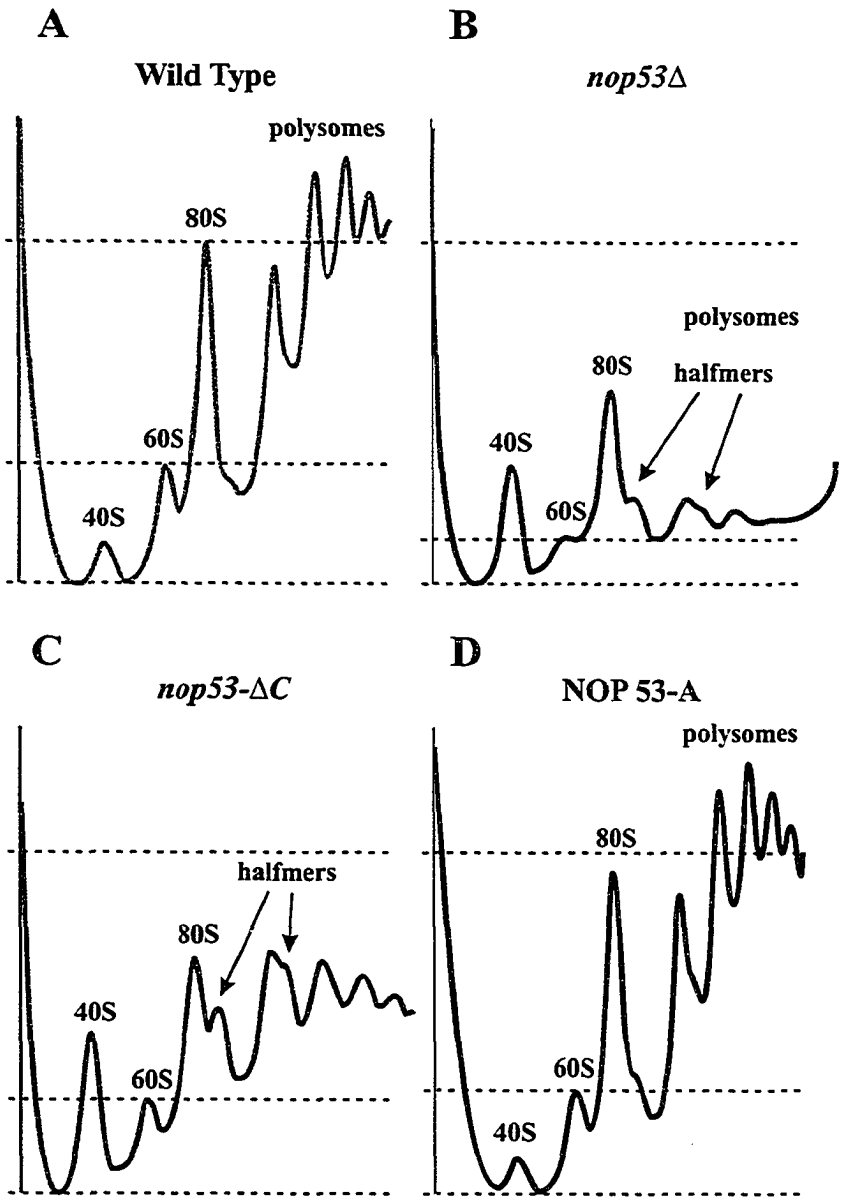

Figure 4.4. Deletion of *NOP53* results in a 60S subunit assembly defect. Polysome profiles for wild-type (A), *nop53Δ* (B), *nop53-ΔC* (C) and *NOP53* genomically tagged with protein A (NOP53-A) (D) were obtained by fractionation of cell lysates on 7-to-42% sucrose gradients and monitoring the optical density at 254 nm. The peaks corresponding to 40S, 60S, 80S and polysomes are indicated. Loads were normalized by OD_{260} prior to fractionation; thus, peak heights are sensitive indicators of the levels of each subunit. The dashed lines indicate the abundance of 80S ribosomes in the wild-type strain. The *nop53* mutant strains (B and C) exhibited a deficit of 60S particles as indicated by the reduction in free 60S, 80 and polysomes, and by the appearance of halfmers. The polysome profile of the NOP53-A strain (D) was indistinguishable from that of the wild-type strain.

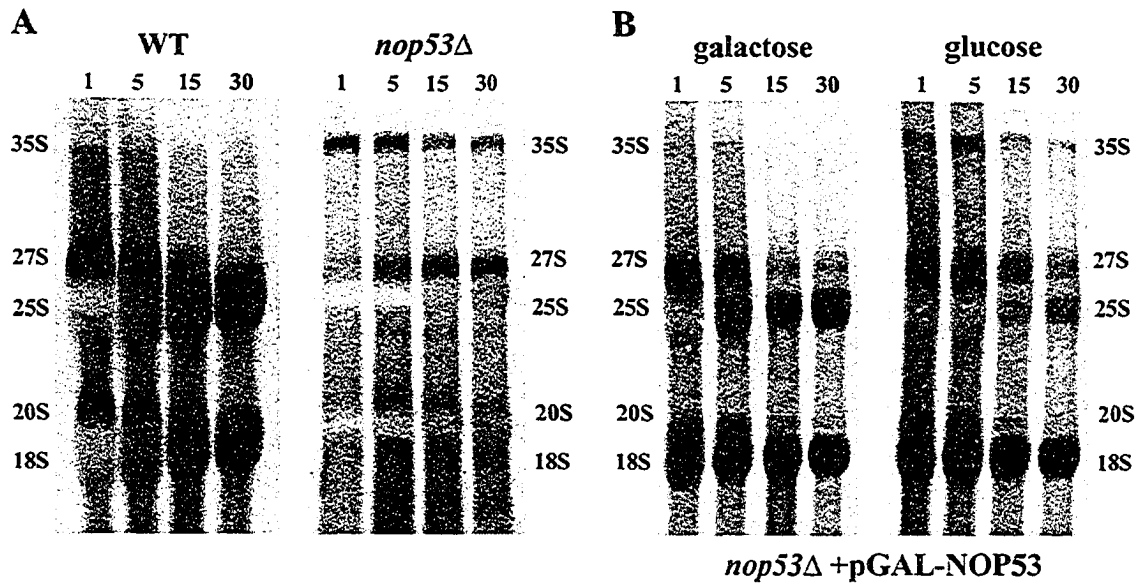

Figure 4.5. Pulse-chase analysis of RNA from *nop53Δ* cells (A) or from cells depleted of Nop53p (B). (A) RNA from wild-type (WT) and *nop53Δ* cells was metabolically labeled with [^{3}H] uracil for 1 min followed by a chase with excess unlabeled uracil for 1, 5, 15 and 30 min (noted above each lane). For each lane, RNA corresponding to 50 000 cpm of starting material was separated on a 1.3% formaldehyde agarose gel prior to autoradiography. (B) *nop53Δ* cells expressing pGAL-NOP53 were grown in either galactose or glucose for 14 hours prior to pulse-chase analysis. The major rRNA species are marked. Cells lacking Nop53p exhibited defects in 27S to 25S processing as indicated by the absence of labeled 25S rRNA and accumulation of the larger 35S and 27S precursor species.

containing Nop53p-pA (Fig. 4.4D) and Nop53p-GFP (data not shown) chimeras as the sole versions of Nop53p, or in *nop53Δ* cells expressing *NOP53* from a plasmid (data not shown).

As the biogenesis of ribosomes is inextricably linked to the complex processing of rRNA we evaluated rRNA processing through pulse-chase, northern hybridization and primer extension analyses (Fig. 4.5 and 4.6) in the presence or absence of Nop53p. The pulse-chase labeling with [^{3}H]-uracil showed that strains lacking Nop53p accumulated pre-rRNA at the 35S and 27S stages (Fig. 4.5A), indicative of a 27S to 25S processing

defect (Fig. 4.3A). Similar results were obtained through depleting Nop53p by controlling its expression using a *GAL1* promoter and repressing the promoter by shifting cells to glucose as the sole carbon source (Fig. 4.5B). In these experiments, there was no evidence of a dramatic perturbation of the 18S biogenesis pathway. In agreement with the ribosome and polysome analyses, such an rRNA processing defect is expected to lead to the observed 60S abnormalities (Venema and Tollervey, 1995). This is similar to the previously observed defects upon loss of Nop2p (Hong et al., 2001), which we detect in association with Nop53p.

Northern blotting was performed using probes designed to identify different intermediates in the processing pathway and thus to reveal rRNA processing defects. Consistent with the pulse-chase results and polysome profiles, the *nop53* strains were unable to produce normal amounts of mature 25S rRNA. An analysis of the intermediates in *nop53* cells revealed an accumulation of 35S and 27S precursors, with a corresponding decrease in 32S and 25S species (Fig. 4.6B). This pattern is typical of mutants with defects early in the processing of rRNA (sites A_0, A_1, A_2 and A_3) or in the processing of the internally transcribed spacer 2 (ITS2) at sites C_1 and C_2. *nop53* cells also accumulated 5'-A_0 fragments along with 7S precursors (Fig. 4.6C), suggesting that exosome function is compromised in the absence of Nop53p (Allmang et al., 2000; de la Cruz et al., 1998). As predicted by results from polysome fractionations and pulse-chase analyses, the biosynthesis of the 40S subunit was relatively normal and we detected no accumulation of the 23S and 20S precursors of the 18S rRNA (Fig. 4.6B).

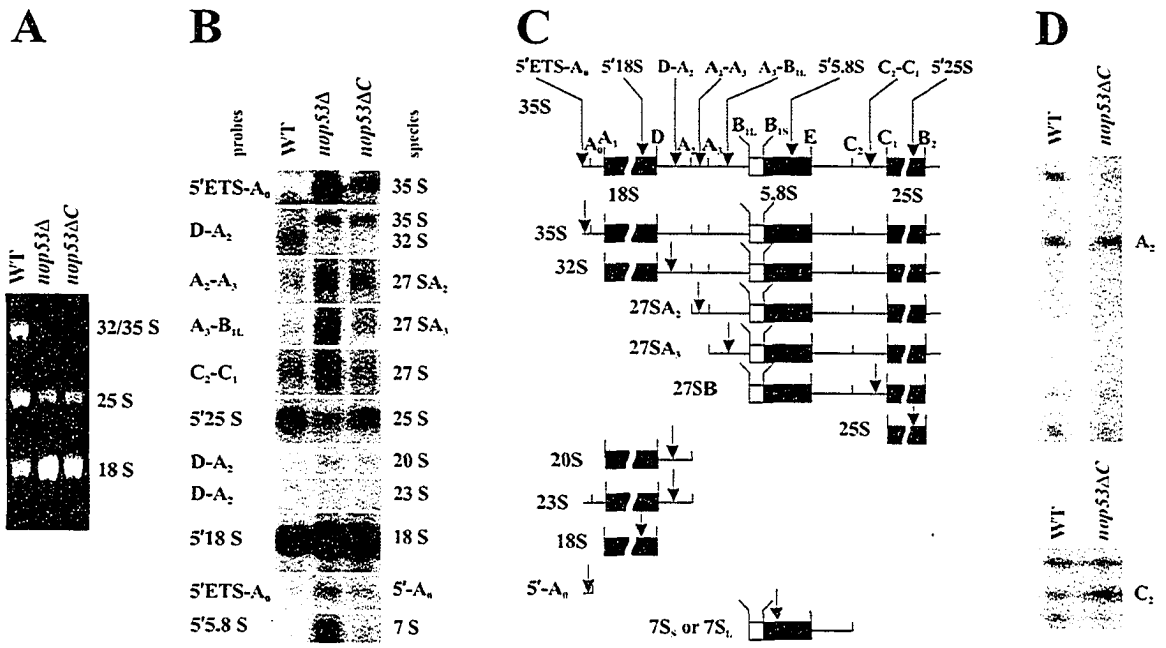

Figure 4.6. Northern hybridization and primer extension analyses reveal defects in rRNA processing in *nop53Δ* and *nop53-ΔC* strains. (A) Total RNA isolated from wild-type (WT) and *nop53Δ* and *nop53-ΔC* cells was separated on a 1.4% formaldehyde-agarose gel and visualized by ethidium bromide staining. To normalize the 18S signal between wild-type and *nop53* strains 2.5 and 2–fold more OD_{260} units were loaded from *nop53Δ* and *nop53-ΔC* cells respectively, relative to wild-type cells. Note that the intensities of the 25S and 32S bands are less in *nop53* cells. (B) Northern analysis of rRNA processing in *nop53* strains shows a specific 60S subunit defect. A gel identical to that shown in panel A was analyzed by northern blotting using oligonucleotide probes used to detect specific rRNA species. The sequences of the probes are listed in Table 2.3. The position of each probe and the rRNA species it is designed to detect are shown in the diagram of probe positions and pre-rRNA processing intermediates (Panel C). Note the accumulation of the steady-state levels of the 35S, 27S and 7S species in *nop53* cells and a decrease in 32S and 25S levels indicating defects in 60S processing. (D) Primer extension analyses were performed on the wild-type and *nop53-ΔC* strains. Analysis through ITS1 was done using a 5' 5.8S primer (marked with * in panel C), which hybridizes within mature 5.8S rRNA, while analysis through ITS2 was done using a 5' 25S primer (marked with * in panel C), that hybridizes within the mature 25S rRNA. Note that the ITS1 and ITS2 regions of the 35S rRNA transcript were not efficiently processed in *nop53* cells as evidenced by the increased A_2 and C_2 signal.

Primer extension studies were also performed to specifically detect the accumulation of uncleaved precursors in the internally transcribed spacers ITS1 and ITS2. Because sufficient high quality RNA could not be isolated from *nop53Δ* cells, *nop53-ΔC* cells were used for this analysis. In these cells primer extension through ITS1 and ITS2 revealed an accumulation of the products cleaved at sites A_2 and C_2 (Fig. 4.6D). These sites are present in the $27SA_2$ and 26S species and are often abundant in 25S deficient mutants (Fig. 4.6C) (Venema and Tollervey, 1995); thus, Nop53p affects events at this stage of ribosome biogenesis as well as earlier events. In the aggregate these results suggest that Nop53p is required for efficient 60S biogenesis and that this manifests primarily by an accumulation of 27S processing intermediates.

4.4 Discussion

Ribosome biogenesis is a temporally and spatially regulated assembly process involving the coordinated activity of numerous protein and nucleic acid cis- and trans-acting factors. In this chapter, we have investigated the role of *S. cerevisiae* Nop53p, a highly conserved eukaryotic ribosomal biogenesis factor. Nop53p is primarily localized to the nucleolus and associates with assembling 60S ribosomal subunits after cleavage of the 90S precursor. Nop53p sediments with ~60S particles, immunopurifies with other ribosome biogenesis factors and loss of Nop53p results in a dramatic decrease in the abundance of mature 60S ribosome subunits, an accumulation of halfmers, but relatively little change in 40S subunit levels. Because Nop53p was absent from the cytoplasm by fluorescence microscopy and from 80S ribosome or polysome fractions, it appears that Nop53p associates early with the assembling 60S subunit following cleavage of the 35S

rRNA / 90S pre-ribosome complex and leaves the assembling 60S complex prior to formation of the mature 80S ribosome.

Large scale interaction studies based on affinity purifications followed by mass spectrometry have detected Nop53p (Ypl146p), and numerous other proteins, in association with several pre-60S biogenesis factors including Nsa3p, Nug1p, Rix1p, Sda1p and Arx1p, Rpl24p, and Nog1p (Bassler et al., 2001; Nissan et al., 2002; Saveanu et al., 2003). In addition, Nop53p was absent from fractions associated with 90S or 40S pre-ribosomal components (Grandi et al., 2002; Schafer et al., 2003). The detection of Nop53p with numerous different 60S biogenesis factors suggests that Nop53p may be associated with a large multicomponent complex, or may bind to several different complexes during the biogenesis of 60S subunits. Our results suggest that one such complex contains Cbf5p, Nop2p, and Fkb3p and Fkb4p each of which was detected associated with Nop53p isolated by affinity purification. These four proteins also appear to be among the most tightly associated with Nop53p as they were resistant to extensive washing of the Nop53p-pA complex with an increasing concentration of $MgCl_2$. Taken together, the abundance of interaction data from this study and others clearly place Nop53p in the 60S biogenesis pathway.

In agreement with this role for Nop53p, pulse-chase and northern blotting revealed that the most dramatic defect in *nop53* cells was in 27S processing to the mature 25S rRNA species. The concomitant accumulation of 35S species is common to 27S processing defects and was also observed in *nop53* cells. Moreover, primer extension analysis also showed defects in processing of $27SA_2$ to 25S. Cells were inefficient in processing both the A_2 and C_2 intermediates, although there was no obvious

accumulation of A_0 or A_1, which are processed quickly, prior to the formation of the 27S intermediate. This is similar to the situation with Nop2p, which we found tightly associated with Nop53p. In particular, the paucity of 60S subunits and the accumulation of 35S and 27S rRNA species are similar phenotypes to those observed upon the loss functional Nop2p (Hong et al., 1997; 2001). Indeed, Nop2p is absolutely required for A_0 processing as well as for efficient A_1 and A_2 processing (Beltrame et al., 1994). While, these steps were the most sensitive to Nop53p (or Nop2p) loss, *nop53* mutants had an overall decrease in the levels of rRNA, suggesting general defects as well as stage-specific defects. This could result from the specific involvement of Nop53p in many different events of 60S processing, and/or the loss of additional proteins (such as the Nop53p-interactors Nop2p and Cbf5p) (Venema and Tollervey, 1999). For example, both Nop2p and Cbf5p are involved in snRNP guiding and base-specific rRNA modifications (pseudouridine formation and 2'-O-ribose methylation, respectively). Lack of pseudouridines or 2'-O-methyl modifications of both rRNA and snoRNAs can slow down or prevent multiple rRNA processing steps leading to general rRNA and ribosome defects (Tollervey et al., 1993; Venema and Tollervey, 1999). rRNA undermodification has also been shown to reduce the efficiency of Rat1p exonuclease activity, perhaps by a quality control mechanism (Venema and Tollervey, 1999). The 5' to 3' exonuclease activity of Rat1p is responsible for $A_3 \rightarrow B1$ trimming ($27SA_3 \rightarrow 27SB$) and $C_2 \rightarrow C_1$ trimming ($25.5S \rightarrow 25S$) (Geerlings et al., 2000). The accumulation of intermediate cleavage products C_1 and possibly A_2 (precursors to 5.8S/25S), revealed by primer extension, may be an indirect result of Nop53p loss leading to inefficient Rat1p function.

Interestingly, similar C_2-C_1 processing delays were observed in *nop2* mutants (Hong et al., 1997), further supporting the contention that Nop53p is important for Nop2p function.

It is interesting to note that while Nop53p interacts with Cbf5p, the most dramatic phenotypes of *nop53* cells are not the same as those resulting from the loss of functional Cbf5p. Cbf5p is proposed to be the pseudouridine synthase and a component of the box H-ACA class of snoRNPs (Lafontaine et al., 1998). Accordingly, depletion of Cbf5p leads to defects in both 60S and 40S biogenesis. In contrast, depletion of Nop53p had very little effect on 18S rRNA biogenesis. Thus the lack of Nop53p did not appear to dramatically alter Cbf5p function, but, like Nop2p, had primary effects on 25S rRNA and 60S subunit biogenesis. We do note, however, that complete absence of Nop53p did lead to phenotypes that were not restricted to the 60S pathway. For example, in order to compare rRNA from wild-type and *nop53Δ* mutants, more than twice the number of *nop53Δ* cells were required to get similar amounts of 18S rRNA, suggesting that the defects associated with *nop53* also (eventually) affect 40S biogenesis. Thus, the observed 60S defect appears to dominate the phenotype and might mask a less significant role in Cbf5p function and 40S biogenesis.

In addition, *nop53* mutants exhibit an accumulation of 7S and 5'-A_0 species, which are indicative of exosome defects (Butler, 2002; Li et al., 1990; Mitchell et al., 1997). However, because the exosome-dependent modifications take place late in the rRNA processing pathway, the accumulation of these fragments may also be attributed to the quality control mechanism, rather than to a specific Nop53p function. Moreover, we have observed such defects associated with Rat1p and its interacting partner, Rai1p, neither of which has been directly implicated in exosome function (Sydorskyy et al.,

2003). Similar results have been observed for Dob1/Mtr4p and Cgr1p (de la Cruz et al., 1998; Moy et al., 2002).

Taken together, our results demonstrate that Nop53p plays an integral role in 60S subunit biogenesis, through its association with key players such as Nop2p and (to a lesser extent) Cbf5p. Based on its association with Nop2p and other factors (Cbf5p, Fpr3p, Fpr4p and numerous ribosomal proteins) we prefer a model in which Nop53p plays more of a structural function than an enzymatic one, performing a base modification; however, an enzymatic activity for Nop53p cannot be ruled out at this point. A molecular understanding of its role in the context of the maturing 60S subunit will demand a more comprehensive analysis of the complex molecular events of ribosome biogenesis.

Chapter 5

Perspectives

5.1 Synopsis

In this study we have used genetic, biochemical and cell biological approaches to identify and characterize two novel yeast proteins, Rai1p and Nop53p, which are involved in ribosomal 60S subunit biogenesis. Both proteins were found to interact physically with pre-60S subunits as well as with several other proteins involved in ribosome biogenesis. Mutations in *RAI1* and *NOP53* strongly impair cell growth causing a dramatic decrease in the abundance of 60S subunits and appearance of halfmers. Rai1p and Nop53p are members of the same pathway, but they act at different stages of that pathway. Rai1p was identified in a *KAP123* genetic screen, and is required for efficient 60S subunit export from the nucleus in the *kap123Δ* background. Nop53p is necessary for one of the early steps of 60S biogenesis, since it associates with the assembling 60S subunits after the 90S precursors split. It dissociates from the 60S subunit before its export from the nucleus and the completion of 80S ribosome maturation. The relevance of these data and my thoughts on future experiments are discussed in the following sections.

5.2 Perspectives on deciphering the pre-60S subunit maturation pathway

The data presented in this thesis clearly place both Nop53p and Rai1p in the pre-60S subunit biogenesis pathway. Hence, further studies of this pathway are essential to improve our understanding of Nop53p and Rai1p functions. This can be achieved by examination of physical interactions of Nop53p and Rai1p in the mutants of other ribosomal biogenesis factors involved in the pathway, comparison of the single and

double-mutant phenotypes, and attempts to reconstitute the 60S biogenesis pathway *in vitro*.

The earliest nucleolar pre-60S ribosomes were isolated along with about 50 non-ribosomal proteins, many of which are important for ribosome biogenesis. However, only 5 non-ribosomal factors are present on the most mature pre-60S subunits after export to the cytoplasm (Nissan et al., 2002). These findings underscore the enormous structural changes that take place in the 60S pre-ribosomes on their path from the nucleolus to the cytoplasm. There were numerous attempts to complete a comprehensive list of protein trans-acting factors involved in the ribosome biogenesis. The recent introduction of a technique utilizing epitope-tagged assembly factors which associate with precursor particles at certain steps in the pathway, followed by subsequent proteomic and rRNA analysis of the isolated precursor particles, have led to great breakthroughs in this area (see Section 1.6.3). Because subunit maturation is a continuous process and different non-ribosomal proteins overlap at its various stages, initially it was dificult to make sense of the bounty of data acquired from these experiments. The ordering of the 60S pre-ribosomes into a sequence of early, medium and late intermediates was established by employing the tagging methodology using well characterized biogenesis factors, such as Nsa3p, Nop7p, Nug1p, Rix1p, Sda1p, Arx1p, and Kre35p (Fig. 1.6) (Nissan et al., 2002). Now that the basic framework of the pathway is available, the same methodology should be applied to all known non-ribosomal proteins involved in the pathway, including Nop53p and Rai1p. This information, along with immuno-electron microscopic localization analysis (Milkereit et al., 2001) of the major ribosome biogenesis factors should provide a comprehensive and

well validated spatial map of the pathway. And it should also provide a basis for further deductive studies of each component's function.

5.3 Perspectives on the search for biochemical function

Most protein factors involved in 60S ribosome biogenesis identified so far may be classified according to their biochemical function. These groups include: proteins that process and modify the pre-rRNAs (endo- and exonucleases, pseudouridine synthases or methyltransferases), mediate RNP folding/remodeling (RNA helicases, RNA chaperones) or facilitate protein association/dissociation (GTPases, AAA-ATPases). Further studies of both Nop53p and Rai1p will likely focus on elucidating their precise biochemical functions, in order to attribute the proteins to one of these or other functional groups. This can be done by using specific *in vitro* assays for enzymatic activity, based on predictions drawn from structural analysis, genetic studies and physical interactions. Such an approach has proven to be an efficient research-guiding tool. For example, GTP hydrolase activity (Sprang, 1997), found in several newly identified biogenesis factors such as Nug1p, Nug2p, Nog1p, and Kre35p (Bassler et al., 2001; Kallstrom et al., 2003), makes them candidates for regulators of ribosome maturation and pre-ribosome transport, through their possible association with signal transduction pathways that coordinate ribosome biogenesis and other cellular pathways (Tschochner and Hurt, 2003). Similarly, other recently identified AAA-type ATPases (Vale, 2000), Rix7p and Mdn1p/Rea1p (Gadal et al., 2001a; Galani et al., 2004) may have chaperone activity that is required for the dissociation of protein-protein interactions. As such, they could be required for the remodeling of the pre-60S subunits in preparation for their export into the

cytoplasm. A structural study showing that Mdn1p/Rea1p is related to the proteins of the dynein motor family suggests that these ATPases could also function as molecular motors along the pre-ribosomal pathway (Garbarino and Gibbons, 2002).

Interestingly, the rRNA analysis of cells lacking Mdn1p/Rea1p showed that, similarly to *nop53Δ* and to a lesser extent *rai1Δ* strains, the maturation of the 3' end of 5.8S rRNA is impaired. This processing reaction is directly dependent upon the exosome, a complex of 11 exonucleases required for 3'→5' trimming of various yeast RNA species and for the degradation of short excised RNA fragments (Butler, 2002; Mitchell et al., 1997). The accumulation of 7S has been used as a marker of the exosome defect (Allmang et al., 2000), but several non-exosome mutants have also been shown to accumulate an unprocessed 7S species. Some of them, such as the putative ATP-dependent RNA helicases, Dob1p and Dob7p, or a putative GTP-ase Nog2p, are predicted to function as exosome cofactors (de la Cruz et al., 1998; Daugeron and Linder 1998; Saveanu et al., 2001). In the case of Dob1p, the prediction is based on its synergistic effect in conjunction with an exosome component Rrp4p (de la Cruz et al., 1998). However, there is no obvious link between the exosome and Rai1p or Nop53p. It is unclear to what extent early events of 60S subunit biogenesis are linked to the exosome, but the observations presented here indicate that that further studies regarding the nature of the 7S accumulation in *nop53Δ* and *rai1Δ* strains are necessary.

5.4 Perspectives on Rat1p/Rai1p interaction

In addition to karyopherins, the synthetic fitness screen employed in this study revealed a complex genetic interaction between *KAP123* and *RAI1*. According to our

data, cells lacking Kap123p are unable to import sufficient quantities of the essential export factor Nmd3p to compensate for the loss of Rai1p. The precise function of Rai1p has yet to be established, but it seems to act in tandem with the nuclear 5'→3' exonuclease Rat1p (Johnson, 1997; Xue et al., 2000). Our biochemical, genetic and localization data (see Sections 3.3 and 3.4 for details) also support this notion. Interestingly, both yeast Rat1p and its human counterpart hXrn2 were recently found to be directly involved in RNA polymerase II (Pol II) transcription termination by digestion of nascent transcripts after endonucleolytic cleavage of the poly-(A) site (Kim et al., 2004; Tollervey, 2004). Furthermore, both degradation of the cleaved poly-(A) site in the Pol II transcript and transcription termination were suppressed in both *rat1-1* and *rai1Δ* strains (Das et al., 2003; Kim et al., 2004). This suggests that Rai1p acts as a Rat1p cofactor and very likely regulates the exonuclease activity or tethers this activity to the reaction site. Despite these observations, a comparison of the quantity of mRNA and rRNA production in *rat1-1* and *rai1Δ* strains implies that the most prominent role for the Rat1p/Rai1p complex remains in the area of ribosome biogenesis.

It is particularly intriguing to speculate that the coordination of the late steps of 60S biogenesis and nuclear export might involve a direct link between Rai1p and Nmd3p, perhaps during the loading of ribosomes with Nmd3p. To address this question, it would be interesting to isolate pre-60S particles, ready for export and charged with Nmd3p, and to examine the stoichiometry of Nmd3p, Rat1p and Rai1p. This, however, may be difficult because of the transient nature of the interactions and the large size of the complex.

5.5 Perspectives on ribosome regulation

Ribosome biogenesis is tightly co-regulated with various cellular processes and in particular with the cell cycle. This makes the understanding of ribosome regulation vital to our understanding of cell growth processes and a very attractive problem for future studies. Several regulators of the cell cycle were also recently found to regulate expression of ribosomal components (see Section 1.5) communicating, through cell cycle controllers, the signals from the nutrient-sensing pathways to the ribosome biogenesis machinery. A model has been proposed in which the critical cell-size threshold at Start is established by rates of ribosome production or, alternatively, by the rates of translation (Jorgensen and Tyers, 2004). In yeast, the common regulators connecting both systems, Sfp1p and Sch9p, were found utilizing high-throughput microarray technology (Jorgensen et al., 2002; 2004). This technology will likely prove useful in searching for other controllers and triggering mechanisms that put various known cellular pathways into action.

Yet another challenge of the field is deciphering the mechanisms enabling temporal decrease of the translation rates, and the mechanisms committing excessive ribosomes to degradation upon nutrient starvation or other environmental cues (see Section 1.5). One may predict that ribosome dissociation and subsequent targeting for degradation can be mediated by post-translational modifications of the r-proteins. Phosphorylation of the S6 small subunit protein is a well established example of this kind of regulation of ribosome function (Ruggero and Pandolfi, 2003). Recently, mass spectrometry has emerged as a tool for high-throughput identification of post-translational modifications such as phosphorylation (Peters et al., 2004), acetylation

(Dormeyer et al., 2005), ubiquitination (Peng et al., 2003) and sumoylation (Wohlschlegel et al., 2004) in complex protein samples. Analysis of r-protein post-translational modifications from enriched ribosome fractions of stressed and exponentially growing cells may spearhead efforts to establish the pathways involved in ribosome regulation.

5.6 Perspectives on future nucleocytoplasmic transport studies

Nucleocytoplasmic exchange occurs strictly through the NPCs. Although small enough to passively diffuse into the nucleus, r-proteins are nevertheless imported actively by the karyopherins (Rout et al., 1997; Schlenstedt et al., 1997). In this context, specific karyopherins have been suggested to function both as transport receptors and chaperones. The chaperone function is proposed to cover the basic domains of r-proteins, thereby preventing their precipitation (Jakel et al., 2002); however, thus far this hypothesis has not found much experimental support which would require a comprehensive study to investigate where and how karyopherins release their r-protein cargoes.

The synthetic fitness screen used in this study yielded three karyopherins: Kap121p/Pse1p, Sxm1p/Kap108p and Nmd5p/Kap119p, each of which likely can substitute for the r-protein import function along with Kap123p (see Section 3.8.1 for discussion). Today, with a comprehensive inventory of transport receptors and an increasing understanding of transport processes, the field is poised to reveal a "universal ribosomal nuclear localization signal" and to decipher its regulation. Indeed, the logic of the ribosome assembly processes predicts that such a sequence, recognizable by multiple

karyopherins, would be needed for the timely and stoichiometric import of r-proteins. Unfortunately, to date there have been no reports of a detailed study of this problem.

Another part of this question is what happens to the NLSs after the import of r-proteins is complete. A newly assembled ribosomal subunit containing several NLSs would be unable to leave the nucleus if there were no mechanisms disabling or overriding the import signal. Therefore the NLS sequences must be modified or screened from the import receptors in order for ribosomal subunits to become qualified for export from the nucleus and to be able to remain in the cytoplasm. If this logic is correct, a long discussed problem, whether or not there are ribosomal export checkpoint mechanisms, provides a very simple solution. One could predict that pre-ribosomal particles would cycle in and out of the nucleus as long as the NLSs of assembling r-proteins were not "neutralized", by obscuring them during the formation and packaging into the subunit. This mechanism could be employed at the late, nucleoplasmic stages of ribosome assembly, when the pre-ribosomal particles are no longer associated with the factors such as the Noc proteins, which are proposed to be involved in intranuclear transport of ribosomal precursor particles (Dlakic and Tollervey, 2004; Milkereit et al., 2001; 2003).

One final question of interest is related to the mechanism of rapid deregulation of ribosome biogenesis during various environmental and intracellular insults (discussed in the Section 1.5). Ribosomal proteins, being small, highly positively charged proteins, with the capacity to readily bind nucleic acids, could be dangerous to the cell, both in the nucleus and the cytoplasm. However, it is likely that to facilitate the control over the unwanted nuclear influx of r-proteins, in addition to regulation of transcriptional and translational levels, the cells also regulate r-protein nucleocytoplasmic transport

processes. Studies directed at this question should provide a better understanding of nucleocytoplasmic transport.

5.7 Perspectives on the 60S export pathway

An analysis of ribosomal export from the nucleus had been very difficult until the development of functional *in vivo* export assays in *S. cerevisiae*, using GFP-tagged variants of r-proteins. Crm1p and the members of its 60S export pathway (see Section 1.4.5) were among first genes shown to be involved in ribosome export (Gadal et al., 2001b; Ho et al., 2000a). Since then, using a combination of genetics and biochemistry, several additional factors have been shown to affect subunit maturation and export (Gadal et al., 2001a; Milkereit et al., 2001; Milkereit et al., 2003). One such protein is Mtr2p, a *bona fide* mRNA export factor, which was demonstrated to form a complex with another conserved mRNA export factor Mex67p (Santos-Rosa et al., 1998). Interestingly, the *mtr2-33* allele had been known previously to accumulate 60S pre-ribosomes at the restrictive temperature and to be synthetically lethal with proteins involved in 60S biogenesis, such as Nug1p, Ecm1p, and Nmd3p (Bassler et al., 2001). More recently, Mtr2p was found to associate with the Arx1p particle, one of the latest pre-60S particles isolated so far (Nissan et al., 2002). Taken together these data place Mtr2p in the 60S export pathway, likely functioning in parallel with the Nmd3p/Crm1p export mechanism (see Section 1.4.5) and thus connecting mRNA export with ribosome export. In the future, it will be very exciting to learn more precisely where Mtr2p belongs in the 60S export pathway.

Although many questions about the 60S export pathway have been solved, new questions continue to emerge. For instance, we showed in this thesis that overexpression of *NMD3* rescued the slow growth phenotype observed in sf17 (*rai1-1/kap123Δ*), *rai1Δ/kap123Δ and rai1Δ* cells. We also directly visualized GFP chimeras containing either Nmd3p NLS or Nmd3p NLS/NES demonstrating that correct and efficient Nmd3p import into the nucleus requires Kap123p (see Section 3.7). Although mislocalization of Nmd3p is evident in *kap123* cells, the lethality of *nmd3Δ* suggests that there are other factors capable of importing Nmd3p in the absence of Kap123p. These alternative import factors have yet to be identified.

The precise role of the numerous trans-acting factors that control ribosomal biogenesis remains elusive. In addition, the composition of the multiple pre-ribosomal particles and details of their dynamic progression from immature to mature ribosomes remain to be characterized. Nevertheless current studies are shedding increasingly more light on the molecular mechanisms that govern this complex process. The studies, mainly conducted in yeast, are establishing a rough model of the ribosome maturation pathway, which in turn is facilitating further research in this field. New data indicate that many ribosome biogenesis factors are involved in the networks regulating a vast array of diverse cellular processes including growth, proliferation and cell cycle progression (Tschochner and Hurt, 2003). It will be very exciting to learn how these seemingly disparate pathways are connected. Furthermore, because of the dependence of ribosome biogenesis on nucleocytoplasmic transport, further characterization of the components necessary for the transport of ribosomal proteins, and associated components, will lead to

a better understanding of the precise mechanisms that regulate their translocation. These studies will greatly contribute to our understanding of this basic cellular process.

References

Aitchison, J.D., G. Blobel, and M.P. Rout. 1995a. Nup120p: a yeast nucleoporin required for NPC distribution and mRNA transport. *J Cell Biol.* 131:1659-75.

Aitchison, J.D., G. Blobel, and M.P. Rout. 1996. Kap104p: a karyopherin involved in the nuclear transport of messenger RNA binding proteins. *Science.* 274:624-7.

Aitchison, J.D., M.P. Rout, M. Marelli, G. Blobel, and R.W. Wozniak. 1995b. Two novel related yeast nucleoporins Nup170p and Nup157p: complementation with the vertebrate homologue Nup155p and functional interactions with the yeast nuclear pore-membrane protein Pom152p. *J Cell Biol.* 131:1133-48.

Albertini, M., L.F. Pemberton, J.S. Rosenblum, and G. Blobel. 1998. A novel nuclear import pathway for the transcription factor TFIIS. *J Cell Biol.* 143:1447-55.

Alberts, B. 1994. Molecular Biology of the Cell. Garland Pub., New York. xliii, 1294, 67 p.

Allen, N.P., L. Huang, A. Burlingame, and M. Rexach. 2001. Proteomic analysis of nucleoporin interacting proteins. *J Biol Chem.* 276:29268-74.

Allmang, C., P. Mitchell, E. Petfalski, and D. Tollervey. 2000. Degradation of ribosomal RNA precursors by the exosome. *Nucleic Acids Res.* 28:1684-91.

Altschul, S.F., T.L. Madden, A.A. Schaffer, J. Zhang, Z. Zhang, W. Miller, and D.J. Lipman. 1997. Gapped BLAST and PSI-BLAST: a new generation of protein database search programs. *Nucleic Acids Res.* 25:3389-402.

Aris, J.P., and G. Blobel. 1988. Identification and characterization of a yeast nucleolar protein that is similar to a rat liver nucleolar protein. *J Cell Biol.* 107:17-31.

Ausubel, F.M. 1994. Current protocols in molecular biology. John Wiley & Sons, New York. 4 v.

Baronas-Lowell, D.M., and J.R. Warner. 1990. Ribosomal protein L30 is dispensable in the yeast Saccharomyces cerevisiae. *Mol Cell Biol.* 10:5235-43.

Bassler, J., P. Grandi, O. Gadal, T. Lessmann, E. Petfalski, D. Tollervey, J. Lechner, and E. Hurt. 2001. Identification of a 60S preribosomal particle that is closely linked to nuclear export. *Mol Cell.* 8:517-29.

Bataille, N., T. Helser, and H.M. Fried. 1990. Cytoplasmic transport of ribosomal subunits microinjected into the Xenopus laevis oocyte nucleus: a generalized, facilitated process. *J Cell Biol.* 111:1571-82.

Beltrame, M., Y. Henry, and D. Tollervey. 1994. Mutational analysis of an essential binding site for the U3 snoRNA in the 5' external transcribed spacer of yeast pre-rRNA. *Nucleic Acids Res.* 22:5139-47.

Ben Ali, A., J. Wuyts, R. De Wachter, A. Meyer, and Y. Van de Peer. 1999. Construction of a variability map for eukaryotic large subunit ribosomal RNA. *Nucleic Acids Res.* 27:2825-31.

Bender, A., and J.R. Pringle. 1991. Use of a screen for synthetic lethal and multicopy suppressee mutants to identify two new genes involved in morphogenesis in Saccharomyces cerevisiae. *Mol Cell Biol.* 11:1295-305.

Bernstein, K.A., J.E. Gallagher, B.M. Mitchell, S. Granneman, and S.J. Baserga. 2004. The small-subunit processome is a ribosome assembly intermediate. *Eukaryot Cell.* 3:1619-26.

Boeke, J.D., J. Trueheart, G. Natsoulis, and G.R. Fink. 1987. 5-Fluoroorotic acid as a selective agent in yeast molecular genetics. *Methods Enzymol.* 154:164-75.

Boon, K., H.N. Caron, R. van Asperen, L. Valentijn, M.C. Hermus, P. van Sluis, I. Roobeek, I. Weis, P.A. Voute, M. Schwab, and R. Versteeg. 2001. N-myc enhances the expression of a large set of genes functioning in ribosome biogenesis and protein synthesis. *EMBO J.* 20:1383-93.

Burnette, W.N. 1981. "Western blotting": electrophoretic transfer of proteins from sodium dodecyl sulfate--polyacrylamide gels to unmodified nitrocellulose and radiographic detection with antibody and radioiodinated protein A. *Anal Biochem.* 112:195-203.

Butler, J.S. 2002. The yin and yang of the exosome. *Trends Cell Biol.* 12:90-6.

Cadwell, C., H.J. Yoon, Y. Zebarjadian, and J. Carbon. 1997. The yeast nucleolar protein Cbf5p is involved in rRNA biosynthesis and interacts genetically with the RNA polymerase I transcription factor RRN3. *Mol Cell Biol.* 17:6175-83.

Cavanaugh, A.H., W.M. Hempel, L.J. Taylor, V. Rogalsky, G. Todorov, and L.I. Rothblum. 1995. Activity of RNA polymerase I transcription factor UBF blocked by Rb gene product. *Nature.* 374:177-80.

Chivian, D., D.E. Kim, L. Malmstrom, P. Bradley, T. Robertson, P. Murphy, C.E. Strauss, R. Bonneau, C.A. Rohl, and D. Baker. 2003. Automated prediction of CASP-5 structures using the Robetta server. *Proteins.* 53 Suppl 6:524-33.

Ciarmatori, S., P.H. Scott, J.E. Sutcliffe, A. McLees, H.M. Alzuherri, J.H. Dannenberg, H. te Riele, I. Grummt, R. Voit, and R.J. White. 2001. Overlapping functions of the pRb family in the regulation of rRNA synthesis. *Mol Cell Biol.* 21:5806-14.

Cosloy, S.D., and M. Oishi. 1973. Genetic transformation in Escherichia coli K12. *Proc Natl Acad Sci U S A.* 70:84-7.

Cross, F.R. 1997. 'Marker swap' plasmids: convenient tools for budding yeast molecular genetics. *Yeast.* 13:647-53.

Da Costa, L., T.N. Willig, J. Fixler, N. Mohandas, and G. Tchernia. 2001. Diamond-Blackfan anemia. *Curr Opin Pediatr.* 13:10-5.

Dai, M.S., S.X. Zeng, Y. Jin, X.X. Sun, L. David, and H. Lu. 2004. Ribosomal protein L23 activates p53 by inhibiting MDM2 function in response to ribosomal perturbation but not to translation inhibition. *Mol Cell Biol.* 24:7654-68.

Das, B., J.S. Butler, and F. Sherman. 2003. Degradation of normal mRNA in the nucleus of Saccharomyces cerevisiae. *Mol Cell Biol.* 23:5502-15.

Daugeron, M.C., and P. Linder. 1998. Dbp7p, a putative ATP-dependent RNA helicase from Saccharomyces cerevisiae, is required for 60S ribosomal subunit assembly. *RNA.* 4:566-81.

de la Cruz, J., D. Kressler, D. Tollervey, and P. Linder. 1998. Dob1p (Mtr4p) is a putative ATP-dependent RNA helicase required for the 3' end formation of 5.8S rRNA in Saccharomyces cerevisiae. *EMBO J.* 17:1128-40.

Delorme, E. 1989. Transformation of Saccharomyces cerevisiae by electroporation. *Appl Environ Microbiol.* 55:2242-6.

Dez, C., and D. Tollervey. 2004. Ribosome synthesis meets the cell cycle. *Curr Opin Microbiol.* 7:631-7.

Dick, F.A., D.P. Eisinger, and B.L. Trumpower. 1997. Exchangeability of Qsr1p, a large ribosomal subunit protein required for subunit joining, suggests a novel translational regulatory mechanism. *FEBS Lett.* 419:1-3.

Dilworth, D.J., A. Suprapto, J.C. Padovan, B.T. Chait, R.W. Wozniak, M.P. Rout, and J.D. Aitchison. 2001. Nup2p dynamically associates with the distal regions of the yeast nuclear pore complex. *J Cell Biol.* 153(7):1465-78.

Dingwall, C., and R.A. Laskey. 1991. Nuclear targeting sequences-a consensus? *Trends in Biochemical Sciences.* 16:478-481.

Dlakic, M., and D. Tollervey. 2004. The Noc proteins involved in ribosome synthesis and export contain divergent HEAT repeats. *RNA.* 10:351-4.

Dolinski, K., S. Muir, M. Cardenas, and J. Heitman. 1997. All cyclophilins and FK506 binding proteins are, individually and collectively, dispensable for viability in Saccharomyces cerevisiae. *Proc Natl Acad Sci U S A.* 94:13093-8.

Dormeyer, W., M. Ott, and M. Schnolzer. 2005. Probing lysine acetylation in proteins: strategies, limitations and pitfalls of in vitro acetyltransferase assays. *Mol Cell Proteomics.*

Doseff, A.I., and K.T. Arndt. 1995. LAS1 is an essential nuclear protein involved in cell morphogenesis and cell surface growth. *Genetics.* 141:857-71.

Draptchinskaia, N., P. Gustavsson, B. Andersson, M. Pettersson, T.N. Willig, I. Dianzani, S. Ball, G. Tchernia, J. Klar, H. Matsson, D. Tentler, N. Mohandas, B. Carlsson,

and N. Dahl. 1999. The gene encoding ribosomal protein S19 is mutated in Diamond-Blackfan anaemia. *Nat Genet.* 21:169-75.

Du, Y.C., and B. Stillman. 2002. Yph1p, an ORC-interacting protein: potential links between cell proliferation control, DNA replication, and ribosome biogenesis. *Cell.* 109:835-48.

Dundr, M., and T. Misteli. 2001. Functional architecture in the cell nucleus. *Biochem J.* 356:297-310.

Eisinger, D.P., F.A. Dick, and B.L. Trumpower. 1997. Qsr1p, a 60S ribosomal subunit protein, is required for joining of 40S and 60S subunits. *Mol Cell Biol.* 17:5136-45.

El-Moghazy, A.N., N. Zhang, T. Ismail, J. Wu, A. Butt, S. Ahmed Khan, C. Merlotti, K. Cara Woodwark, D.C. Gardner, S.J. Gaskell, and S.G. Oliver. 2000. Functional analysis of six novel ORFs on the left arm of chromosome XII in Saccharomyces cerevisiae reveals two essential genes, one of which is under cell-cycle control. *Yeast.* 16:277-88.

Elion, E.A., J. Trueheart, and G.R. Fink. 1995. Fus2 localizes near the site of cell fusion and is required for both cell fusion and nuclear alignment during zygote formation. *J Cell Biol.* 130:1283-96.

Eng, J.K., A.L. McCormack, and J.R. Yates III. 1994. An approach to correlate tandem mass spcral data of peptides with amino acid sequences in a protein database. *J. Am. Soc. Mass Spectrom.* 5:976-989.

Fatica, A., and D. Tollervey. 2002. Making ribosomes. *Curr Opin Cell Biol.* 14:313-8.

Fink, G.R., J. Hicks, P. Hieter, M.D. Rose, F. Sherman, F.M. Winston, and Cold Spring Harbor Laboratory. 1990. Methods in yeast genetics: a laboratory course manual. Cold Spring Harbor Laboratory, Cold Spring Harbor. v, 198 p.

Fischer, U., M. Michael, R. Luhrmann, and G. Dreyfuss. 1996. Signal-mediated nuclear export pathways of proteins and RNAs. *Trends Cell Biol.* 6:290-293.

Fisher, E.M., P. Beer-Romero, L.G. Brown, A. Ridley, J.A. McNeil, J.B. Lawrence, H.F. Willard, F.R. Bieber, and D.C. Page. 1990. Homologous ribosomal protein genes on the human X and Y chromosomes: escape from X inactivation and possible implications for Turner syndrome. *Cell.* 63:1205-18.

Foiani, M., A.M. Cigan, C.J. Paddon, S. Harashima, and A.G. Hinnebusch. 1991. GCD2, a translational repressor of the GCN4 gene, has a general function in the initiation of protein synthesis in Saccharomyces cerevisiae. *Mol Cell Biol.* 11:3203-16.

Fromont-Racine, M., B. Senger, C. Saveanu, and F. Fasiolo. 2003. Ribosome assembly in eukaryotes. *Gene.* 313:17-42.

Gadal, O., D. Strauss, J. Braspenning, D. Hoepfner, E. Petfalski, P. Philippsen, D. Tollervey, and E. Hurt. 2001a. A nuclear AAA-type ATPase (Rix7p) is required for biogenesis and nuclear export of 60S ribosomal subunits. *EMBO J.* 20:3695-704.

Gadal, O., D. Strauss, J. Kessl, B. Trumpower, D. Tollervey, and E. Hurt. 2001b. Nuclear export of 60s ribosomal subunits depends on Xpo1p and requires a nuclear export sequence-containing factor, Nmd3p, that associates with the large subunit protein Rpl10p. *Mol Cell Biol.* 21:3405-15.

Gadal, O., D. Strauss, E. Petfalski, P.E. Gleizes, N. Gas, D. Tollervey, and E. Hurt. 2002. Rlp7p is associated with 60S preribosomes, restricted to the granular component of the nucleolus, and required for pre-rRNA processing. *J Cell Biol.* 157:941-51.

Galani, K., T.A. Nissan, E. Petfalski, D. Tollervey, and E. Hurt. 2004. Rea1, a dynein-related nuclear AAA-ATPase, is involved in late rRNA processing and nuclear export of 60 S subunits. *J Biol Chem.* 279:55411-8.

Garbarino, J.E., and I.R. Gibbons. 2002. Expression and genomic analysis of midasin, a novel and highly conserved AAA protein distantly related to dynein. *BMC Genomics.* 3:18.

Geerlings, T.H., J.C. Vos, and H.A. Raue. 2000. The final step in the formation of 25S rRNA in Saccharomyces cerevisiae is performed by 5'-->3' exonucleases. *RNA.* 6:1698-703.

Gerace, L. 1995. Nuclear export signals and the fast track to the cytoplasm. *Cell.* 82:341-4.

Gerbi, S.A., A.V. Borovjagin, M. Ezrokhi, and T.S. Lange. 2001. Ribosome biogenesis: role of small nucleolar RNA in maturation of eukaryotic rRNA. *Cold Spring Harb Symp Quant Biol.* 66:575-90.

Gill, T., T. Cai, J. Aulds, S. Wierzbicki, and M.E. Schmitt. 2004. RNase MRP cleaves the CLB2 mRNA to promote cell cycle progression: novel method of mRNA degradation. *Mol Cell Biol.* 24:945-53.

Gorlich, D., and U. Kutay. 1999. Transport between the cell nucleus and the cytoplasm. *Annu Rev Cell Dev Biol.* 15:607-60.

Grandi, P., V. Rybin, J. Bassler, E. Petfalski, D. Strauss, M. Marzioch, T. Schafer, B. Kuster, H. Tschochner, D. Tollervey, A.C. Gavin, and E. Hurt. 2002. 90S pre-ribosomes include the 35S pre-rRNA, the U3 snoRNP, and 40S subunit processing factors but predominantly lack 60S synthesis factors. *Mol Cell.* 10:105-15.

Guthrie, C., and G.R. Fink. 1991. Guide to yeast genetics and molecular biology. *Methods Enzymol.* 194:1-863.

Harel, A., and D.J. Forbes. 2004. Importin beta: conducting a much larger cellular symphony. *Mol Cell.* 16:319-30.

Harnpicharnchai, P., J. Jakovljevic, E. Horsey, T. Miles, J. Roman, M. Rout, D. Meagher, B. Imai, Y. Guo, C.J. Brame, J. Shabanowitz, D.F. Hunt, and J.L. Woolford, Jr. 2001. Composition and functional characterization of yeast 66S ribosome assembly intermediates. *Mol Cell.* 8:505-15.

Hayashi, F., K.D. Smith, A. Ozinsky, T.R. Hawn, E.C. Yi, D.R. Goodlett, J.K. Eng, S. Akira, D.M. Underhill, and A. Aderem. 2001. The innate immune response to bacterial flagellin is mediated by Toll- like receptor 5. *Nature.* 410:1099-103.

Hedges, J., M. West, and A.W. Johnson. 2005. Release of the export adapter, Nmd3p, from the 60S ribosomal subunit requires Rpl10p and the cytoplasmic GTPase Lsg1p. *EMBO J.* 24:567-79.

Heiss, N.S., S.W. Knight, T.J. Vulliamy, S.M. Klauck, S. Wiemann, P.J. Mason, A. Poustka, and I. Dokal. 1998. X-linked dyskeratosis congenita is caused by mutations in a highly conserved gene with putative nucleolar functions. *Nat Genet.* 19:32-8.

Henras, A.K., C. Dez, and Y. Henry. 2004. RNA structure and function in C/D and H/ACA s(no)RNPs. *Curr Opin Struct Biol.* 14:335-43.

Ho, J.H., G. Kallstrom, and A.W. Johnson. 2000a. Nascent 60S ribosomal subunits enter the free pool bound by Nmd3p. *RNA.* 6:1625-34.

Ho, J.H., G. Kallstrom, and A.W. Johnson. 2000b. Nmd3p is a Crm1p-dependent adapter protein for nuclear export of the large ribosomal subunit. *J Cell Biol.* 151:1057-66.

Hong, B., J.S. Brockenbrough, P. Wu, and J.P. Aris. 1997. Nop2p is required for pre-rRNA processing and 60S ribosome subunit synthesis in yeast. *Mol Cell Biol.* 17:378-88.

Hong, B., K. Wu, J.S. Brockenbrough, P. Wu, and J.P. Aris. 2001. Temperature sensitive *NOP2* alleles defective in synthesis of 25S rRNA and large ribosomal subunits in Saccharomyces cerevisiae. *Nucleic Acids Res.* 29:2927-37.

Hurt, E., S. Hannus, B. Schmelzl, D. Lau, D. Tollervey, and G. Simos. 1999. A novel in vivo assay reveals inhibition of ribosomal nuclear export in ran-cycle and nucleoporin mutants. *J Cell Biol.* 144:389-401.

Iouk, T.L., J.D. Aitchison, S. Maguire, and R.W. Wozniak. 2001. Rrb1p, a yeast nuclear WD-repeat protein involved in the regulation of ribosome biosynthesis. *Mol Cell Biol.* 21:1260-71.

Jakel, S., J.M. Mingot, P. Schwarzmaier, E. Hartmann, and D. Gorlich. 2002. Importins fulfill a dual function as nuclear import receptors and cytoplasmic chaperones for exposed basic domains. *EMBO J.* 21:377-86.

Jin, A., K. Itahana, K. O'Keefe, and Y. Zhang. 2004. Inhibition of HDM2 and activation of p53 by ribosomal protein L23. *Mol Cell Biol.* 24:7669-80.

Johnson, A.W. 1997. Rat1p and Xrn1p are functionally interchangeable exoribonucleases that are restricted to and required in the nucleus and cytoplasm, respectively. *Mol Cell Biol.* 17:6122-30.

Jones, D.T. 1999. Protein secondary structure prediction based on position-specific scoring matrices. J Mol Biol. 292:195-202.

Jones, D.T., and J.J. Ward. 2003. Prediction of disordered regions in proteins from position specific score matrices. Proteins. 53 Suppl 6:573-8.

Jorgensen, P., J.L. Nishikawa, B.J. Breitkreutz, and M. Tyers. 2002. Systematic identification of pathways that couple cell growth and division in yeast. *Science.* 297:395-400.

Jorgensen, P., I. Rupes, J.R. Sharom, L. Schneper, J.R. Broach, and M. Tyers. 2004. A dynamic transcriptional network communicates growth potential to ribosome synthesis and critical cell size. *Genes Dev.* 18:2491-505.

Jorgensen, P., and M. Tyers. 2004. How cells coordinate growth and division. *Curr Biol.* 14:R1014-27.

Ju, Q., and J.R. Warner. 1994. Ribosome synthesis during the growth cycle of Saccharomyces cerevisiae. *Yeast.* 10:151-7.

Kallstrom, G., J. Hedges, and A. Johnson. 2003. The putative GTPases Nog1p and Lsg1p are required for 60S ribosomal subunit biogenesis and are localized to the nucleus and cytoplasm, respectively. *Mol Cell Biol.* 23:4344-55.

Kim, M., N.J. Krogan, L. Vasiljeva, O.J. Rando, E. Nedea, J.F. Greenblatt, and S. Buratowski. 2004. The yeast Rat1 exonuclease promotes transcription termination by RNA polymerase II. *Nature*. 432:517-22.

King, M.Y., and K.L. Redman. 2002. RNA methyltransferases utilize two cysteine residues in the formation of 5-methylcytosine. *Biochem.* 41:11218-25.

Kipper, J., C. Strambio-de-Castillia, A. Suprapto, and M.P. Rout. 2002. Isolation of nuclear envelope from Saccharomyces cerevisiae. *Methods Enzymol.* 351:394-408.

Kongsuwan, K., Q. Yu, A. Vincent, M.C. Frisardi, M. Rosbash, J.A. Lengyel, and J. Merriam. 1985. A Drosophila Minute gene encodes a ribosomal protein. *Nature.* 317:555-8.

Kranz, J.E., and C. Holm. 1990. Cloning by function: an alternative approach for identifying yeast homologs of genes from other organisms. *Proc Natl Acad Sci U S A.* 87:6629-33.

Kressler, D., J. de la Cruz, M. Rojo, and P. Linder. 1997. Fal1p is an essential DEAD-box protein involved in 40S-ribosomal- subunit biogenesis in Saccharomyces cerevisiae. *Mol Cell Biol.* 17:7283-94.

Kressler, D., M. Doere, M. Rojo, and P. Linder. 1999a. Synthetic lethality with conditional dbp6 alleles identifies rsa1p, a nucleoplasmic protein involved in the assembly of 60S ribosomal subunits. *Mol Cell Biol.* 19:8633-45.

Kressler, D., P. Linder, and J. de La Cruz. 1999b. Protein trans-acting factors involved in ribosome biogenesis in Saccharomyces cerevisiae. *Mol Cell Biol.* 19:7897-912.

Kufel, J., C. Allmang, E. Petfalski, J. Beggs, and D. Tollervey. 2002. Lsm proteins are required for normal processing and stability of ribosomal RNAs. *J Biol Chem.*

Lafontaine, D., and D. Tollervey. 1995. Trans-acting factors in yeast pre-rRNA and pre-snoRNA processing. *Biochem Cell Biol.* 73:803-12.

Lafontaine, D.L., C. Bousquet-Antonelli, Y. Henry, M. Caizergues-Ferrer, and D. Tollervey. 1998. The box H + ACA snoRNAs carry Cbf5p, the putative rRNA pseudouridine synthase. *Genes Dev.* 12:527-37.

Lambertsson, A. 1998. The minute genes in Drosophila and their molecular functions. *Adv Genet.* 38:69-134.

Leslie, D.M., B. Grill, M.P. Rout, R.W. Wozniak, and J.D. Aitchison. 2002. Kap121p-mediated nuclear import is required for mating and cellular differentiation in yeast. *Mol Cell Biol.* 22:2544-55.

Li, H.D., J. Zagorski, and M.J. Fournier. 1990. Depletion of U14 small nuclear RNA (snR128) disrupts production of 18S rRNA in Saccharomyces cerevisiae. *Mol Cell Biol.* 10:1145-52.

Lohrum, M.A., R.L. Ludwig, M.H. Kubbutat, M. Hanlon, and K.H. Vousden. 2003. Regulation of HDM2 activity by the ribosomal protein L11. *Cancer Cell.* 3:577-87.

Lupas, A., M. Van Dyke, and J. Stock. 1991. Predicting coiled coils from protein sequences. *Science.* 252:1162-4.

Maniatis, T., J. Sambrook, and E.F. Fritsch. 1982. Molecular cloning: a laboratory manual. Cold Spring Harbor Laboratory, Cold Spring Harbor, N.Y. x, 545 p.

Marelli, M., J.D. Aitchison, and R.W. Wozniak. 1998. Specific binding of the karyopherin Kap121p to a subunit of the nuclear pore complex containing Nup53p, Nup59p, and Nup170p. *J Cell Biol.* 143:1813-30.

Matsudaira, P. 1987. Sequence from picomole quantities of proteins electroblotted onto polyvinylidene difluoride membranes. *J Biol Chem.* 262:10035-8.

Mattaj, I.W., and L. Englmeier. 1998. Nucleocytoplasmic transport: the soluble phase. *Annu Rev Biochem.* 67:265-306.

Menssen, A., and H. Hermeking. 2002. Characterization of the c-MYC-regulated transcriptome by SAGE: identification and analysis of c-MYC target genes. *Proc Natl Acad Sci U S A.* 99:6274-9.

Milkereit, P., O. Gadal, A. Podtelejnikov, S. Trumtel, N. Gas, E. Petfalski, D. Tollervey, M. Mann, E. Hurt, and H. Tschochner. 2001. Maturation and intranuclear transport of pre-ribosomes requires Noc proteins. *Cell.* 105:499-509.

Milkereit, P., D. Strauss, J. Bassler, O. Gadal, H. Kuhn, S. Schutz, N. Gas, J. Lechner, E. Hurt, and H. Tschochner. 2003. A Noc complex specifically involved in the formation and nuclear export of ribosomal 40 S subunits. *J Biol Chem.* 278:4072-81.

Mitchell, P., E. Petfalski, A. Shevchenko, M. Mann, and D. Tollervey. 1997. The exosome: a conserved eukaryotic RNA processing complex containing multiple 3'-->5' exoribonucleases. *Cell.* 91:457-66.

Moy, T.I., D. Boettner, J.C. Rhodes, P.A. Silver, and D.S. Askew. 2002. Identification of a role for Saccharomyces cerevisiae Cgr1p in pre-rRNA processing and 60S ribosome subunit synthesis. *Microbiology.* 148:1081-90.

Neufeld, T.P., A.F. de la Cruz, L.A. Johnston, and B.A. Edgar. 1998. Coordination of growth and cell division in the Drosophila wing. *Cell.* 93:1183-93.

Nissan, T.A., J. Bassler, E. Petfalski, D. Tollervey, and E. Hurt. 2002. 60S pre-ribosome formation viewed from assembly in the nucleolus until export to the cytoplasm. *EMBO J.* 21:5539-47.

Nissen, P., J. Hansen, N. Ban, P.B. Moore, and T.A. Steitz. 2000. The structural basis of ribosome activity in peptide bond synthesis. *Science.* 289:920-30.

Noller, H.F., V. Hoffarth, and L. Zimniak. 1992. Unusual resistance of peptidyl transferase to protein extraction procedures. *Science.* 256:1416-9.

Oliver, E.R., T.L. Saunders, S.A. Tarle, and T. Glaser. 2004. Ribosomal protein L24 defect in belly spot and tail (Bst), a mouse Minute. Development. 131:3907-20.

Palade, G.E. 1955. A small particulate component of the cytoplasm. *J Biophys Biochem Cytol.* 1:59-68.

Paule, M.R., and R.J. White. 2000. Survey and summary: transcription by RNA polymerases I and III. *Nucleic Acids Res.* 28:1283-98.

Pemberton, L.F., G. Blobel, and J.S. Rosenblum. 1998. Transport routes through the nuclear pore complex. *Curr Opin Cell Biol.* 10:392-9.

Peng, J., D. Schwartz, J.E. Elias, C.C. Thoreen, D. Cheng, G. Marsischky, J. Roelofs, D. Finley, and S.P. Gygi. 2003. A proteomics approach to understanding protein ubiquitination. *Nat Biotechnol.* 21:921-6.

Porter, K.R., A. Claude, E.F. Fullam. 1945. A study of tissue culture cells by electron microscopy. *J. Exp. Med.* 81:233-246.

Peters, E.C., A. Brock, and S.B. Ficarro. 2004. Exploring the phosphoproteome with mass spectrometry. *Mini Rev Med Chem.* 4:313-24.

Rosenblum, J.S., L.F. Pemberton, and G. Blobel. 1997. A nuclear import pathway for a protein involved in tRNA maturation. *J Cell Biol.* 139:1655-61.

Rosenblum, J.S., L.F. Pemberton, N. Bonifaci, and G. Blobel. 1998. Nuclear import and the evolution of a multifunctional RNA-binding protein. *J Cell Biol.* 143:887-99.

Rout, M.P., and J.D. Aitchison. 2001. The nuclear pore complex as a transport machine. *J Biol Chem.* 29:29.

Rout, M.P., J.D. Aitchison, M.O. Magnasco, and B.T. Chait. 2003. Virtual gating and nuclear transport: the hole picture. *Trends Cell Biol.* 13:622-8.

Rout, M.P., J.D. Aitchison, A. Suprapto, K. Hjertaas, Y. Zhao, and B.T. Chait. 2000. The yeast nuclear pore complex: composition, architecture, and transport mechanism. *J Cell Biol.* 148:635-51.

Rout, M.P., G. Blobel, and J.D. Aitchison. 1997. A distinct nuclear import pathway used by ribosomal proteins. *Cell.* 89:715-25.

Rout, M.P., and J.V. Kilmartin. 1990. Components of the yeast spindle and spindle pole body. *J Cell Biol.* 111:1913-27.

Rudra, D., and J.R. Warner. 2004. What better measure than ribosome synthesis? *Genes Dev.* 18:2431-6.

Ruggero, D., S. Grisendi, F. Piazza, E. Rego, F. Mari, P.H. Rao, C. Cordon-Cardo, and P.P. Pandolfi. 2003. Dyskeratosis congenita and cancer in mice deficient in ribosomal RNA modification. *Science*. 299:259-62.

Ruggero, D., and P.P. Pandolfi. 2003. Does the ribosome translate cancer? *Nat Rev Cancer*. 3:179-92.

Sabatini, D.D., Y. Tashiro, and G.E. Palade. 1966. On the attachment of ribosomes to microsomal membranes. *J Mol Biol*. 19:503-24.

Sanger, F., S. Nicklen, and A.R. Coulson. 1977. DNA sequencing with chain-terminating inhibitors. *Proc Natl Acad Sci U S A*. 74:5463-7.

Santos-Rosa, H., H. Moreno, G. Simos, A. Segref, B. Fahrenkrog, N. Pante, and E. Hurt. 1998. Nuclear mRNA export requires complex formation between Mex67p and Mtr2p at the nuclear pores. *Mol Cell Biol*. 18:6826-38.

Saveanu, C., D. Bienvenu, A. Namane, P.E. Gleizes, N. Gas, A. Jacquier, and M. Fromont-Racine. 2001. Nog2p, a putative GTPase associated with pre-60S subunits and required for late 60S maturation steps. *EMBO J*. 20:6475-84.

Saveanu, C., A. Namane, P.E. Gleizes, A. Lebreton, J.C. Rousselle, J. Noaillac-Depeyre, N. Gas, A. Jacquier, and M. Fromont-Racine. 2003. Sequential protein association with nascent 60S ribosomal particles. *Mol Cell Biol*. 23:4449-60.

Schachman, H.K., A.B. Pardee, and R.Y. Stanier. 1952. Studies on the macro-molecular organization of microbial cells. *Arch Biochem Biophys*. 38:245-60.

Schafer, T., D. Strauss, E. Petfalski, D. Tollervey, and E. Hurt. 2003. The path from nucleolar 90S to cytoplasmic 40S pre-ribosomes. *EMBO J*. 22:1370-80.

Schaffer, A.A., L. Aravind, T.L. Madden, S. Shavirin, J.L. Spouge, Y.I. Wolf, E.V. Koonin, and S.F. Altschul. 2001. Improving the accuracy of PSI-BLAST protein database searches with composition-based statistics and other refinements. *Nucleic Acids Res.* 29:2994-3005.

Schlenstedt, G., E. Smirnova, R. Deane, J. Solsbacher, U. Kutay, D. Gorlich, H. Ponstingl, and F.R. Bischoff. 1997. Yrb4p, a yeast ran-GTP-binding protein involved in import of ribosomal protein L25 into the nucleus. *EMBO J.* 16:6237-49.

Schmitt, M.E., T.A. Brown, and B.L. Trumpower. 1990. A rapid and simple method for preparation of RNA from Saccharomyces cerevisiae. *Nucleic Acids Res.* 18:3091-2.

Schwarzacher, H.G., and W. Mosgoeller. 2000. Ribosome biogenesis in man: current views on nucleolar structures and function. *Cytogenet Cell Genet.* 91:243-52.

Seedorf, M., M. Damelin, J. Kahana, T. Taura, and P. Silver. 1999. Interactions between a nuclear transporter and a subset of nuclear pore complex proteins depend on Ran GTPase. *Mol Cell Biol.* 19:1547-1557.

Seedorf, M., and P.A. Silver. 1997. Importin/karyopherin protein family members required for mRNA export from the nucleus. *Proc Natl Acad Sci U S A.* 94:8590-5.

Shan, X., Z. Xue, and T. Melese. 1994. Yeast NPI46 encodes a novel prolyl cis-trans isomerase that is located in the nucleolus. *J Cell Biol.* 126:853-62.

Sherr, C.J., and J.D. Weber. 2000. The ARF/p53 pathway. *Curr Opin Genet Dev.* 10:94-9.

Shevchenko, A., M. Wilm, O. Vorm, and M. Mann. 1996. Mass spectrometric sequencing of proteins silver-stained polyacrylamide gels. *Anal Chem.* 68:850-8.

Shimomura, O. 2005. The discovery of aequorin and green fluorescent protein. *J Microsc.* 217:1-15.

Shimomura, O., F.H. Johnson, and Y. Saiga. 1962. Extraction, purification and properties of aequorin, a bioluminescent protein from the luminous hydromedusan, Aequorea. *J Cell Comp Physiol.* 59:223-39.

Sikorski, R.S., and P. Hieter. 1989. A system of shuttle vectors and yeast host strains designed for efficient manipulation of DNA in Saccharomyces cerevisiae. *Genetics.* 122:19-27.

Spingola, M., L. Grate, D. Haussler, and M. Ares, Jr. 1999. Genome-wide bioinformatic and molecular analysis of introns in Saccharomyces cerevisiae. *RNA.* 5:221-34.

Sprang, S.R. 1997. G protein mechanisms: insights from structural analysis. *Annu Rev Biochem.* 66:639-78.

Stade, K., C.S. Ford, C. Guthrie, and K. Weis. 1997. Exportin 1 (Crm1p) is an essential nuclear export factor. *Cell.* 90:1041-50.

Stage-Zimmermann, T., U. Schmidt, and P.A. Silver. 2000. Factors affecting nuclear export of the 60S ribosomal subunit in vivo. *Mol Biol Cell.* 11:3777-89.

Strambio-de-Castillia, C., G. Blobel, and M.P. Rout. 1995. Isolation and characterization of nuclear envelopes from the yeast Saccharomyces. *J Cell Biol.* 131:19-31.

Sydorskyy, Y., D.J. Dilworth, B. Halloran, E.C. Yi, T. Makhnevych, R.W. Wozniak, and J.D. Aitchison. 2005. Nop53p is a novel nucleolar 60S ribosomal subunit biogenesis protein. *Biochem J.* 388:819-26.

Sydorskyy, Y., D.J. Dilworth, E.C. Yi, D.R. Goodlett, R.W. Wozniak, and J.D. Aitchison. 2003. Intersection of the Kap123p-mediated nuclear import and ribosome export pathways. *Mol Cell Biol.* 23:2042-54.

Tissieres, A., and J.D. Watson. 1958. Ribonucleoprotein particles from Escherichia coli. *Nature.* 182:778-80.

Tollervey, D. 2004. Molecular biology: termination by torpedo. *Nature.* 432:456-7.

Tollervey, D., H. Lehtonen, M. Carmo-Fonseca, and E.C. Hurt. 1991. The small nucleolar RNP protein NOP1 (fibrillarin) is required for pre-rRNA processing in yeast. *EMBO J.* 10:573-83.

Tollervey, D., H. Lehtonen, R. Jansen, H. Kern, and E.C. Hurt. 1993. Temperature-sensitive mutations demonstrate roles for yeast fibrillarin in pre-rRNA processing, pre-rRNA methylation, and ribosome assembly. *Cell.* 72:443-57.

Tschochner, H., and E. Hurt. 2003. Pre-ribosomes on the road from the nucleolus to the cytoplasm. *Trends Cell Biol.* 13:255-63.

Udem, S.A., and J.R. Warner. 1972. Ribosomal RNA synthesis in Saccharomyces cerevisiae. *J Mol Biol.* 65:227-42.

Uechi, T., T. Tanaka, and N. Kenmochi. 2001. A complete map of the human ribosomal protein genes: assignment of 80 genes to the cytogenetic map and implications for human disorders. *Genomics.* 72:223-30.

Vale, R.D. 2000. AAA proteins. Lords of the ring. *J Cell Biol.* 150:F13-9.

Venema, J., and D. Tollervey. 1995. Processing of pre-ribosomal RNA in Saccharomyces cerevisiae. *Yeast.* 11:1629-50.

Venema, J., and D. Tollervey. 1999. Ribosome synthesis in Saccharomyces cerevisiae. *Annu Rev Genet.* 33:261-311.

Voit, R., K. Schafer, and I. Grummt. 1997. Mechanism of repression of RNA polymerase I transcription by the retinoblastoma protein. *Mol Cell Biol.* 17:4230-7.

Warner, J.R. 1999. The economics of ribosome biosynthesis in yeast. *Trends Biochem Sci.* 24:437-40.

Warner, J.R., A. Kumar, S.A. Udem, and R.S. Wu. 1972. Ribosomal proteins and the assembly of ribosomes in eukaryotes. *Biochem J.* 129:29P-30P.

Watanabe, M., A.R. Zinn, D.C. Page, and T. Nishimoto. 1993. Functional equivalence of human X- and Y-encoded isoforms of ribosomal protein S4 consistent with a role in Turner syndrome. *Nat Genet.* 4:268-71.

Wente, S.R. 2000. Gatekeepers of the nucleus. *Science.* 288:1374-7.

Winzeler, E.A., D.D. Shoemaker, A. Astromoff, H. Liang, K. Anderson, B. Andre, R. Bangham, R. Benito, J.D. Boeke, H. Bussey, A.M. Chu, C. Connelly, K. Davis, F. Dietrich, S.W. Dow, M. El Bakkoury, F. Foury, S.H. Friend, E. Gentalen, G. Giaever, J.H. Hegemann, T. Jones, M. Laub, H. Liao, R.W. Davis, and et al. 1999. Functional characterization of the S. cerevisiae genome by gene deletion and parallel analysis. *Science.* 285:901-6.

Wohlschlegel, J.A., E.S. Johnson, S.I. Reed, and J.R. Yates, 3rd. 2004. Global analysis of protein sumoylation in Saccharomyces cerevisiae. *J Biol Chem.* 279:45662-8.

Wootton, J.C., and S. Federhen. 1996. Analysis of compositionally biased regions in sequence databases. *Methods Enzymol.* 266:554-71.

Wozniak, R.W., M.P. Rout, and J.D. Aitchison. 1998. Karyopherins and kissing cousins. *Trends Cell Biol.* 8:184-8.

Xue, Y., X. Bai, I. Lee, G. Kallstrom, J. Ho, J. Brown, A. Stevens, and A.W. Johnson. 2000. Saccharomyces cerevisiae RAI1 (YGL246c) is homologous to human DOM3Z and encodes a protein that binds the nuclear exoribonuclease Rat1p. *Mol Cell Biol.* 20:4006-15.

Zhang, Y., Z. Yu, X. Fu, and C. Liang. 2002. Noc3p, a bHLH protein, plays an integral role in the initiation of DNA replication in budding yeast. *Cell.* 109:849-60.